

1981

The influence of electrode material, viscosity, and magnetic field upon prebreakdown current in dielectric oil.

Mohammad A. Abiri
University of Windsor

Follow this and additional works at: <http://scholar.uwindsor.ca/etd>

Recommended Citation

Abiri, Mohammad A., "The influence of electrode material, viscosity, and magnetic field upon prebreakdown current in dielectric oil." (1981). *Electronic Theses and Dissertations*. Paper 4055.

This online database contains the full-text of PhD dissertations and Masters' theses of University of Windsor students from 1954 forward. These documents are made available for personal study and research purposes only, in accordance with the Canadian Copyright Act and the Creative Commons license—CC BY-NC-ND (Attribution, Non-Commercial, No Derivative Works). Under this license, works must always be attributed to the copyright holder (original author), cannot be used for any commercial purposes, and may not be altered. Any other use would require the permission of the copyright holder. Students may inquire about withdrawing their dissertation and/or thesis from this database. For additional inquiries, please contact the repository administrator via email (scholarship@uwindsor.ca) or by telephone at 519-253-3000ext. 3208.



National Library of Canada

Cataloguing Branch
Canadian Theses Division

Ottawa, Canada
K1A 0N4

Bibliothèque nationale du Canada

Direction du catalogage
Division des thèses canadiennes

NOTICE

The quality of this microfiche is heavily dependent upon the quality of the original thesis submitted for microfilming. Every effort has been made to ensure the highest quality of reproduction possible.

If pages are missing, contact the university which granted the degree.

Some pages may have indistinct print especially if the original pages were typed with a poor typewriter ribbon or if the university sent us a poor photocopy.

Previously copyrighted materials (journal articles, published tests, etc.) are not filmed.

Reproduction in full or in part of this film is governed by the Canadian Copyright Act, R.S.C. 1970, c. C-30. Please read the authorization forms which accompany this thesis.

**THIS DISSERTATION
HAS BEEN MICROFILMED
EXACTLY AS RECEIVED**

AVIS

La qualité de cette microfiche dépend grandement de la qualité de la thèse soumise au microfilmage. Nous avons tout fait pour assurer une qualité supérieure de reproduction.

S'il manque des pages, veuillez communiquer avec l'université qui a conféré le grade.

La qualité d'impression de certaines pages peut laisser à désirer, surtout si les pages originales ont été dactylographiées à l'aide d'un ruban usé ou si l'université nous a fait parvenir une photocopie de mauvaise qualité.

Les documents qui font déjà l'objet d'un droit d'auteur (articles de revue, examens publiés, etc.) ne sont pas microfilmés.

La reproduction, même partielle, de ce microfilm est soumise à la Loi canadienne sur le droit d'auteur, SRC 1970, c. C-30. Veuillez prendre connaissance des formules d'autorisation qui accompagnent cette thèse.

**LA THÈSE A ÉTÉ
MICROFILMÉE TELLE QUE
NOUS L'AVONS REÇUE**

THE INFLUENCE OF ELECTRODE MATERIAL,
VISCOSITY, AND MAGNETIC FIELD
UPON PREBREAKDOWN CURRENT
IN DIELECTRIC OIL

A Thesis
submitted to the Faculty of Graduate Studies through the
Department of Electrical Engineering in Partial Fulfilment
of the Requirements for the Degree of
Master of Applied Science at the
University of Windsor

by



Mohammad A. Abiri

Windsor, Ontario, Canada

August, 1980

© Mohammad A. Abiri - 1980

758973

To My Parents, and four
wonderful nephews and nieces,
Mansour, Ali, Tabassoam, and
Parisa

ABSTRACT

Experimental measurements of the current conduction in dimethylsiloxane fluid (DC 200) are presented. Reproducible current measurements have been made in the range of high voltage leading up to breakdown using a slow ramp application technique. Electrode materials were investigated in the high field regime for their capability of injecting charge as a function of applied voltage. Silicone oils with the same chemical composition but with different viscosities were used.

A plot of current versus voltage (log-log) has been obtained for large electrode spacings. This plot displays a linear portion prior to breakdown indicating that current flows according to a law of the form $I = KV^n$. The slope of the linear plots of the logarithm of current against logarithm of applied voltage varied linearly according to electrode spacing. The lines relating slope with electrode spacing were found to be displaced when the viscosity was altered. This influence of viscosity is presented for four kinds of electrode material.

Attention was also given to the influence upon prebreakdown of oil in the presence of a magnetic field acting transverse to the electric field and with strength of 200 gauss. The prebreakdown current has been observed to be either increased slightly or reduced according to the electrode spacing; for small spacings between 3.1 mm and 10 mm the inverse value of the slope was increased, reaching a maximum

and thereafter lowered progressively until it became negative. This effect was found to be influenced by the nature of the electrode surface as evidenced by using four kinds of electrode material, and one type of oil viscosity:

ACKNOWLEDGEMENTS

The author would like to express his sincere thanks and appreciation to Professor A. Watson, for his invaluable advice, help, and constructive criticisms during the course of this research.

The author also wishes to thank Dr. M. R. Raghuveer of the Department of Electrical Engineering, University of Manitoba, for his valuable assistance in the experimental setup and discussions on part of this work.

The author also extends his thanks to Messrs L. Reiter, J. M. Novosad, and D. K. Liebsch for their technical assistance in the construction of the apparatus.

Thanks are also extended to colleagues for their suggestions and Mrs. K. Kennedy for her excellent typing of this thesis.

The author expresses his sincere thanks to his parents without their constant encouragement, moral support, and love, though far away, this work would not have been completed.

TABLE OF CONTENTS

	<u>Page</u>
ABSTRACT	ii
ACKNOWLEDGEMENTS	iv
TABLE OF CONTENTS	v
LIST OF ILLUSTRATIONS	vii
LIST OF TABLES	xi
I. INTRODUCTION	1
II. A REVIEW OF CONDUCTION AND BREAKDOWN PHENOMENA IN DIELECTRIC LIQUIDS	6
2.1 Introduction	6
2.2 Electron Emission	7
2.3 Factors Influencing the Properties of Liquids	9
2.3.1 Dissolved Gases	9
2.3.2 Electrode Effects	13
2.3.2.1 Electrode Material and Surface Nature	13
2.3.2.2 Influence of Electrode Area	19
2.3.3 Moisture Content and its Effect on Breakdown Strength	19
2.3.4 Effect of Impurities	22
2.3.5 Conditioning Process	23
2.3.6 Magnetic Field Effect	24

Table of Contents Cont'd

	<u>Page</u>
III. EXPERIMENTAL SYSTEM	26
3.1 High Voltage Circuitry (The Ramp Generator)	26
3.2 The Test Chamber	32
3.3 Current Measurement Circuitry	34
3.4 The X-Y Recorder	38
3.5 The Magnet Supply Circuit	39
IV. EXPERIMENTAL PROCEDURES AND RESULTS	43
4.1 Breakdown Voltage	43
4.2 V-I Plot	44
4.3 Magnetic Field	47
4.4 Additional Observations	47
4.5 Experimental Results	48
V. CONCLUSIONS AND DISCUSSION	88
5.1 Summary	88
5.2 Major Conclusions	89
5.3 Discussion of Results	91
5.4 Suggestions for Further Studies	96
REFERENCES	98
APPENDICES	105
VITA AUCTORIS	136

LIST OF ILLUSTRATIONS

<u>Figure</u>		<u>Page</u>
2.1	The Effect of Separate Cathode or Anode Oxidation on the Strength of Liquified Argon	16
2.2	Typical Current/Stress Characteristics for Coated and Uncoated Electrodes	17
2.3	Variation of Moisture Content of Transformer Oil in Contact with Moist Air with Temperature	21
3.1	Ramp Generator Circuit	27
3.2	Wave Shape of Output Voltage of the Ramp Generator	28
3.3	Motorized Variac Switching Circuit	29
3.4	Sectional View of Test Chamber	33
3.5	General Schematic Diagram of Measuring Circuitry	37
3.6	Magnet Circuit Diagram	40
3.7	Variation of Flux Density between the Magnetic Poles	41
4.1	Experimental Procedure for Fixed Electrode Spacing	46
4.2	Voltage Versus Current Characteristics for Fifteen Consecutive Stress Cycles with Copper Electrodes in 5 ^{C.S.} Silicone Oil	49

List of Illustrations Cont'd:

<u>Figure</u>	<u>Page</u>
4.3 The Current-Voltage Characteristics for CU Electrodes and 5 ^{C.S.} Silicone Oil	51
4.4 The Current-Voltage Characteristics for CU Electrodes with Different Viscosities	53
4.5 The Current-Voltage Characteristics for Filtered and Unfiltered Silicone Oil	54
4.6 The Current-Voltage Characteristics for Different Electrode Materials with 5 ^{C.S.} Silicone Oil	55
4.7 The Current-Voltage Characteristics for Different Electrode Materials with 350 ^{C.S.} Silicone Oil	56
4.8 The Current-Voltage Characteristics for Different Electrode Materials with 1000 ^{C.S.} Silicone Oil	57
4.9 The Current-Voltage Characteristics for Copper Electrodes and 1000 ^{C.S.} Silicone Oil for Different Number of Ramp Cycles	59
4.10.1 The Current-Voltage Characteristics (log-log) for CU Electrodes and 5 ^{C.S.} Silicone Oil	60
4.10.2 The Current-Voltage Characteristics (log-log) for CU Electrodes and 350 ^{C.S.} Silicone Oil	61
4.10.3 The Current-Voltage Characteristics (log-log) for CU Electrodes and 1000 ^{C.S.} Silicone Oil	62

List of Illustrations Cont'd:

<u>Figure</u>	<u>Page</u>
4.10.4 The Current-Voltage Characteristics (log-log) for Al Electrodes and 5 ^{C.S.} Silicone Oil	63
4.10.5 The Current-Voltage Characteristics (log-log) for Al Electrodes and 350 ^{C.S.} Silicone Oil	64
4.10.6 The Current-Voltage Characteristics (log-log) for Al Electrodes and 1000 ^{C.S.} Silicone Oil	65
4.10.7 The Current-Voltage Characteristics (log-log) for Mg Electrodes and 5 ^{C.S.} Silicone Oil	66
4.10.8 The Current-Voltage Characteristics (log-log) for Mg Electrodes and 350 ^{C.S.} Silicone Oil	67
4.10.9 The Current-Voltage Characteristics (log-log) for Mg Electrodes and 1000 ^{C.S.} Silicone Oil	68
4.10.10 The Current-Voltage Characteristics (log-log) for Zn Electrodes and 5 ^{C.S.} Silicone Oil	69
4.10.11 The Current-Voltage Characteristics (log-log) for Zn Electrodes and 350 ^{C.S.} Silicone Oil	70
4.10.12 The Current-Voltage Characteristics (log-log) for Zn Electrodes and 1000 ^{C.S.} Silicone Oil	71
4.11 The Current-Voltage Characteristics (log-log) at Room Temperature for Different Relative Humidity.	74
4.12.1 $d(\ln V)/d(\ln I)$ as a Function of Electrode Spacing for Hemispherical Copper Electrodes	75
4.12.2 $d(\ln V)/d(\ln I)$ as a function of Electrode Spacing for Hemispherical Al Electrodes	76

List of Illustrations Cont'd:

<u>Figure</u>	<u>Page</u>
4.12.3 $d(\ln V)/d(\ln I)$ as a Function of Electrode Spacing for Hemispherical Mg Electrodes	77
4.12.4 $d(\ln V)/d(\ln I)$ as a Function of Electrode Spacing for Hemispherical Zn Electrodes	78
4.13.1 Dependence of $d(\ln V)/d(\ln I)$ on Electrode Spacing for a Number of Electrode Materials using 5 ^{C.S.} Silicone Oil	80
4.13.2 Dependence of $d(\ln V)/d(\ln I)$ on Electrode Spacing for a Number of Electrode Materials using 350 ^{C.S.} Silicone Oil	81
4.13.3 Dependence of $d(\ln V)/d(\ln I)$ on Electrode Spacing for a Number of Electrode Materials using 1000 ^{C.S.} Silicone Oil	82
4.14 $d(\ln V)/d(\ln I)$ for Hemispherical Copper Electrodes as a Function of Electrode Spacing for Four Successive Sets of 15 Recordings in the Presence of a Magnetic Field	84
4.15 The Average $d(\ln V)/d(\ln I)$ for Different Electrode Materials as a Function of Electrode Spacing With and Without Applying a Magnetic Field	85
4.16 The Current-Voltage Characteristics with CU Electrodes and 350 ^{C.S.} Silicone Oil for Different Ramp Slow Rates	87

LIST OF TABLES

<u>Table</u>		<u>Page</u>
4.1	B/D Voltage in KV as a Function of Electrode Spacing	45

I. INTRODUCTION

Electrical insulating oils for transformers, capacitors, cables and switch gear have long since been refined from naphthenic petroleum crude oil. In addition to being short in supply [1], they present fire hazards [2], which can not be eliminated even by the use of fire resistants such as askarel [3]. It is, therefore, advisable to use synthesized fluids such as silicones, alkylbenzenes and polyolefins as alternatives [1]. This has the possibility of abundant supply, excellent electrical properties such as high dielectric strength, chemical stability, good thermal conductivity and non-inflammability.

It is of importance to know the behaviour of the current stress characteristic in the region immediately below breakdown, since the breakdown itself in the liquid dielectric is the ultimate point of the conduction stage. It is, therefore, worthy to characterize more fully their dielectric performance in this region of electric field.

Recently a preliminary research on the prebreakdown current of silicone oil resulted in several publications [4-6]. It has been shown [4-10] that prebreakdown current versus voltage characteristics for uniform fields have three parts, being divided into low, intermediate and high field regions. At low fields the current is ohmic, in the intermediate region current saturates and at higher fields a non-linear relationship between current and voltage exists.

Watson [5] has shown that two sharply divided portions of the high field regime of the I-V characteristics of silicone oil displays, a linear relationship between the logarithm of the current and of the voltage and the ultimate slope was a function of electrode spacing. He has also shown this phenomenon to be consistent with a model involving Fowler-Nordheim emission which initiates a convective charge transport mechanism with the fluid flowing in a vortex cell enclosing a steady irrotational funnel flow through its core at the cathode. The I-V characteristics of dimethyl-siloxane fluid under ambient temperature and humidity has been studied by Hackim et al [6]. He has shown that, on a log-log scale, at low fields, the current is ohmic (slope of 1) but the slope decreased to 50% at intermediate voltages only to increase again at high fields. It is also observed that the above relationship strongly depends on the relative humidity. There is still, however, a great deal that is unclear, such as, the influence of viscosity, electrode material, and an applied magnetic field on the prebreakdown mechanism under high electric fields.

The principal objectives of the foregoing thesis are threefold:

1. To investigate the influence of viscosity of the liquid upon the prebreakdown current.
2. To investigate the effect of electrode material upon the prebreakdown current from the viewpoint of their capability to inject charge under stress.

3. To investigate the possible influence of a magnetic field upon the liquid prebreakdown process.

In the first part of this work a dimethyl-siloxane fluid (Dow Corning DC 200, 5, 350, and 1,000^{C.S.}) and hemispherically tipped cylinders of copper were chosen for studies to investigate the significance of the viscosity influencing the prebreakdown current which has not been previously studied.

The same experiments were repeated for the case of aluminium, magnesium and zinc to study the effect of the electrode material upon the mechanism of prebreakdown current in silicone liquid under non-uniform fields.

Thirdly, there are two possible ways in which the influence of a magnetic field is manifested:

a) By studying the relationship between breakdown voltage and magnetic field strength with constant electrode spacing (Secker and Hilton's method [11]).

b) By studying relationships between the prebreakdown current and electrode spacing with constant magnetic field (Watson and Girgis's method [5]).

Magnetic influence upon breakdown has been observed in other situations. For instance a magnetic perturbation in vacuum breakdown was reported by Watson [12] as being a surface phenomenon in the oxide layer present on metallic electrode surfaces, upon exposure of the metal to the atmosphere. It has been suggested that a weak magnetic field acting transverse to the electric field can influence the current emitted by a protrusion through a magneto-transport effect and

the resulting current reduction modifies the breakdown voltage [13].

Zaky and Hawley reported [9] that the electrode material has an effect on the current emitted in the high field regime of liquid dielectrics which display a similar effect upon the I-V characteristics as in vacuum. Thus one may expect similar effects due to magnetic field to occur in liquid dielectrics since each is thought to conduct current primarily by field emission. Saveanu and Mondescu [14] report a small magnetic field perturbation of current transport, particularly in polar liquids and a dependence of breakdown voltage of brass spheres on a crossed magnetic field for a fixed electrode spacing in the dielectric liquid hexane has been reported by Secker and Hilton [11] and Gallagher [15]. Recently Watson and Girgis [5] have observed that a weak magnetic field has an effect upon prebreakdown current of copper hemispheres in silicone oil for different electrode spacing.

In addition to complementing the early treatment by Watson and Girgis [5] of the influence of a crossed magnetic field on the prebreakdown current in silicone oil the present investigation deals with the importance of the electrode material, using aluminium, copper, magnesium and zinc electrodes. An assumption was made that dissimilar results for copper and aluminium with the same liquid obtained earlier [5] were dominantly an electrode phenomenon which was not accounted. A voltage growth rate of 12.8 kVs^{-1} was provided by a ramp generator with which the current versus voltage characteristics

could be obtained with a fixed magnetic field strength at five different electrode spacings. This investigation moreover has shown that the applied magnetic flux actually influences the conditioning process.

In order to place the present work in perspective, recent work concerning electrical breakdown and conduction in dielectric liquids is reviewed briefly in Chapter 2. Chapter 3 deals with experimental arrangements and techniques. The results obtained are given in Chapter 4. The last chapter is devoted to the discussion and conclusion of the research work presented in this thesis.

II. A REVIEW OF CONDUCTION AND BREAKDOWN PHENOMENA IN DIELECTRIC LIQUIDS

2.1 Introduction

A voluminous literature has evolved concerning breakdown and conduction in dielectric liquids. This has been summarized in many books and reviews of which those written by Lewis [16], Adamczewski [17] and Zaky and Hawley [9] are the best known. It is not the purpose here to review all the factors which influence breakdown and conduction in dielectric liquids but only to summarize the literature up-to-date which is most relevant to the dissertation in hand.

The theory behind dielectric breakdown has always been to a great extent equal parts of speculation, art and science. Relating to the reliability and cost of equipment designs, liquids and gases are known to be self-healing media, i.e., the dielectric properties are recoverable after breakdown.

Studies in the past 60 years have confirmed that the dielectric strength of insulating liquids is influenced by material properties, a host of external environmental factors, assorted test conditions which may exist and most important of all purity of the liquid itself.

The breakdown mechanism is, however, governed by the behaviour of pure liquids (which are free from containing gases) as well as impure liquids (which are contained of dissolved gases) [9].

In the review article by Lewis [16], the emphasis was

mainly on work carried out on "pure" liquids, since their study was believed to provide a better understanding of the processes involved in conduction and behaviour.

2.2 Electron Emission

The introduction of free electrons into liquids is a method of testing conduction in dielectric liquids. This can be done by means of photo electric effect, field-assisted thermionic emission, field-aided electron emission (cold cathode field emission, as used here) or by superimposing a β -radiating substance on one of the electrodes.

It has been reported [9] that at high stresses there is more or less exponential form of increase in current with increasing field. This current is known to be electronic since it must result from injection of carriers from an electrode or multiplication in the material, or both.

Field emission (tunnelling) and schottky emission are the two main mechanisms of emission of electrons from the cathode into the insulation postulated by many investigators to explain the exponential current/voltage relationship [16]. Electron and ion multiplication analogous to that in a gas discharge may also occur at the higher stresses. The space-charge of the injected electrons (whether moving or trapped) within the insulator will have the effect of decreasing the field at the cathode and modifying the current/voltage relation [57]. Where liquids are concerned there are at least two other possible means of charge transfer which make the conduction in dielectric liquids to be complex.

First the tendency of oil to display movement when under stress [48, 54] suggests that charges injected into the liquid from an electrode attaching themselves to oil molecules in the neighbourhood cause this oil to be attracted to the opposite electrode where some of its charge may be given up, thus producing a convection of charge independent of conductivity [57]. The second possibility is that particles, which at highly stressed regions move to and fro between the electrodes, will ferry charge from one electrode to the other. Electron emission from metals under the influence of an electric field is, however, a surface phenomenon and depends on electrode material, and the method of preparation. The phenomenon occurring in the liquid itself depends on the volume of liquid and hence the electrode spacing. They include such effects as dependence of conductivity on viscosity, density, temperature and molecular structure, secondary ionization processes in the liquid and the influence of previous electrical breakdown.

Fowler and Nordheim [58] introduced an equation for emission current from the metal caused by an electric field E having the form:

$$I = AE^2 \exp(-B/E)$$

where A and B are functions of the work function ϕ . This equation is applicable in very high fields. The various effects of electrode surfaces were explained as being due to different values of the work function for electrons to escape from a metal.

2.3 Factors Influencing the Properties of Liquids

Several factors do affect both conductivity and breakdown measurements of liquid dielectrics, namely, temperature, pressure, electrode material and its geometry, electrode area and the nature of their surfaces, content of dissolved gas, water and other impurities, and stressed volume which are common to all liquid insulants. A brief description of these factors is given below.

2.3.1 Dissolved Gases

A recent discovery concerning the influence of dissolved gases is that reported by Sletten [18]. In his report the electric strength of hexane, using direct voltage, increased from 0.7 MVcm^{-1} for the gas free liquid to 1.3 MVcm^{-1} for an oxygen content corresponding to an equilibrium partial pressure of about 130 torr; no further increase in strength was observed for larger amounts of dissolved oxygen.

Sletten and Lewis [19] reported that nitrogen and hydrogen have no effect, even when the amounts dissolved were large. Their report indicates that carbon dioxide shows some effect on the strength. Thus the first few breakdown measurements corresponded to the breakdown voltage of degassed hexane; however, as the number of breakdown increased, the strength rose to a value corresponding to the maximum breakdown strength of the hexane with oxygen in solution. It was concluded that the observed increase in strength was entirely due to a progressive accumulation of oxygen released during the breakdown. They have attributed the beneficial

effect of oxygen to its electro-negative properties.) Electrons emitted from the cathode form negative oxygen ions, so that the available number of electrons is effectively reduced.

Gosling and Tropper [20] carried out an investigation of the effect of dissolved gases on the breakdown strength of transformer oil under carefully controlled conditions and found that the variation of the breakdown strength of oil with gas content depended on the type of gas dissolved. Their interpretation of the effect is based on the results of the variation of the breakdown voltage with electrode spacing for oil containing dissolved nitrogen, oxygen, and air. These results showed that, in all three cases, the uniform field breakdown voltage versus electrode spacing characteristics of oil gives an apparent intercept when extrapolated to zero spacing.

It should be noted that Sletten and Lewis [19] found a similar zero-spacing intercept in the breakdown voltage versus electrode spacing characteristics of hexane when it contained dissolved oxygen, and the intercept was attributed to the presence of this gas.

Gosling and Tropper [20] reported also that, for each individual gas, the intercept increases with increasing gas content. The intercepts with dissolved oxygen were always greater than those with dissolved nitrogen, while the intercepts with dissolved air were greater than those for either oxygen or nitrogen at the same equilibrium pressure.

Since, under identical test conditions, no intercept was obtained with degassed oil, the existence of the apparent intercepts in oil containing dissolved gases was attributed [20] to the formation of insulating layers on one or both electrodes. The total breakdown voltage would then be distributed partly across this layer (or layers) and partly across the bulk liquid. Nelson et al [21] studied the effect of dissolved gas on the 50 Hz electric strength of transformer oil as a function of temperature using uniform field. The results for stationary oil and for oil circulating with an average velocity of 3 mms^{-1} were compared and it has been shown that, as a result of circulation for temperatures above 60°C , there is a large reduction in the breakdown strength. The reason for this drop has been thought to be the reduction in the surface tension at high temperatures; causing small bubbles to break away from the electrode surfaces under the sweeping action of the flow. The released bubbles will slowly rise and elongate, leading to the final breakdown of the oil.

In an attempt to reproduce Gosling's [20] results, Nossier and Hawley [22] carried out a detailed investigation of the effect of dissolved sulphur-hexafluoride on the breakdown strength of transformer oil, and found that extrapolation of the breakdown voltage versus electrode spacing characteristics to zero spacing gave apparent intercepts on the voltage axis. They had the same interpretation as Gosling [20], thereby giving a finite breakdown voltage for zero spacings.

Zein Eldine and Trapper [23] investigated the effect of dissolved air on the breakdown strength of transformer oil in non-uniform fields using a point to plane electrode geometry. Their findings showed that by saturating oil with air, there was an increase with the point negative but a decrease with the point positive. These results have been confirmed by breakdown measurements in technically clean transformer oil using direct voltage [24]. The results are attributed [9] in terms of negative space charge formation, due to the presence of oxygen, reducing the field at the negative point, whereas, with the point positive, a negative space charge would increase the field there. The higher strengths obtained by Zein Eldine and Tropper [23] with a negative point polarity are in agreement with the results of Kao and Highan [25] for air-saturated hexane, but are in contrary to the results obtained for air-saturated hexane by Lewis [26].

The above contradiction is thought [9] to be due to the different electrode spacings used by these workers, whereas the first four workers used spacings greater than 300 μM , the electrode spacings used by Lewis [26] did not exceed 90 μM .

In an investigation concerning the optical state of the liquid hexane under electric stress, Farazmand [27] noted the existence of a prebreakdown disturbance in the liquid. The disturbance was characterized to be of spherical forms and grew with increasing time. These investigations were continued by

other workers [28] to verify and extend the results stated above. Chadband and Wright [28] represented the region of disturbance (or the changed density) by a sphere which maintains contact with the point cathode and grows progressively larger as time goes by, and considered it to be a region of weak plasma formed by electrons emitted at the cathode. Since the disturbance is considered to be a region of weak plasma the electric field in it is regarded as zero. The plasma will then grow by the action of the anode field on the electrons and negative ions at its boundary. If the applied voltage is large enough the region grows to span approximately four-fifths of the electrode spacing and leading to instability and breakdown. Chadband and Wright [28] concluded that the rate of movement of the plasma boundary indicates a much higher electron mobility than is measured at lower, pre-ionization fields. It was suggested that at high fields electrons spend a greater proportion of their time in free flight and that the electron mobility becomes field dependent and rises rapidly.

2.3.2 Electrode Effects

2.3.2.1 Electrode Material and Surface Nature

In general electrode surfaces form the physical boundaries between which the final breakdown takes place and so it is not surprising to find that both the conduction current and the breakdown strength for a given electrode spacing is dependent on the material of the electrode.

Studies of the prebreakdown current of different materials have recently been made by Watson and Girgis [5]. The ranking of materials in order of decreasing prebreakdown conduction current under direct ramp voltage for a given spacing with conditioned electrodes is copper and aluminium. In paper this ranking, however, was not conclusive.

The thin oxide layer formed at the electrode interface differs in electrical properties from those of the underlying electrode material and it also affects the properties of the liquid under stress. Such a film of oxide is formed almost instantly on most, if not all, technically cleaned metal surfaces, and has been known [29] to grow with gap performance time after preparation (the time in which freshly surfaced electrodes were exposed to air before immersion in the dielectric liquid), indicating that oxide growth between preparation, which varies with different electrode materials, and the installation of these electrodes might be a possible factor significant to breakdown voltage, accounting for some of the conflicting data obtained from past experiments. This oxide film together with the adsorbed layers of gases, constitute an effective insulating layer which may be important to liquid insulation as regard neutralization of the ions arriving at the electrode surfaces and affect the rate of electron emission from the cathode. Therefore, by using electrodes of various metals which have been allowed to oxidize in dry air after polishing, it is

possible to alter the electric strength in a controlled manner.

Swan and Lewis [30] found that the electric strength of liquid argon containing small amounts of oxygen in solution increased with increasing cathode-oxidation time and decreased with increasing anode-oxidation time (Fig. 1). The anode effect is emphasized to be due to the formation of negative space charge layers at the surface. This was later confirmed when the oxygen was removed or microsecond-pulse voltages were used, even with oxygen present, no anode effect was observed, since negative ions could not form in the anode region [31].

The current relationship with stress (Fig. 2) obtained by Cullingford et al [32] and Zein Eldine et al [33] under similar conditions has also confirmed the earlier explanation [30] of ionization processes at the anode. With regard to the influence of electrode coatings on the breakdown strength of air-saturated mineral oil, Zaky et al [34] found that under direct voltages, the minimum breakdown for either of the electrodes being coated was greater than when both electrodes were bare. This breakdown voltage was higher than for the case when both the electrodes were coated. Zaky et al [35] concluded that with only the cathode coated, by a thin insulating film, most of the applied voltage will appear across the film and set up an intense field in the film and at the underlying metal surface. The field emission process causes electron emission from the cathode which increases with

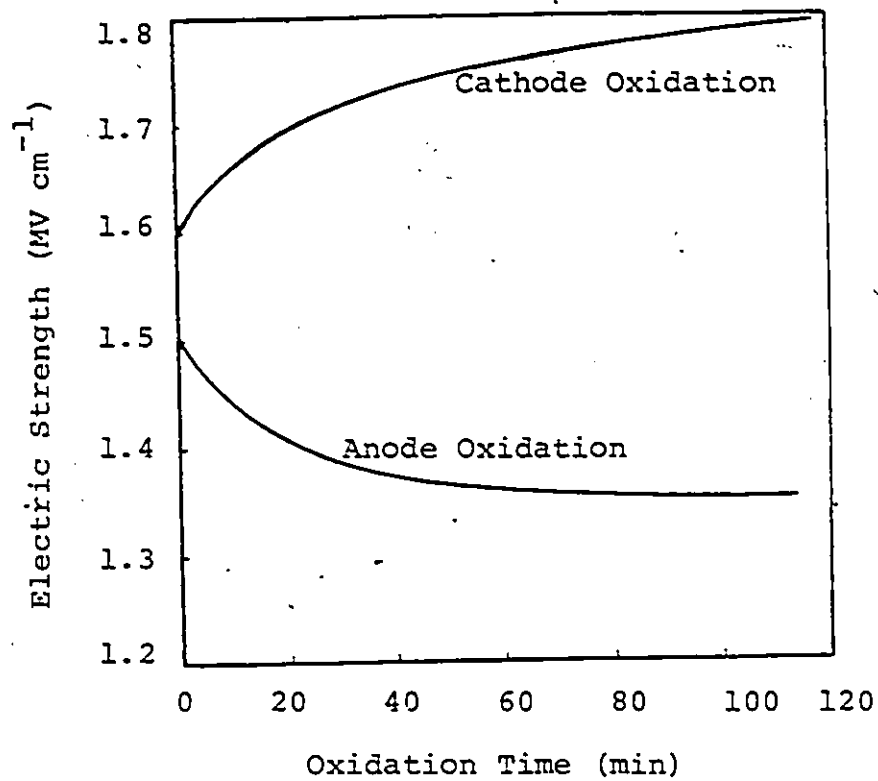
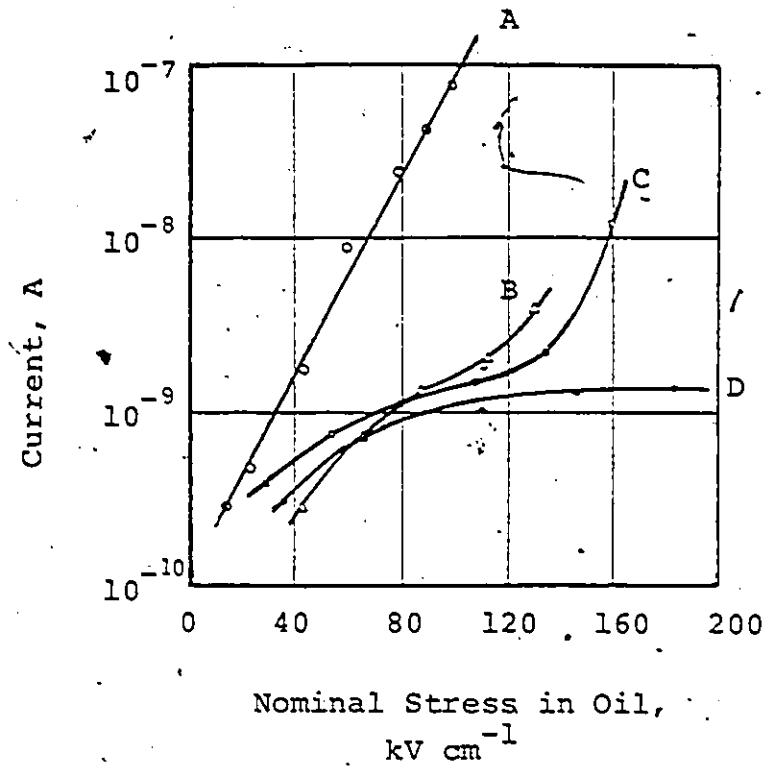


Figure 2.1: The Effect of Separate Cathode or Anode Oxidation on the Strength of Liquified Argon

(After Lewis, 1968, [50])



Oil Gap = 1.5 mm
 Film Thickness = 0.5 mm
A Both electrodes uncoated
B Both electrodes coated
C Cathode uncoated; Anode coated
D Cathode coated, Anode uncoated

(After Cullingford et al., 1963; Zein Eldine et al., 1965, [32])

Figure 2.2: Typical Current/Stress Characteristics for Coated and Uncoated Electrodes

increase in the applied voltage, causing local heating. This local heating deteriorates the effectiveness of the film and results into lowering the breakdown strength. With an insulating film on the anode it was found [35] that the formation of negative ions will enhance the field across the film. More recently, an investigation of the influence of surface oxide film on the apparent zero spacing breakdown voltage of mineral oil has been conducted by Zaky et al [36]. While confirming the previous results of the apparent intercepts, they indicated that although a large intercept is associated with the presence of a highly insulating barrier on one of the electrodes, the presence of such a barrier does not necessarily lead to such an intercept. They interpreted their results by taking into account the space charges present at the electrode surfaces prior to extrapolation to zero spacing. They concluded, however, that the magnitude of the intercept may be determined by the combined action of the cathode and anode, rather than by either of these electrodes, as well as by the presence or absence of dissolved gas.

Hosticka [4] has recently reported on the influence of electrode coatings on the breakdown strength of dimethyl-silicone oil under impulse and 60 HZ voltages. He used bare and insulating electrodes for a uniform field spacing and showed that, by insulating the electrodes, there is an appreciable increase in the dielectric strength of silicone oil. He concluded that the uniform field insulating characteristics of silicone oil are comparable to those of transformer oils.

2.3.2:2 Influence of Electrode Area

Studies of the dependence of the breakdown strength of organic liquids on the electrode area, for a fixed spacing has shown [33] that increasing the area of a stressed surface reduced the strength of liquid insulant for both alternating and direct voltages. This dependence was further investigated by Weber and Endicott [37-38], using 60 HZ voltages and uniform field Rogowski profile and finally concluded that the relationship, for a fixed gap, was logarithmic. The results of Nelson et al [21] on the effect of electrode area on the breakdown strength of air-saturated transformer oil, using 50 HZ and impulse, showed good experimental agreement with the logarithmic law expressed by Weber and Endicott [37-38].

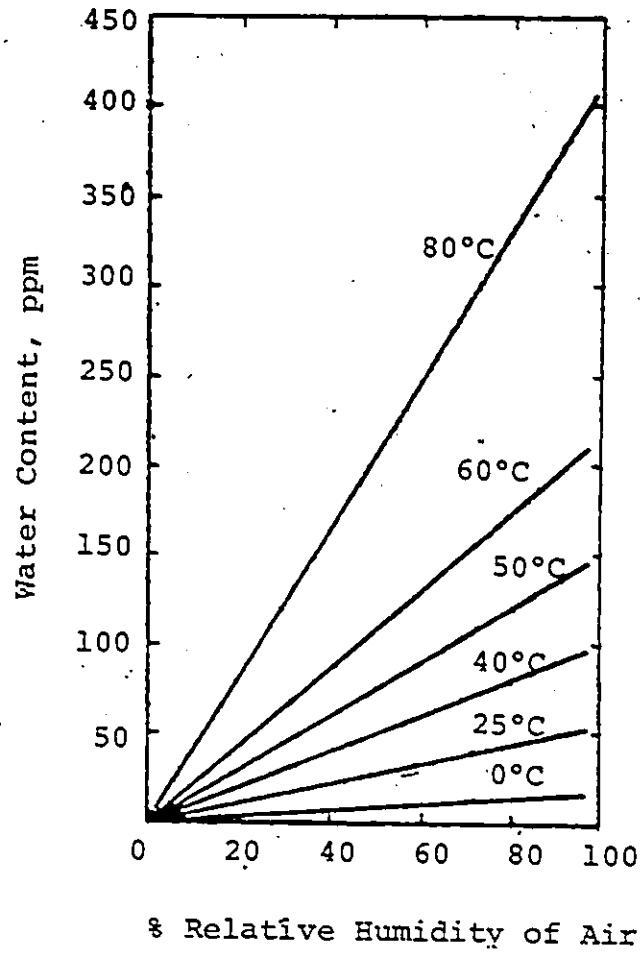
Most investigators [9, 33, 39] explained the area effect by suggesting that the larger the area the greater the probability of having high local fields at asperities on the electrode surfaces. There are, however, some other factors such as gas bubbles trapped in pits on the electrode surfaces, areas of low work functions on the cathode and high work function on the anode, which may constitute weak links in the insulation process, which were recently mentioned by Zaky and Hawley [9].

2.3.3 Moisture Content and Its Effect on Breakdown Strength

Traces of water and other electrolytic impurities are naturally the most important [17]. The amount of water dissolved in a mineral oil, under normal conditions, is

reported to be extremely small in the form of free water [9] or a by-product of oxidation taking place in the oil [40]. However, the most important source of water in oils is that absorbed from a humid environment. When dry oil, therefore, is exposed to an atmosphere which contains water vapour, the oil will absorb water from it. A linear relationship between the water content of a new transformer oil and the relative humidity of the air was found by Kaufman et al [41], Fig. (3), and has been shown [42] to be valid for new and non-oxidized oils. Moreover for a given relative humidity of air, the amount of water dissolved in an oil increases with its degree of oxidation.

It has been reported [9] that the presence of water in an insulating oil has little effect on the breakdown strength of the oil, but if the oil contains solid particles, even small amounts of hygroscopic impurities, the presence of moisture can largely reduce its breakdown strength, by as much as 50%. It has also been shown [43] that particles and fibers present in a dry oil do not tend to form bridges across the test spacing, whereas in the presence of moisture bridge formation invariably takes place. This has been explained [9] that high relative permittivity of the moist particles and fibers (ϵ_r of water, ~ 80) causes them to be drawn into the high field interelectrode region where they become polarised and form dipole chains along the field lines. When the concentration of impurities in the spacing becomes sufficiently high, these form a bridge across the



(after Kaufman et al., 1955, [41])

Figure 2.3: Variation of Moisture Content of Transformer Oil in Contact with Moist Air with Temperature

spacing and lead to a bridge breakdown.

The effect of moisture on the breakdown strength of transformer oil for a large spacing with uniform and non-uniform fields under direct and alternating voltages has been found [44] to be similar for both types of voltage excitation. Kaplan and Kutichinski's [44] results for a 1.5 mm spacing showed that there was a sharp decrease in breakdown strength as the water content increased to 150 ppm and it reached to its lowest value at a concentration of about 200 ppm. For 10 mm spacings and hemispherical electrodes (12.5 mm radius), the drop in strength with increasing moisture content was less marked than for smaller spacings.

Recently a study has been made by Hakim et al [6] on the dielectric properties of silicone liquids. It is shown that the D.C. conductivity of the silicone oil is significantly dependent on the ambient humidity. The conduction current at a fixed voltage and 5 mm spacing will decrease by more than one order of magnitude as a function of drying process time.

2.3.4 Effect of Impurities

Purity of the liquids is important as no reproducible results can be obtained with liquids of insufficient purity, and the characteristic properties of a liquid can be covered by phenomenon arising due to the presence of impurities, such as traces of water, electrolytic impurities, gas and vapour bubbles, dust and other suspensions, especially when the liquids are to be studied in high electric fields. On the application of electric stress these impurities could be

removed [17]. This fact is also stated [9, 17] that when a liquid is subjected to an electric stress for a long period, the electric conduction is reduced by as much as several orders of magnitude and the conduction current does not return to its previous value unless impurities are introduced again.

2.3.5 Conditioning Process

Problems encountered in conduction current measurements are those concerned with the stability and the reproducibility of the results. Zaky and Hawley [9] reported that a conditioned state may be achieved either by spark conditioning or by stress conditioning. Ferrant's [45] results on spark conditioning led him to the conclusion that conditioning is an electrode surface effect and was confirmed by many other investigators [21, 23, 26, 46]. He observed that a conditioned state similar to that of spark conditioning could be attained by forming a process in which a voltage slightly below the breakdown voltage is being applied for a prolonged period, without breaking down the spacing. From the tests with degassed oil and point-plane electrode geometries, Eldine and Tropper [23] found a conditioning effect only when the point was positive, indicating that it was the cathode which was responsible for the conditioning effect. Zaky and Hawley [9] interpreted the results to be dependent on the presence of an adequate supply of electrons from the cathode. When the point is negative, the very high cathode field ensures the supply of a sufficient number of electrons

so that the ultimate breakdown stress will depend only on the existence of a suitable field in the bulk liquid. Hence no conditioning effect is expected to occur. Zaky and Hawley [9] also reported that when the point is positive electron emission from the plane cathode is restricted. This will depend on surface conditions. A high conditioning effect is expected when large cathode area is used.

Observations on the behaviour of microscopic particles, in stressed liquid dielectrics, have shown [20,47] that the gap becomes clear of particle activities after a period of time. Gosling and Tropper [20] found that conduction current measurements during the stress conditioning process are erratic and when the gap was cleared, they were steady and reproducible.

2.3.6 Magnetic Field Effect

Relatively very little work has been published on the possible influence of an applied field upon the conduction of breakdown process of liquid dielectrics due to the importance of other factors. Saveanu and Mondescu [14] however, report a small magnetic field perturbation of conduction, particularly in polar liquids. A dependence of the breakdown voltage on a crossed magnetic field in the dielectric liquid hexane has been reported by Secker and Hilton [11] and Gallagher [15]. Secker and Hilton [11] found that upon application of ramp voltage with a growth rate of 0.625 KVS^{-1} and a varying crossed magnetic field for a fixed electrode spacing, the breakdown voltage of brass spheres in hexane

enhanced for a magnetic flux density less than 0.15 Tesla and it showed reduction with higher flux densities. These results are in conformity with Gallagher's [15] results. Secker assumed that the magnetic field interacts with charge-carriers in the interelectrode spacing, therefore, modifying their trajectories so as to perturb the onset of breakdown. For such trajectory modification, he suggested that the majority of the charged particles, present in the inter-electrode space, must be free electrons to explain such effects. These results of investigation, however, did not positively confirm the existence of a magnetic perturbation of the conduction process itself. Watson et al proceeded in this investigation [5] and confirmed the existence of such an effect in the case of prebreakdown current of copper hemispheres in silicone liquid which, like hexane, is non polar. He showed that, under the action of a weak magnetic field, for spacings between 0.6 cm and 1.0 cm there is a decrease in the prebreakdown current but it increases from then up to 1.4 cm. Watson compared his results with the results obtained by Secker and suggested that these effects originate in the field emission mechanism itself, rather than in the intervening dielectric.

III. EXPERIMENTAL SYSTEM

The experimental facilities can be considered as grouped into five parts; the high voltage circuitry, test vessel, current measurement circuitry, current voltage recorder, and magnet supply circuitry.

3.1 High Voltage Circuitry (The Ramp Generator)

Preliminary current measurements at fixed voltages and for a long interval of time produced non-steady values and non-reproducible results. This was supposed to be due to thermal runaway occurring in the liquid. To overcome the thermal effect Secker and Hilton's [11] method of ramp application was used with success. The ramp generator was constructed from a motorized variac and normal high voltage D.C. supply as shown in Fig. (3.1).

The motorized variac—consisting of a variable autotransformer, the specifications of which are given in Appendix I, was used to modify the ordinary high voltage supply in order to give an output voltage as shown in Fig. (3.2)— was driven by an induction stepping motor as shown in Fig. (3.3).

When power is initiated by turning on the line switch S_1 , as shown in Fig. (3.3), the "LINE ON" indicator DS_1 will light. If the servomotor is at zero position its lower limit switch is actuated and 115^V is across the "POWERSTAT AT ZERO" indicator DS_2 through the contact K_3 and the "POWERSTAT AT ZERO" indicator will light. By closing the "HIGH VOLTAGE ON"

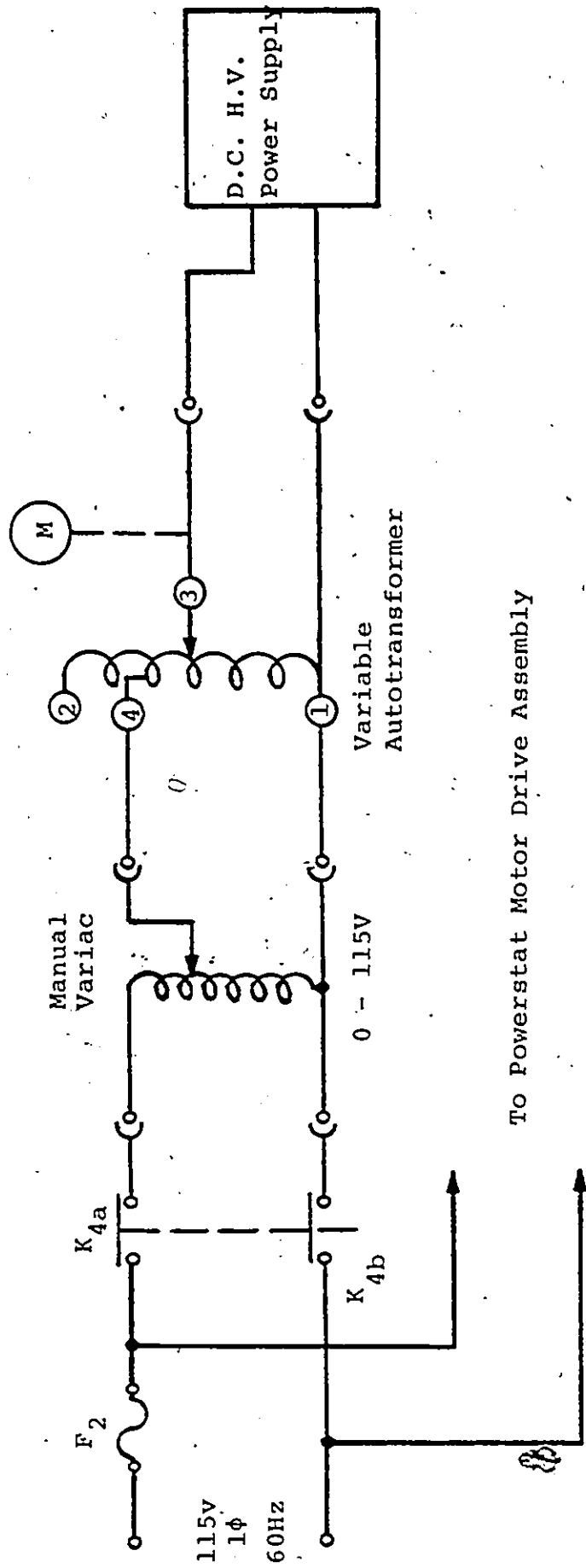


Figure 3.1: Ramp Generator Circuit

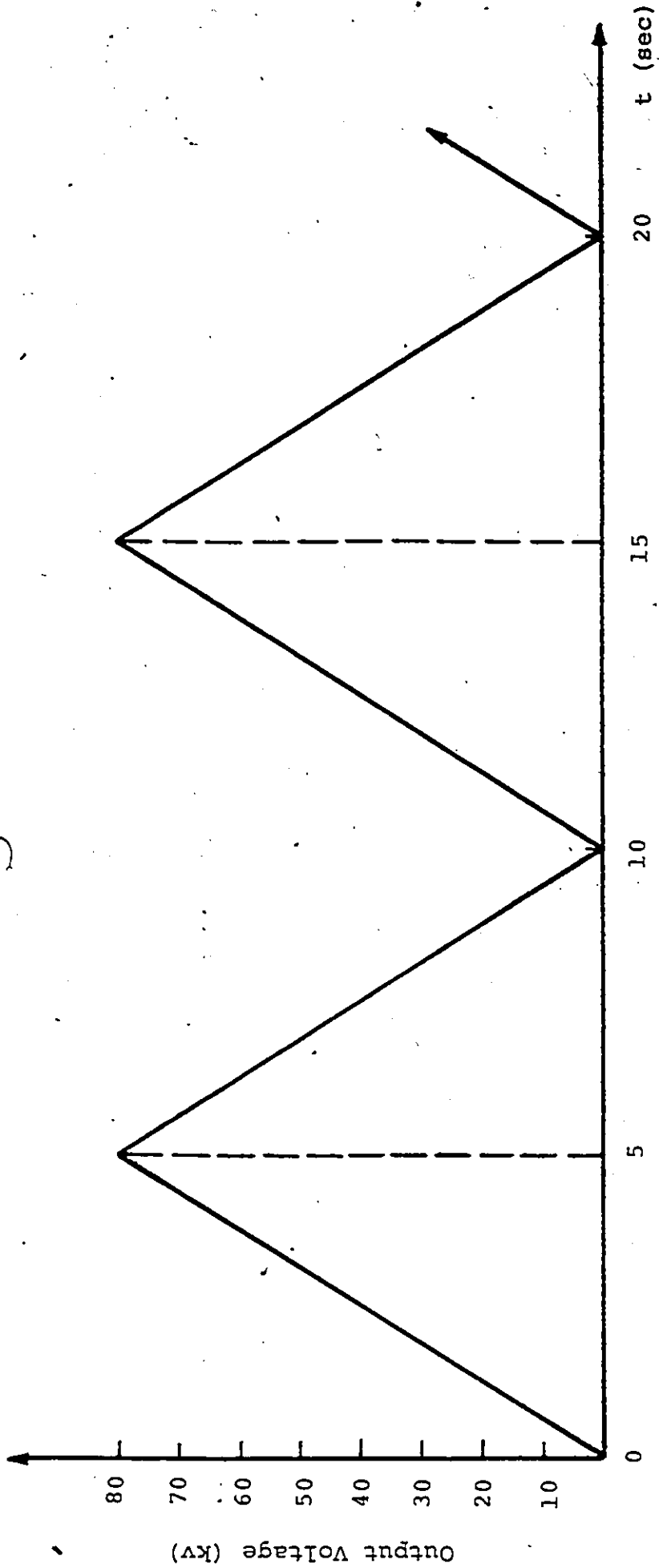
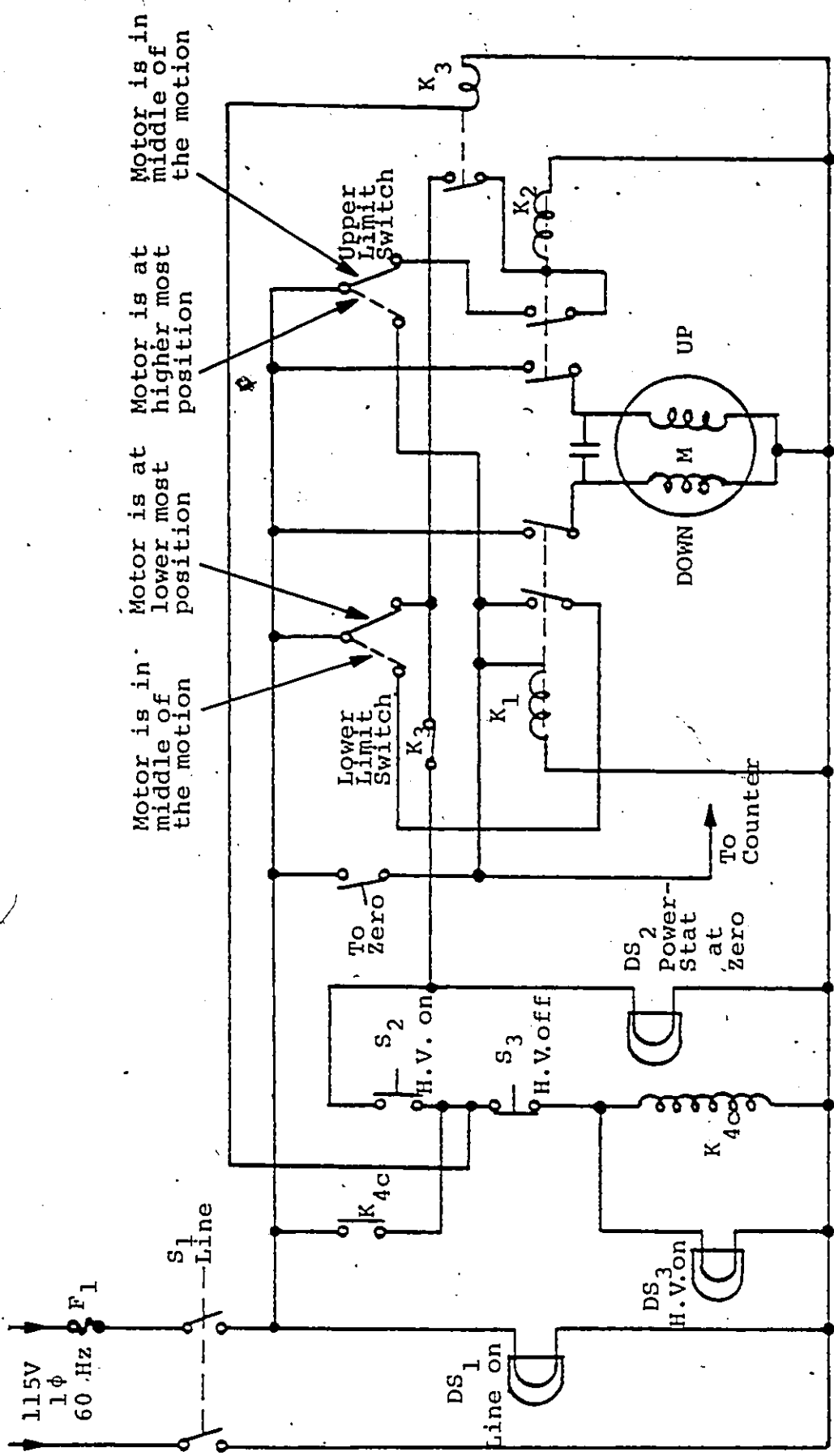


Figure 3.2: Wave Shape of Output Voltage of the Ramp Generator



Motor is in middle of the motion

Motor is at lower most position

Motor is at higher most position

Motor is in middle of the motion

Figure 3.3: Motorized Variac Switching Circuit

switch S_2 will energize the winding of K_4 , the contactor in the main line. Closing these contacts will apply power to the variable autotransformer and the winding K_3 . The "HIGH VOLTAGE ON" (DS_3) indicator will light, the contacts of K_3 will apply power to the raise winding of the servomotor through the contacts of K_2 . The contactor K_2 will stay energized through the upper limit switch. While the relay K_2 remains energized, the output voltage linearly increases with time until it reaches its maximum value, preset by a manual variac, in 5 seconds. The output voltage linearly decreases to zero, in an interval of 5 seconds, when the relay K_1 automatically is energized. The main contactor K_4 will stay energized through its own contact which bypasses the momentary high voltage on switch S_2 . The contact on K_4 will drop out if the power is interrupted to the winding of K_4 by depressing the momentary "HIGH VOLTAGE OFF" switch S_3 . The linearity of the ramp voltage (both rising and lowering) was checked out by a cathode ray oscilloscope. The slope of the ramp voltage can be changed by changing the value of the adjustable output voltage through the manual variac, because the time interval of the voltage rise is fixed. The powerstat motor drive assembly has a zero-start interlock, with a control panel light indicating the zero position.

The high voltage D.C. power supply used was from Del Electronics Corporation and consisted of two separate subassemblies; a PSO-80-5-9 power supply tank and an RM6 control panel. The output voltage of the model PSO-80-5-9

high voltage D.C. generator was continuously variable from zero to rated Maximum DC of the output voltage, 80 Kv, when operated from a 115V, 60 HZ, single phase source. The variations in this voltage due to ripple and regulation were within 0.5% of the output voltage for output currents from 0-5 ma, the maximum available DC output current. It featured reversible output polarity. The RM6 control panel contained an electrically controlled voltage and current overload protection, could be set and reset over the full range from 0-120% of fully rated output voltage and current with front panel indication. The high voltage output of the unit was automatically de-energized when the output voltage or current exceeded these settings. For the reason of safety the unit had zero-start interlock which withheld AC input from the high voltage transformer unless high voltage output control had been returned to zero. An automatic shorting solenoid also discharged the energy stored in the output capacitor, through a 2 M Ω bleeder resistor, immediately on shutdown. The control is mounted on a standard rack type panel 17.5 in. high. The high voltage supply is mounted in a metal frame support and immersed in a tank filled with a high grade insulating oil. A good external ground was connected to the case of the power supply. The high voltage bushing of the test vessel was connected to the high voltage DC generator with a shielding polyethylene output cable supplied by the manufacturer.

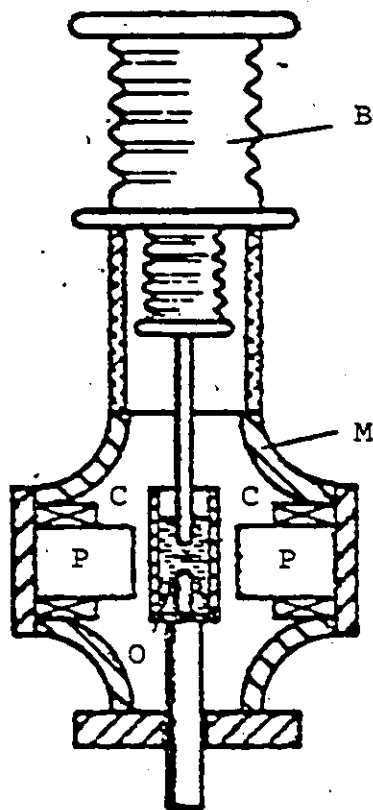
The output voltage of the generator (the gap voltage) was measured with a resistive voltage divider coupled to a

digital voltmeter. The divider ratio was calibrated with an electrostatic voltmeter accurate to $\pm 0.5\%$ of the applied voltage, at voltages below 50 Kv, and with a 15 cm sphere diameter and 1.8 cm to 2.8 cm spacings in the voltage range from 50 Kv to 80 Kv. The calibration assured an accuracy in the measurement of the applied voltage of within $\pm 2\%$ (Kuffel, 1970) for the range of voltage applied throughout the experimental work.

3.2 The Test Chamber

A sectional view of the test chamber used in the experimental work is illustrated in Fig. (3.4). The internal diameter, height, and the thickness of the cylindrical plexiglass wall of the test vessel was 5.7 cm, 8.9 cm, and 0.5 cm respectively. These dimensions were large relative to the electrode spacings used, and therefore it was not expected that the vessel would have any extraneous effect on the prebreakdown between the electrodes. The base plate of the vessel was also of plexiglass material.

The electrodes were attached to two 1.25 cm diameter connecting rods. The upper rod passed through a 75 Kv Corona-free bushing and the negative electrode protruded from the base plate. Electrodes were supported in the liquid in such a way that their spacing could be controlled from outside the container. The lower rod can be displaced vertically using a threading arrangement. A micrometer gauge at the bottom of the base plate indicated the vertical displacement with a precision of 0.01 mm. The cylindrical



- B - 75 kV corona free bushing
- C - Magnetic excitation coils
- M - Cast steel magnetic yoke and outer chamber
- O - Silicone oil, vessel and test electrodes
- P - Polepieces

Figure 3.4: Sectional View of Test Chamber

electrodes having hemispherical tips were 1.6 cm long and of 1.25 cm diameter for all the experiments. The electrodes which screwed onto the electrode shafts in each group were of Al, Cu, Mg and Zn material.

Before each test series, the surface of the electrodes was polished mechanically with 600, 800 and 1,000 grade silicon carbide powder. When the surface was free of visible scratches, it was cleaned with a clean mop and finally washed with acetone in an ultra sonic vibrator to remove the contamination of the surface by polishing materials. To remove any remaining amounts of the acetone and to soak the surface oxide layer on the electrode so that to avoid having a composite dielectric, the electrodes were finally immersed in a boiling silicone oil.

The dielectric test liquid was vacuum filtered through a 2.0-2.5 micron size filter to remove fine solid particles.

The electrode spacing was adjusted by first carefully raising the lower electrode until contact between the two electrodes was attained, as indicated by an ohmmeter. The electrode spacing was then set by rotating the lower connecting rod for the required number of revolutions, to raise the lower electrode. Errors in the gap setting introduced by the tolerance limitations of the thread were negligible.

3.3 Current Measurement Circuitry

The dielectric prebreakdown current measurements have been made using ramp voltage up to 64 Kv, a digital electrometer, Keithley type model 616, inserted in series with the

test gap. The Model 616 Digital Electrometer was an automatic ranging multi-purpose DC measuring tool featuring sensitivity to $10 \mu\text{V}$ per digit. It provides 0.2% voltage accuracy for a wide range of measurements all with the convenience of automatic polarity and decimal points. The Model 616 was essentially a digital multimeter, optimized for measurements from high source impedance, which provides wide range capability when measuring current, resistance, and charge in addition to voltage. The Model 616 was Keithley's most accurate, versatile digital electrometer which provided all the needed precision and wide range required in a laboratory.

With an input resistance greater than 2×10^{14} ohms and offset current lower than 5×10^{-15} A at the input, the Model 616 accurately measures voltage over a wide range of source resistance with negligible error. As a current detector, the electrometer was capable of measuring DC currents of magnitude ranging from 10^{-15} A to 2^{mA} maximum. The prebreakdown current of the dielectric liquid was measured by passing it from the cathode through a high stability resistor ($24 \times 10^6 \Omega$) and protection circuit connected to the electrometer circuit. Currents down to 10^{-9} A could be measured. If any solid particles were observed to collect on the electrodes the liquid was replaced with a visibly clear sample. The presence of a particle during an experiment is usually detected by large fluctuations in the current.

Current measurements can be made by one of two methods:

1) Normal Mode When the FAST/NORMAL switch is set to NORMAL, the Model 616 operates as a shunt-type pico-ammeter in which a resistor is connected directly across the input terminals. The Model 616 measures the voltage drop across the shunt resistors where $V_{IN} = I_{IN} \times R_S$. This method of measurement is typical of most multi-meter current measuring techniques.

2) Fast Mode (Useable for currents from 10^{-5} A and smaller). In this mode (which was used in the experiments) the Model 616 measures very small currents with fast response. When the FAST/NORMAL switch is set to FAST, the Model 616 operates as a feedback-type pico-ammeter in which the current flows through the feedback resistor of the voltage amplifier. The Model 616 indicates the voltage developed across the range resistor where $V_F = I_{IN} \times R_F$. This method of measurement provides fast response since the slowing effect of the input capacitance from lengthy cable is diminished. (The specifications of the electrometer, Model 616, are given in Appendix I).

A divider 10/1 across the Model 616 output receptacle was used as shown in Fig. (3.5). For the purpose of protecting the electrometer, used in the prebreakdown current measurement of the liquid samples, from excessive current resulting from a breakdown of the test spacing, a paper gap which fires at 500 V.C.C., a gas filled surge arrester operating at 90 V.D.C. and back to back Zener diodes operating at 10V, all of which were tested by a curve tracer, were included in

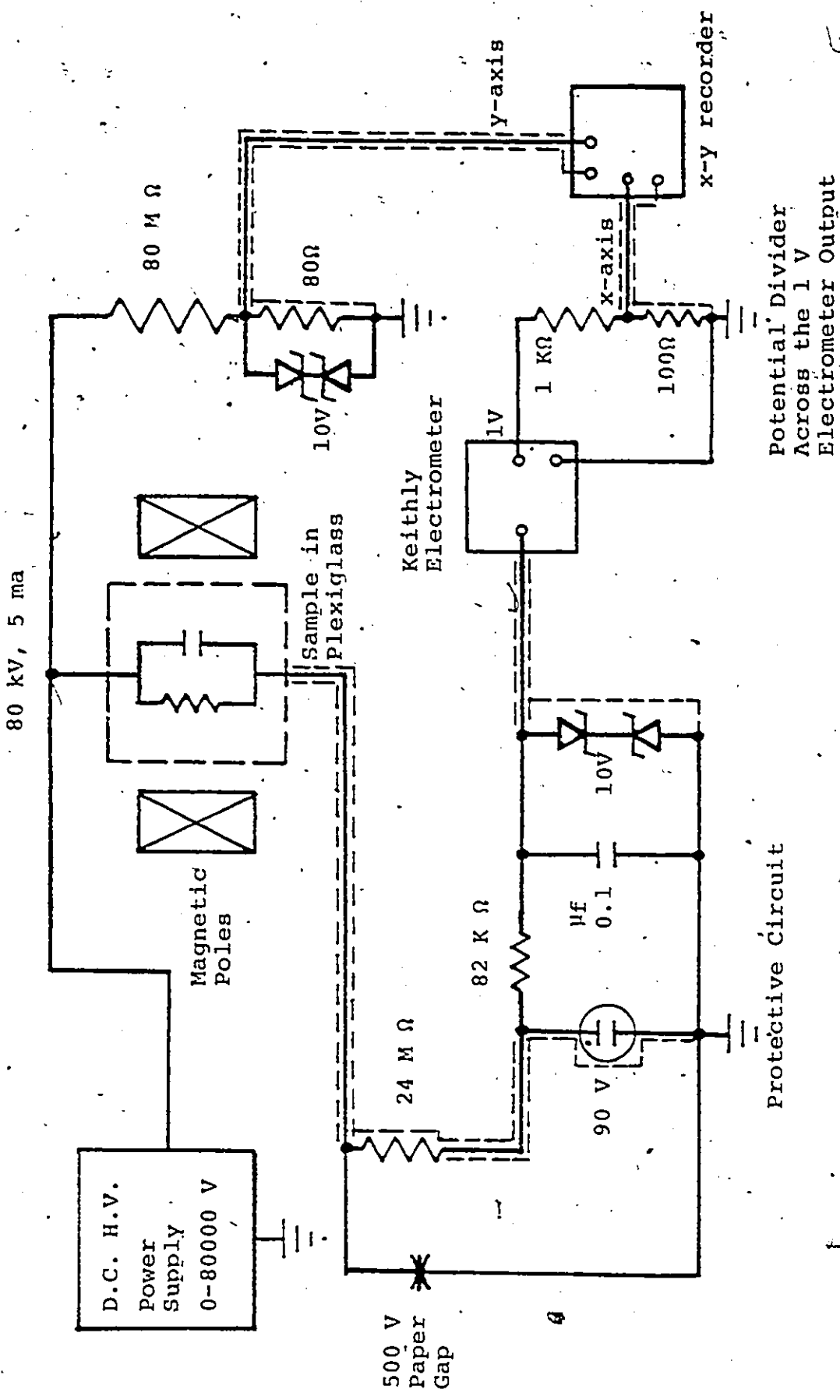


Figure 3.5: General Schematic Diagram of Measuring Circuitry

the circuit. Current measurements with and without protection circuit, under the same conditions, showed no effect of the protection circuit on the values of the measured currents.

3.4 The x-y Recorder

The x-y recorder used was the Model 99.414 variplotter (115 V.A.C., 60 HZ, 1 ϕ , 115 watts). It is a self-balancing potentiometer recorder which plots one variable D.C. voltage as a function of a second variable D.C. voltage. One variable is applied to the arm servomechanism which controls the arm movement along the x-axis (abscissa); the other variable is applied to the pen servomechanism which controls the pen movement along the y-axis (ordinate). The combination of the two motions generates a plot of x versus y. The data is plotted as a continuous inked line on standard 11" x 17" graph paper (10" x 15" plotting area) held on the vinyl covered plotting surface by a vacuum system. Separate parallax and stepped scale controls for the pen arm servo systems permit the presentation of the x and y 0-0 point at any desired location on the plotting surface, and the expansion of the input signal for maximum deflection of the pen and arm respectively.

The pen and arm servo input units accept plug-in sensitivity networks which provide for the acceptance of a greater range of input data signals than would otherwise be possible. A high sensitivity set namely 0.01 volts per inch was used for the pen and arm servo systems in the experiments. One of the two inputs to the recorder was

obtained from the gap voltage via a resistive potential divider ($80\text{ M}\Omega$ and 80Ω). The other input was from the 1 volt analog output of the electrometer. The static accuracy of pen and arm is 0.075%.

3.5 The Magnet Supply Circuit

As shown in Fig. (3.6), the magnetic circuit consists of an AC supply, fed through an isolation transformer (115V, 500 VA, 50/60 HZ), varying from 0 to 140 V, by a variable autotransformer (I.V. 120, out V. 0-140, A 4.5, 0.63 KVA, 50/60 HZ, 1 ϕ), rectified into DC, through a bridge rectifier, a DC ammeter, and two parallel coils (32Ω , 188 mH) connected in series with the other components. The magnetic coils are wound on iron cores to concentrate and increase the magnetic field. The DC current can vary from zero to 4.5 amperes as the variable autotransformer changes. The corresponding transverse DC magnetic field between the pole pieces varies in the range of 0 to 900 gauss (1,800 gauss for series cumulative combination). DC polarity is preserved so as not to lose direction information when tracing and plotting fields. When coils were in parallel cumulative combination, the magnetic flux density was measured at various distances within the effective area between the poles (4" spacing), the North pole being the reference. Each curve of Fig. (3.7) represents an average of six observations taken at the selected points as mentioned earlier. In the active region between the electrodes an approximately uniform transverse magnetic flux density up to 900 gauss (1,800 gauss in series coil

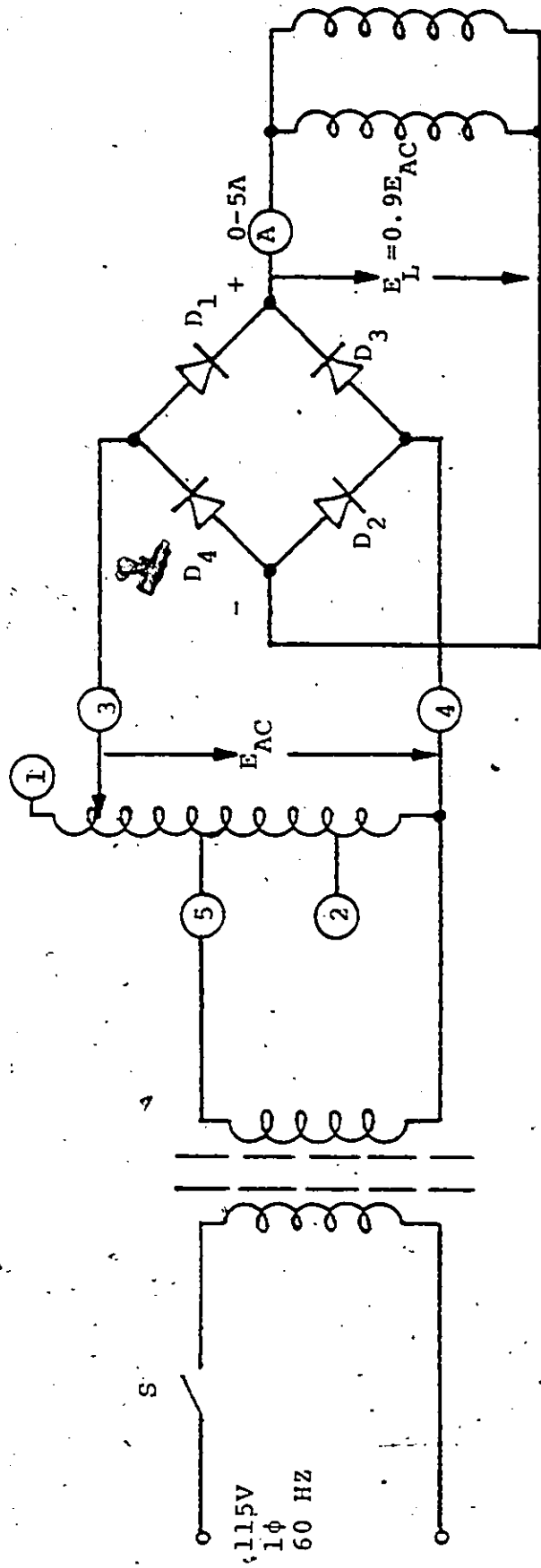


Figure 3.6: Magnetic Circuit Diagram

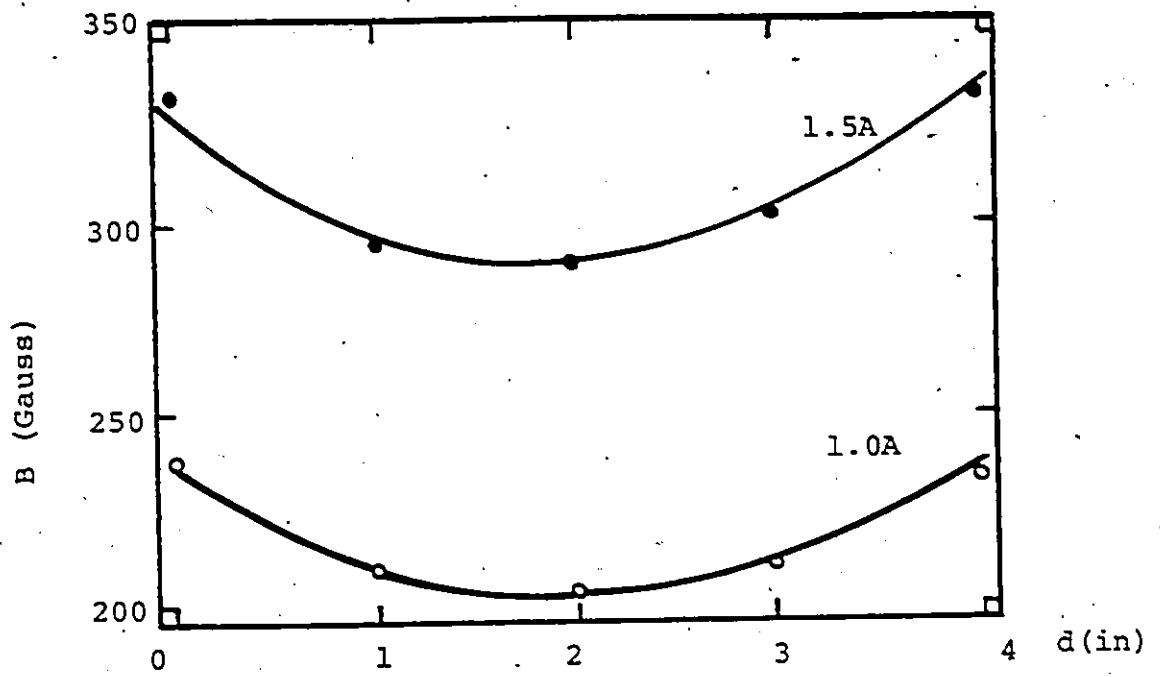


Figure 3.7: Variations of Flux Density Between the Magnetic Poles

combination) could be maintained and can be measured by a Gaussmeter instrument.

The Gaussmeter used to measure magnetic field was the Model 1890 Radio Frequency Lab Inc. (115/230 volts, 50/60 cps., output 18 volts DC at 18 mA). It was a precision magnetic flux measuring tool for making direct measurements of gap flux density in normal or axial fields from 0.1 to over 20,000 gauss. A basic 1,000 gauss HB 9272 permanent reference magnet with $\pm 0.75\%$ accuracy, was provided for calibrating a HB 15950 (0.039" thick x 3/64" x 1" long) flat probe to full scale in transverse field measurements. The accuracy of the Gaussmeter was $\pm 1\%$ plus accuracy of the reference magnet.

IV. EXPERIMENTAL PROCEDURES AND RESULTS

4.1 Breakdown Voltage

All the oil used in experiments was filtered (vacuum filtration) through a 2.0-2.5 micron size filter, and the electrodes were polished with 600, 800 and 1,000 grade silicon carbide, and fine emery cloth, followed by cleaning with acetone (to remove the contamination of the surface by the polishing materials). The breakdown voltage was determined for electrode spacings of $r/2$, r , $3r/2$, $2r$, and $5r/2$ (where r is the radius of the hemispherically tipped electrode and equal to 6.2 mm) with no applied magnetic field. Different electrode materials (Al, Cu, Mg, and Zn) and oils ($5^{\text{C.S.}}$, $350^{\text{C.S.}}$ and $1,000^{\text{C.S.}}$) were used, i.e., four electrode materials, five electrode spacings, and three oil viscosities, therefore, requiring sixty breakdown measurements. The procedure for obtaining the breakdown voltage was as follows:

The gap was set at a required spacing. The electrodes were completely immersed in the silicone dielectric liquid, the volume of which throughout the experiments was approximately constant and equal to three-quarter of the test cell volume. The applied voltage was ramped up and down ten times starting with an upper limit of 5 kv and then the maximum level was increased in 5 kv steps until breakdown was obtained. Once breakdown had occurred, ramping was discontinued for that configuration. It has to be noted that only three breakdowns for each combination of electrode, electrode spacing, and oil

type was obtained. After each breakdown the oil was changed and a freshly prepared electrode was used.

The average breakdown values for each electrode spacing in the vessel filled with silicone oil are shown in Table 1.

From Table 1 it can be seen that aluminium and magnesium maintain a relatively higher breakdown voltage than the copper and zinc.

4.2 V-I Plot

For each combination of electrode, spacing and oil type, an initial conditioning procedure was followed (in a manner similar to the one described by Girgis [59]) by establishing the maximum voltage swing at 5 kv and ramping up and down 15 times. This was repeated in 5 kv steps up to a voltage level V which was 5 kv lower than the breakdown voltage previously measured. At any specific voltage, 15 consecutive V-I plots were superimposed on the same graph paper. The configuration was then subjected to 50 further ramping cycles at the same voltage without recording V-I data.

The above procedure was carried out four times, i.e. four sets of 15 superimposed data plots were made with 50 cycle intervals in each case without record as explained in Fig. (4.1). The data recorded in these blocks was referred to as series 1, 2, 3, and 4 respectively.

From Fig. (4.1) one can see that 210 complete cycles were performed corresponding to $r/2 = 3.1$ mm electrode spacing. The results were recorded only as indicated in the diagram by series 1, 2, 3, and 4. The first set of recordings

Table 4.1 Breakdown Voltage in KV as a Function
of Electrode Spacing

OIL c.s.	d mm	Zn	Cu	Al	Mg
5	3.1	52	53	57	57
350		56	58	62	61
1000		58	61	63	64
5	6.2	61	64	67	66
350		*	*	*	*
1000		*	*	*	*
5	9.3	66	68	69	69
350		*	*	*	*
1000		*	*	*	*
5	12.4				
350	&	*	*	*	*
1000	15.5				

* - Breakdown limited at 70 KV by factors other than
oil breakdown.

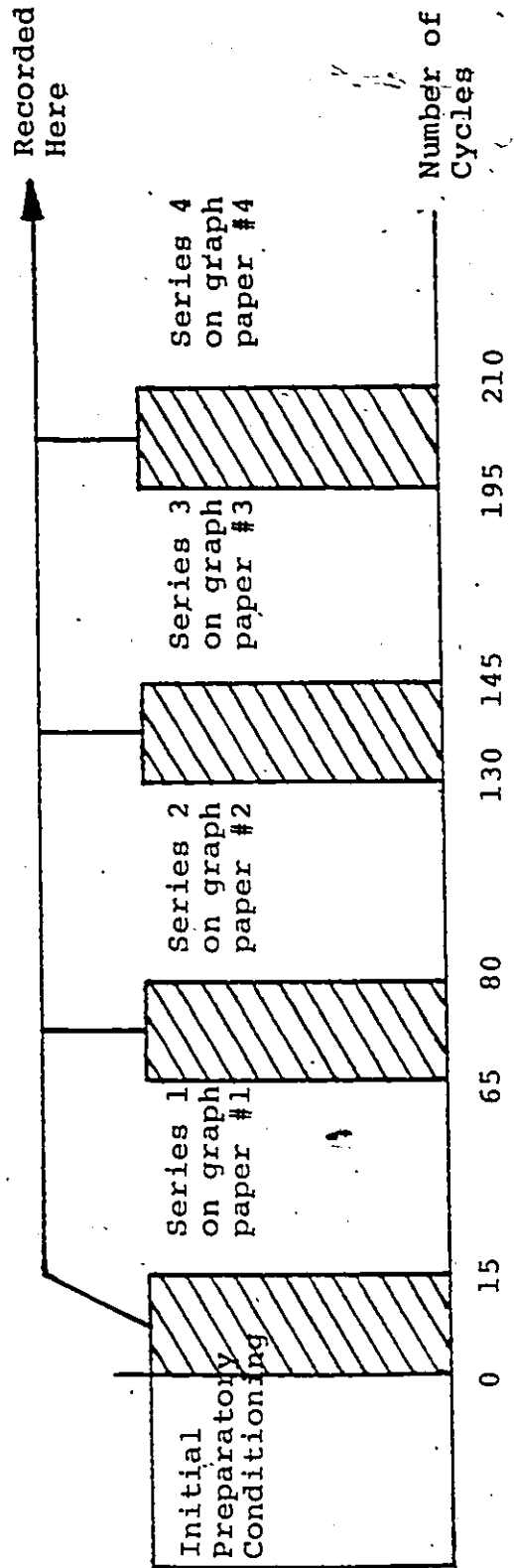


Figure 4.1: Experimental Procedure for Fixed Electrode Spacing

permitted estimation of the statistical scattering of the data due to short term stress conditioning. The second to the fourth sets of 15 recordings permitted an estimate to be made of reproducibility over longer intervals of stress conditioning. This procedure was carried out for five different electrode spacings varying from 0.5 r to 2.5 r in 0.5 r intervals, and another set of recorded measurements corresponding to each of these electrode spacings was obtained.

4.3 Magnetic Field

The complete procedure described in the preceding section was carried out for all electrodes and spacings and for one oil type (350^{C.S.}) in the presence of an applied transverse magnetic flux density of 2×10^{-2} Tesla (200 gauss) in the active region between the electrodes.

The two preceding steps have been used to demonstrate the role played by the electrode spacing, viscosity, surface layer of oxide of different electrode material, as well as of a transverse magnetic field on prebreakdown current of silicone liquid.

4.4 Additional Observations

1. All experiments were conducted at room temperature and atmospheric pressure, with a relative humidity of 55% over most of the period of the experiments.

2. Sometimes, when the spacing was of the order of 0.5r, after a few cycles of ramp application, small suspended particles started oscillating between the electrodes, in the

rising ramp, and developed too early into a complete breakdown.

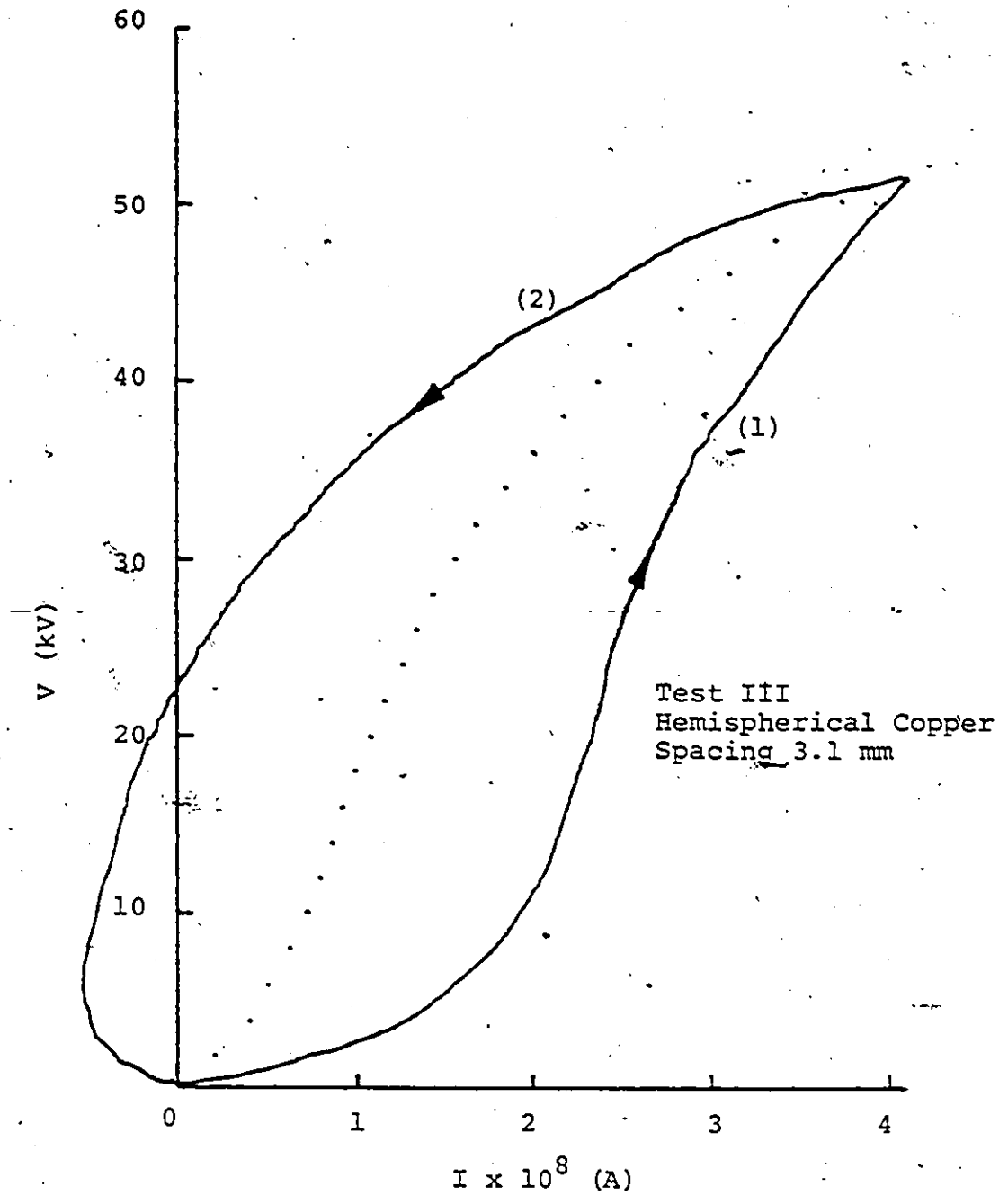
3. In most cases, strong electric fields produced some motion which was observed as a local rise in level of the liquid around the region of highest field intensity. In the case of low viscosity liquid, 5^{c.s.}, disruptive sprays of dielectric liquid in intense fields were moreover commonly observed.

4.5 Experimental Results

From the x-y recorder, the prebreakdown voltage versus current characteristics of the liquid were obtained for each set of 15 complete cycles.

When the voltage applied to a liquid sample is a ramp function the resulting current consists of two components one of which is displacement current, due to charging and discharging of the capacitance of the equipment, and the other is current passing through the test volume. Charge may move through the volume by conduction or convection but the term "conduction" current will be used to describe it from now on.

A copy of the recorded V-I characteristics is presented in Fig. (4.2) for fifteen successive cycles, showing the reproducibility of the data. The loop appears because the displacement current adds to the "conduction" component when dv/dt is positive, curve (1), but it is subtracted from it when the voltage ramp is reversed, curve (2). In order to extract the "conduction" component from the data given in Fig. (4.2), it was only necessary to plot the average current



(1) Voltage rising; (2) voltage falling.

Dotted points represent average of the curves (1) and (2).

Figure 4.2: Voltage Versus Current Characteristics for Fifteen Consecutive Stress Cycles with Copper Electrodes in 5C.S. Silicone Oil

for any particular applied voltage (dotted points in Fig. (4.2)). The method of separation can be illustrated from the following two equations:

$$I_1 = I_c + I_d \quad \dots 4.1$$

$$I_2 = I_c - I_d \quad \dots 4.2$$

Where,

I_1 = the total current when the voltage increases

I_2 = the total current when the voltage decreases

I_c = the "conduction" current

I_d = the "displacement" current

By adding the equations (4.1) and (4.2) we obtain the following equation:

$$I_c = 1/2 (I_1 + I_2) \quad \dots 4.3$$

indicating that at any fixed voltage the "conduction" current, I_c , is the average value of the curves (1) and (2) of the Fig. (4.2) and should be caused by the movement of free electrons and ions.

A set of "conduction" current characteristics for a pair of copper electrodes is shown in Fig. (4.3). The curves give the relationship of the prebreakdown "conduction" current to the applied voltage for five values of electrode spacing and for 5^{C-S} silicone liquid. It will be seen that the well known general form of relationship between voltage and current exists. The V-I characteristics is divided into three typical

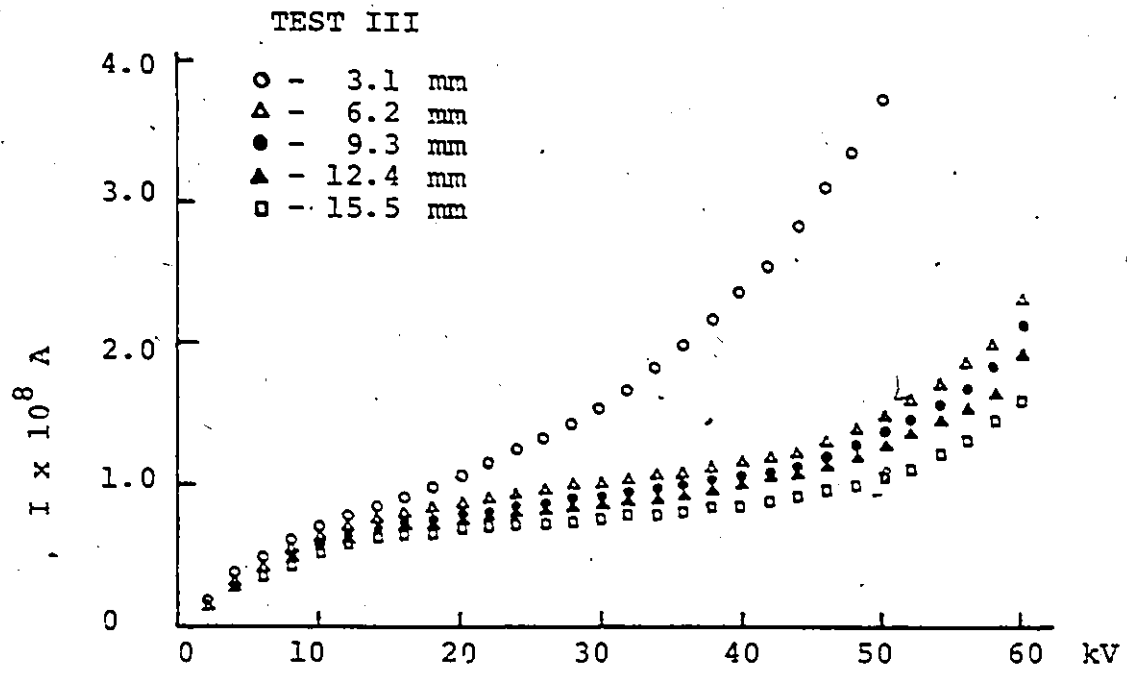


Figure 4.3: The Current-Voltage Characteristics for Copper Electrodes and 5C-S. Silicone Oil at Room Temperature and Ambient Humidity

regions designated as the low, intermediate, and the high field region, except that the saturation region is less marked. Over the entire stress range the curves remain distinctly defined for each electrode spacing. The plotted experimental results of Fig. (4.3), however, show that in the high field region current increases strongly with increasing voltage. It will also be seen that increase in the electrode spacing (3.1 mm to 15.5 mm), and hence in the volume of the oil, shows a significant decrease in the prebreakdown "conduction" current, with the electrode area kept constant.

Fig. (4.4) shows the experimental results obtained with oils of higher viscosity (filtered by vacuum filtration). The general shape of the curves is similar to that of Fig. (4.3) but shows that the current is slightly smaller than that of lower viscosity.

Fig. (4.5) indicates the dependence of the "conduction" current upon impurities. It can be seen that the prebreakdown current of silicone oil has a tendency to decrease when it is purified through filters of pore size of 2.0-2.5 micron.

The relationship of the "conduction" current to the applied voltage obtained for pairs of different electrode materials (Al, Cu, Mg, and Zn) in 5^{C.S.} silicone oil and 3.1 mm electrode spacing is shown in Fig. (4.6). The general shape of the curves in Fig. (4.6) is similar to that of Fig. (4.3). The relationship between prebreakdown "conduction" current values and applied voltage for different electrode materials is shown in Figs. (4.7-4.8) for 350^{C.S.} and 1,000^{C.S.} silicone

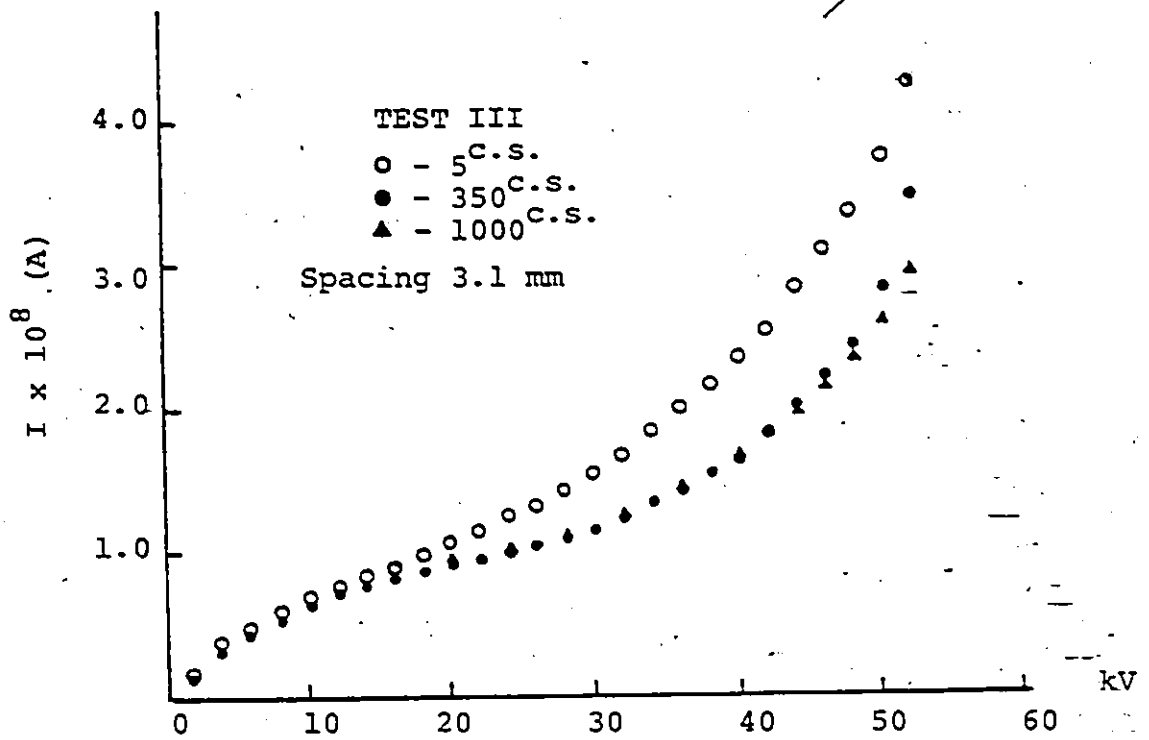


Figure 4.4: The Current-Voltage Characteristics, for Copper Electrodes with Different Viscosities at Room Temperature and Ambient Humidity .

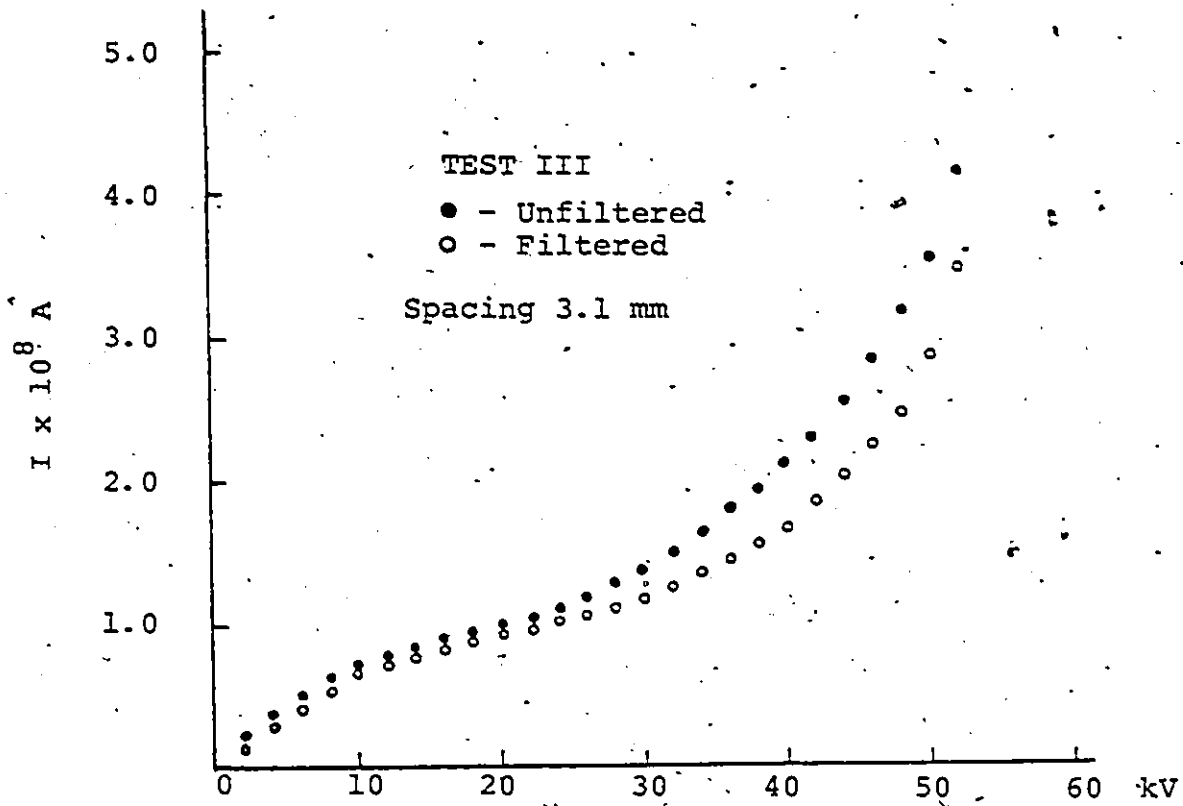


Figure 4.5: The Current-Voltage Characteristics for Hemispherical Copper Electrodes with 350^{c.s.} Silicone Oil, at Room Temperature and Ambient Humidity

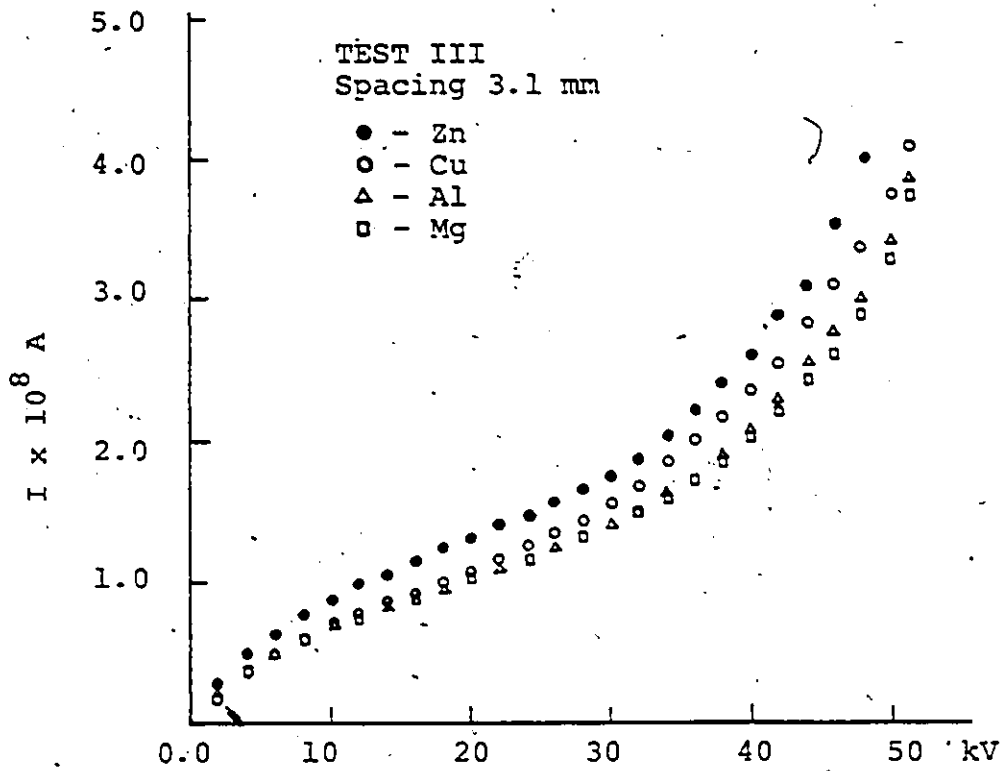


Figure 4.6: The Current - Voltage Characteristics (log-log) for Different Electrode Materials using 5^{C.S.} Silicone Oil at Room Temperature and Ambient Humidity

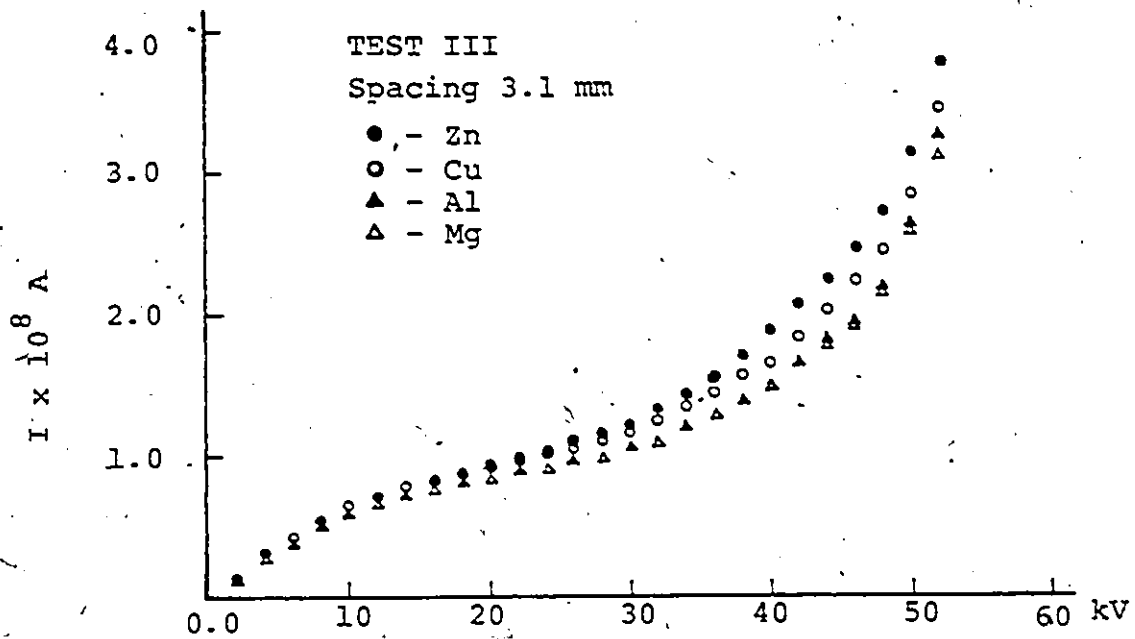


Figure 4.7: The Current-Voltage Characteristics (log-log) for Different Electrode Materials using 350°C-S Silicone Oil at Room Temperature and Ambient Humidity

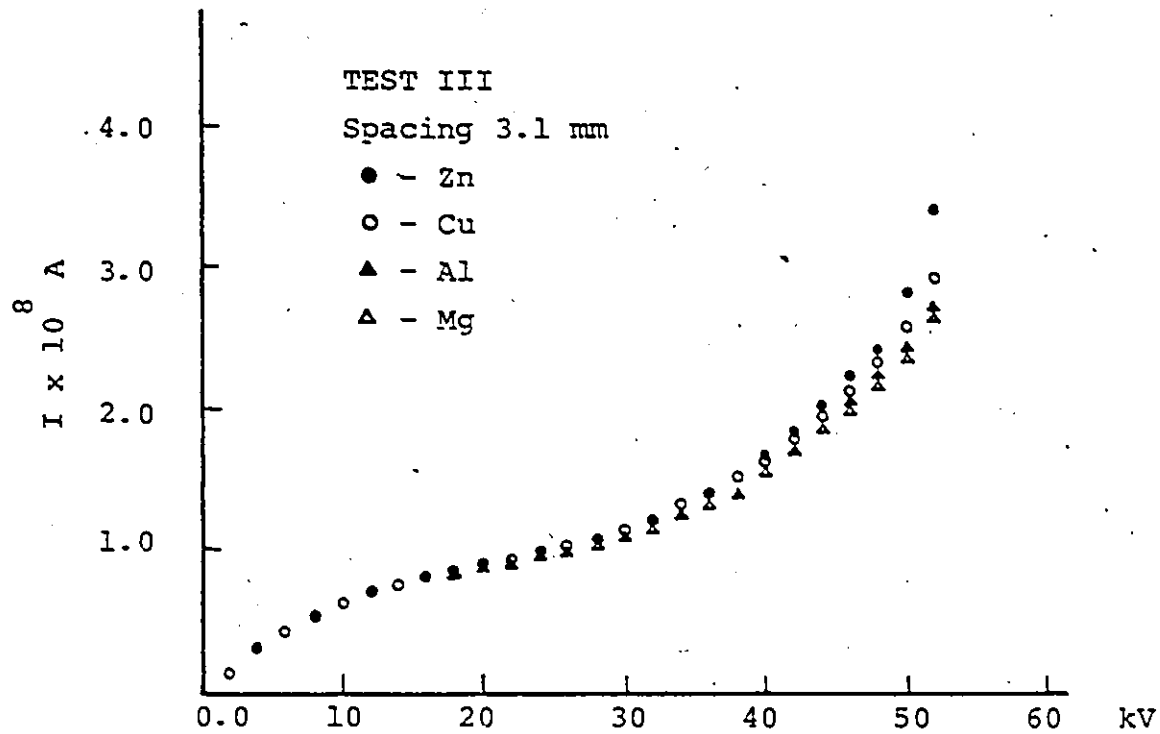


Figure 4.8: The Current-Voltage Characteristics (log-log) for Different Electrode Materials using 1000^{C-S} Silicone Oil at Room Temperature and Ambient Humidity

oil and 3.1 mm electrode spacing respectively. The ranking of the materials, in order of decreasing "conduction" current under ramp voltage conditions for a given spacing and conditioned electrodes is magnesium, aluminium, copper, and zinc, there being no significant difference between magnesium and aluminum.

For all three viscosities (5,350 and 1,000^{C.S.}) investigated the "conduction" current decreased with ramp application time, although, the time required for the current to reach its steady value varied from one viscosity to another and between samples of the same viscosity. Similar findings have been reported by other investigators [8]. Fig. (4.9) shows such an effect for copper electrodes and a 1,000^{C.S.} liquid sample.

Replotting the experimental "conduction" current versus the applied voltage on a log-log scale, as shown in Fig. (4.10) indicates a sharp division between the intermediate and high field region. This plot was made for five different electrode spacings varying from 0.5 r through to 2.5 r (with r being the radius of the tip of the electrode and equal to 6.2 mm) in 0.5 r intervals, oil viscosity (5^{C.S.}, 350^{C.S.}, and 1,000^{C.S.}) and electrode material (Al, Cu, Mg and Zn). The data showed in all cases, Figs. (4.101 - 4.1012), that there were low, intermediate, and a distinct and quite sharp division of the high field "conduction" regions.

It will be seen, in all cases, that $\log I_c$ varies linearly with $\log V$, i.e., $\log I_c = n \log V$. Since the data

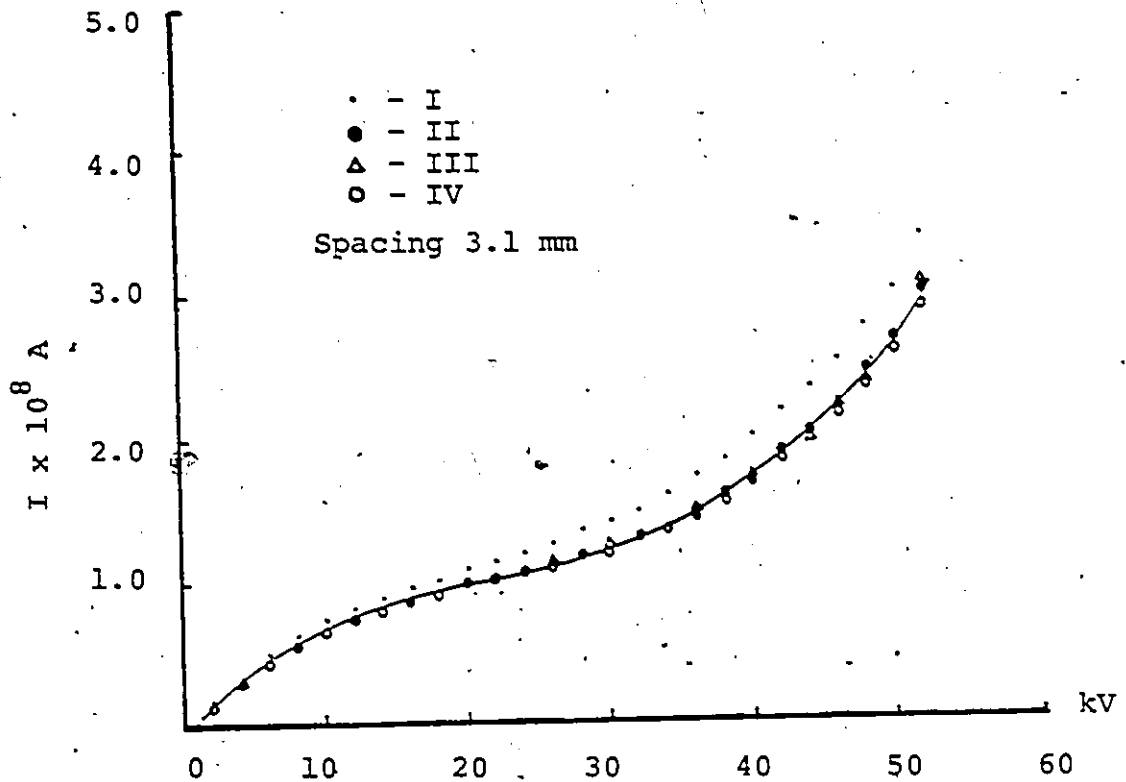


Figure 4.9: The Current-Voltage Characteristics for Copper Electrodes and 1000C.S. Silicone Oil for Different Number of Ramp Cycles

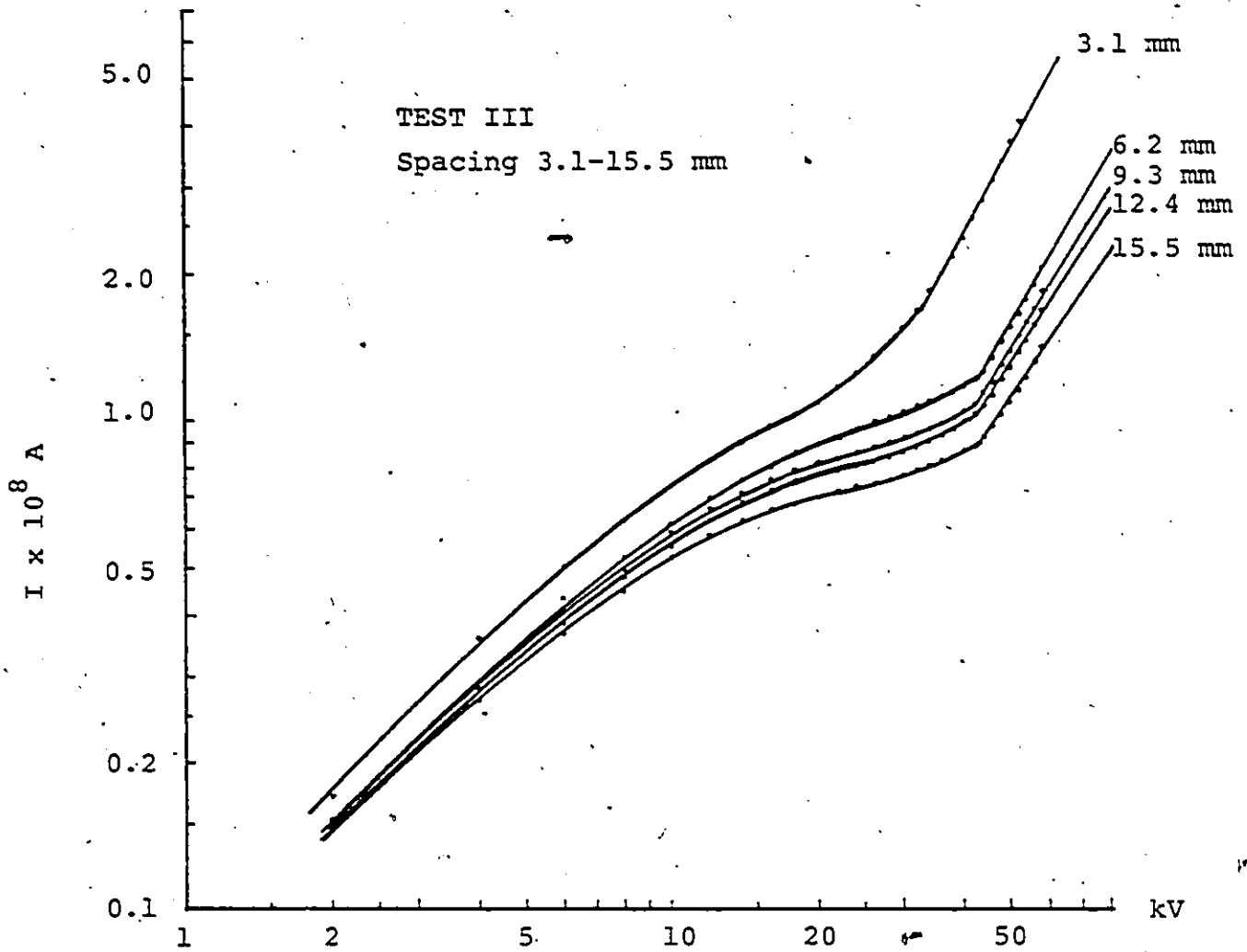


Figure 4.10.1: The Current-Voltage Characteristics (log-log) for Copper Electrodes and 5C-S. Silicone Oil at Room Temperature and 55% Relative Humidity

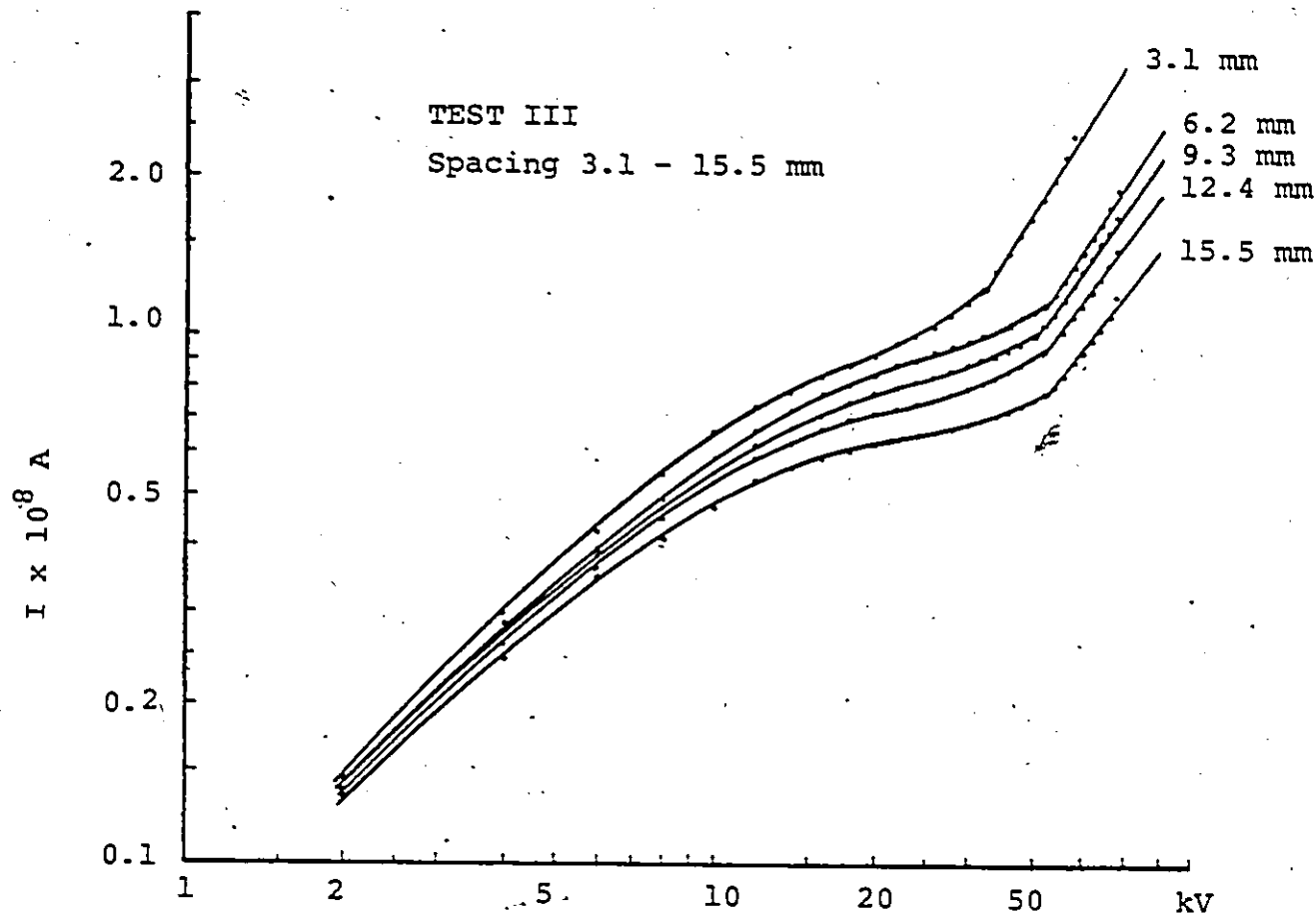


Figure 4.10.2: The Current-Voltage Characteristics (log-log) for Copper Electrodes and 350C.s. Silicone Oil at Room Temperature and 55% Relative Humidity

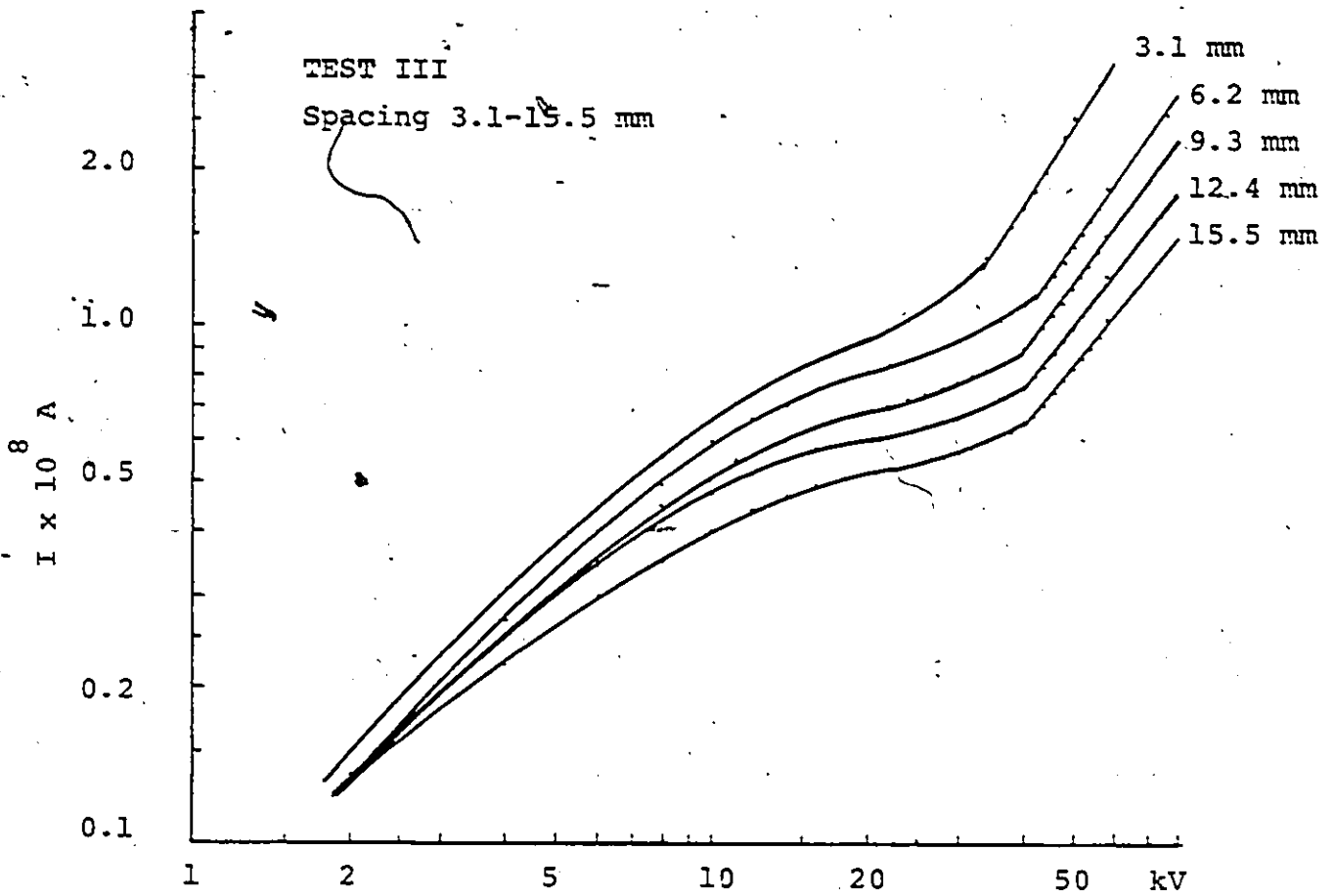


Figure 4.10.3: The Current-Voltage Characteristics (log-log) for Copper Electrodes and 1000C.S. Silicone Oil at Room Temperature and 55% Relative Humidity

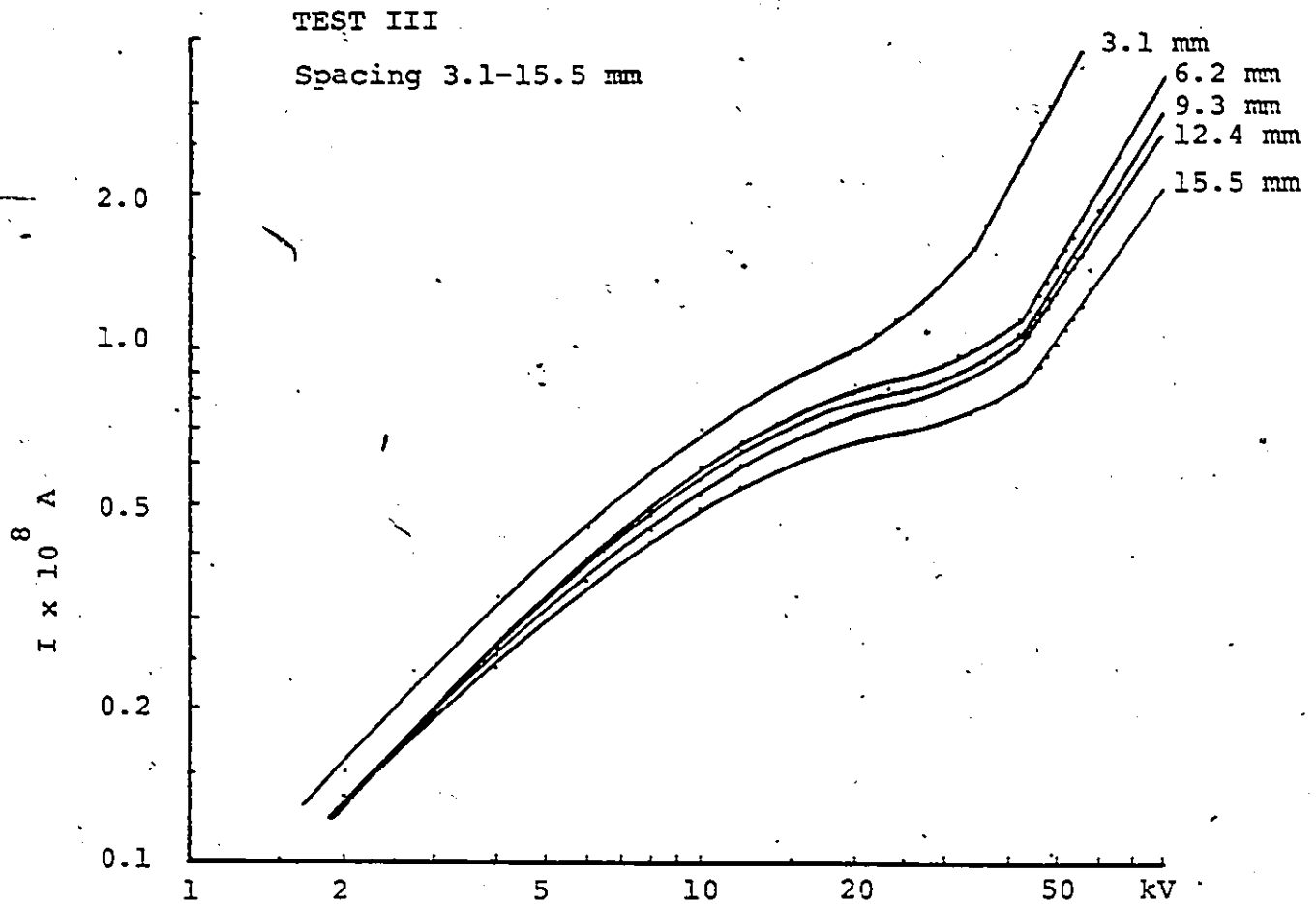


Figure 4.10.4: The Current-Voltage Characteristics (log-log) for Aluminum Electrodes and 5C-S. Silicone Oil at Room Temperature and 55% Relative Humidity

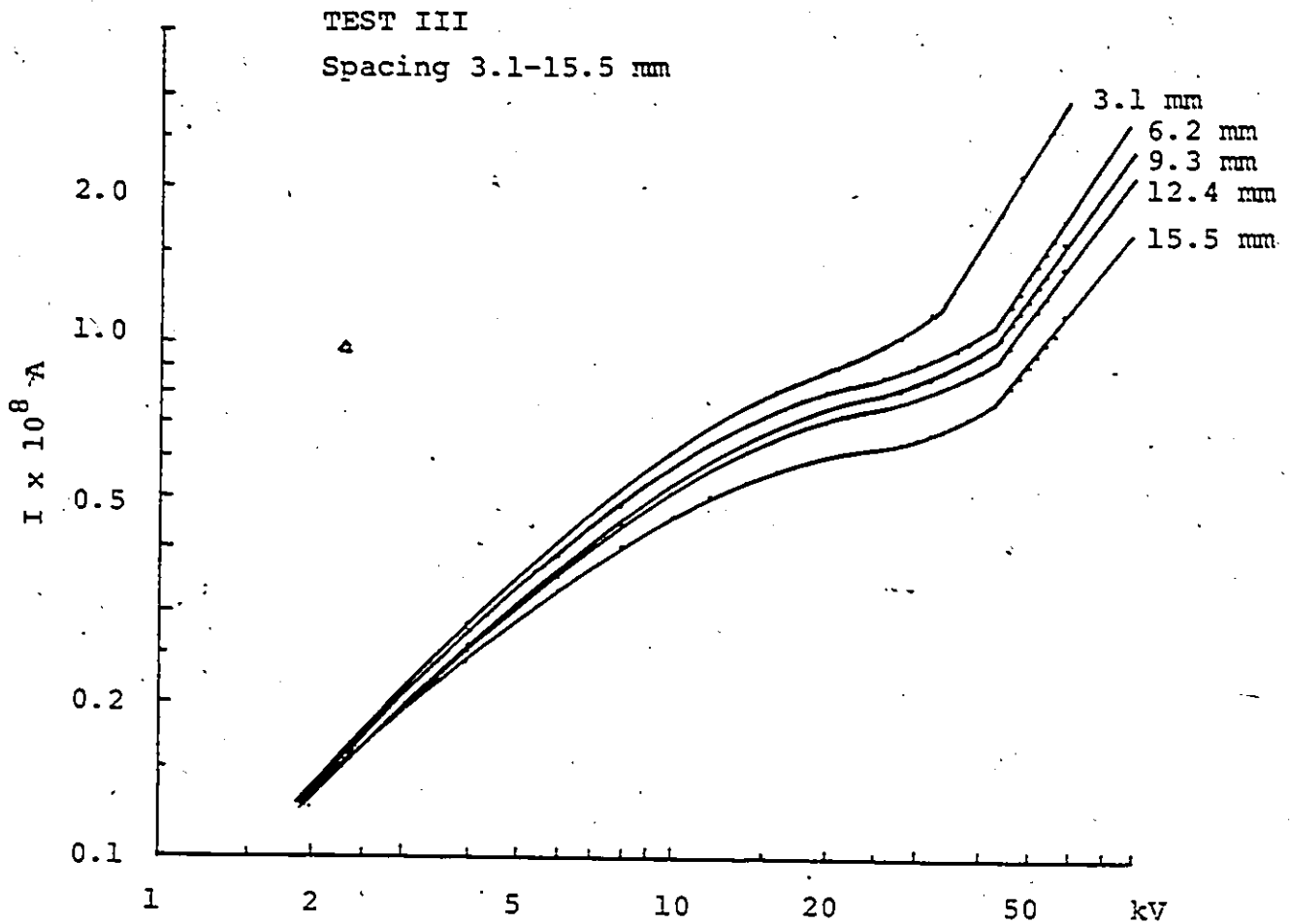


Figure 4.10.5: The Current-Voltage Characteristics (log-log) for Aluminum Electrodes and 350°C.S. Silicone Oil at Room Temperature and 55% Relative Humidity

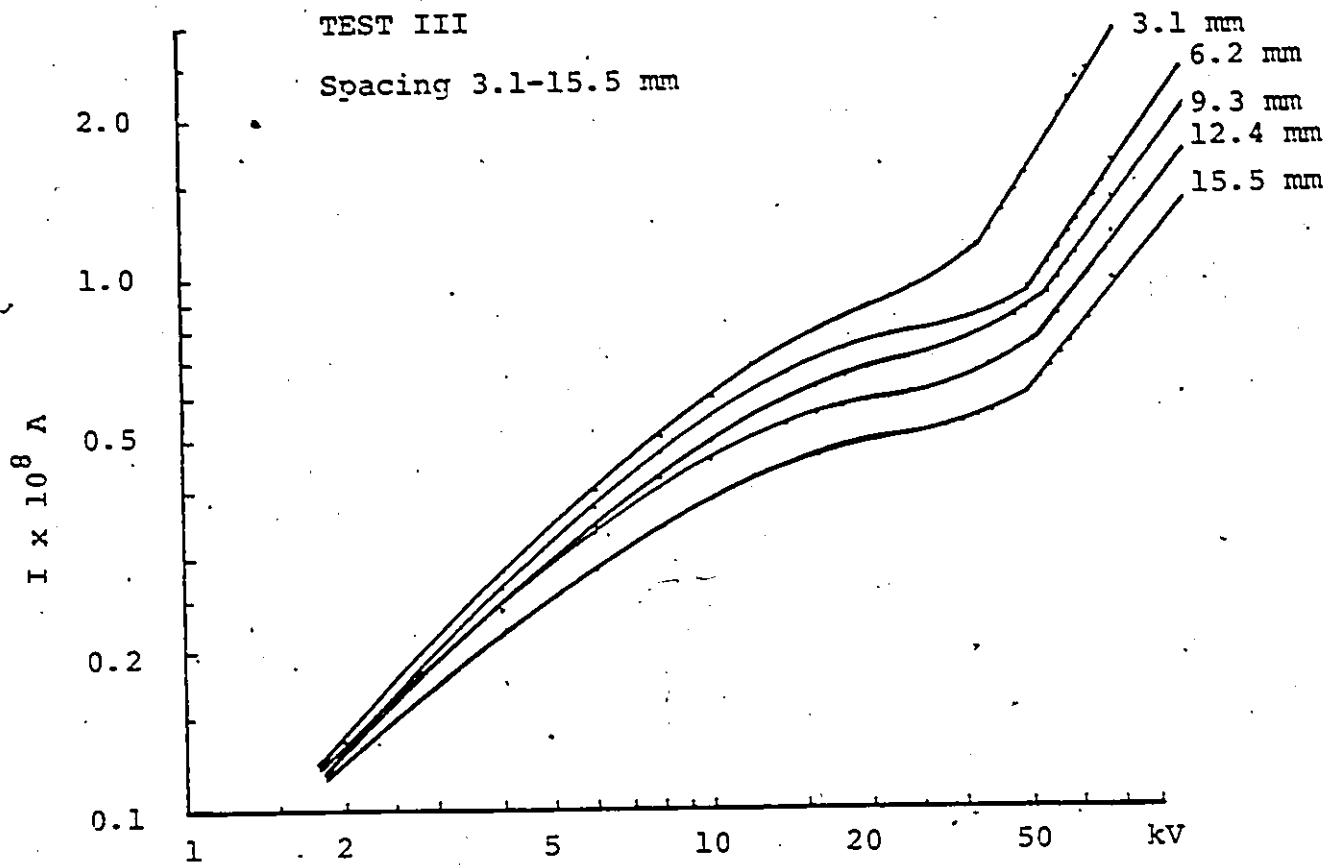


Figure 4.10.6: The Current-Voltage Characteristics (log-log) for Aluminum Electrodes and 1000C.S. Silicone Oil at Room Temperature and 55% Relative Humidity

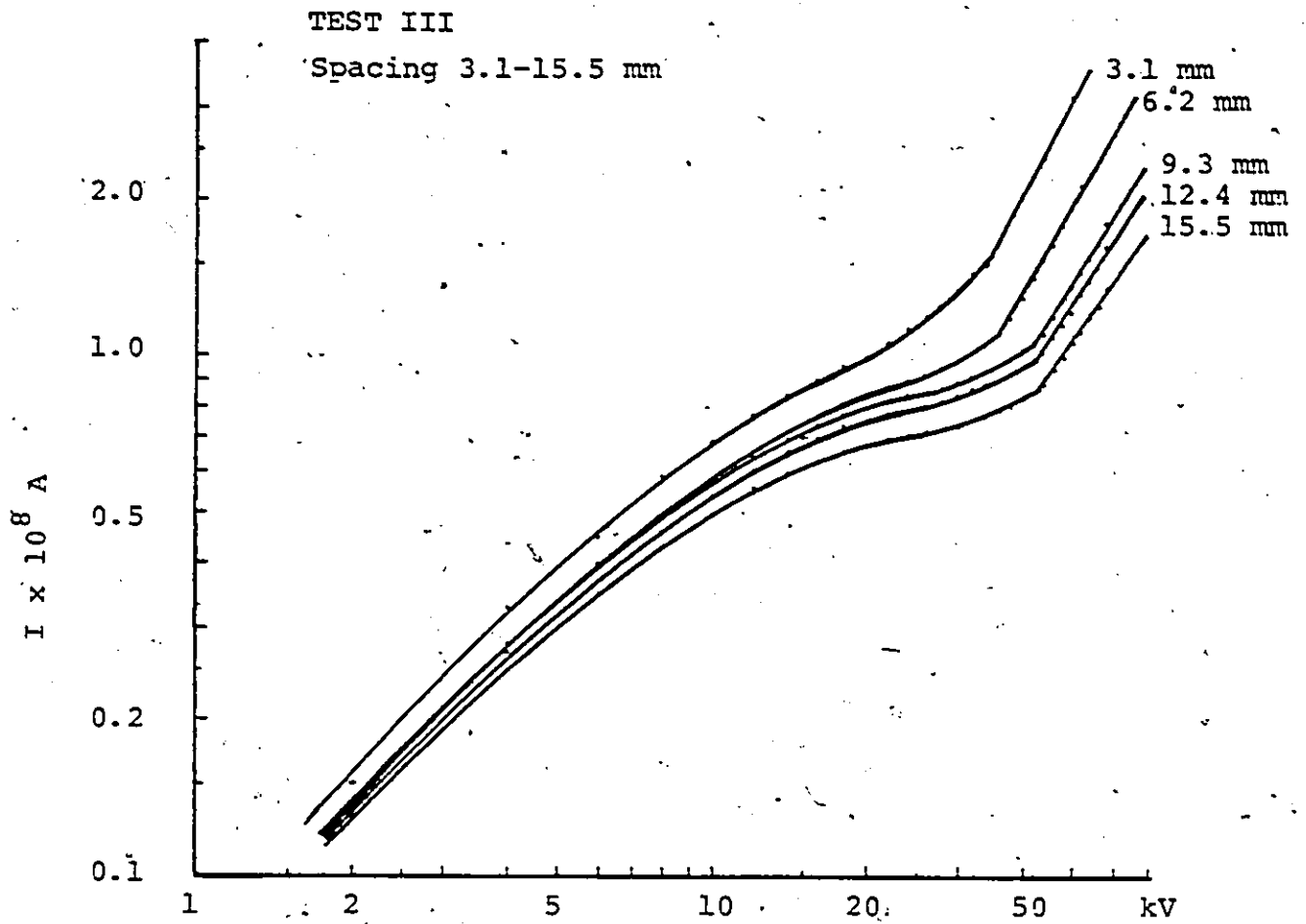


Figure 4.10.7: The Current-Voltage Characteristics (log-log) for Magnesium Electrodes and 5C-S. Silicone Oil at Room Temperature and 55% Relative Humidity

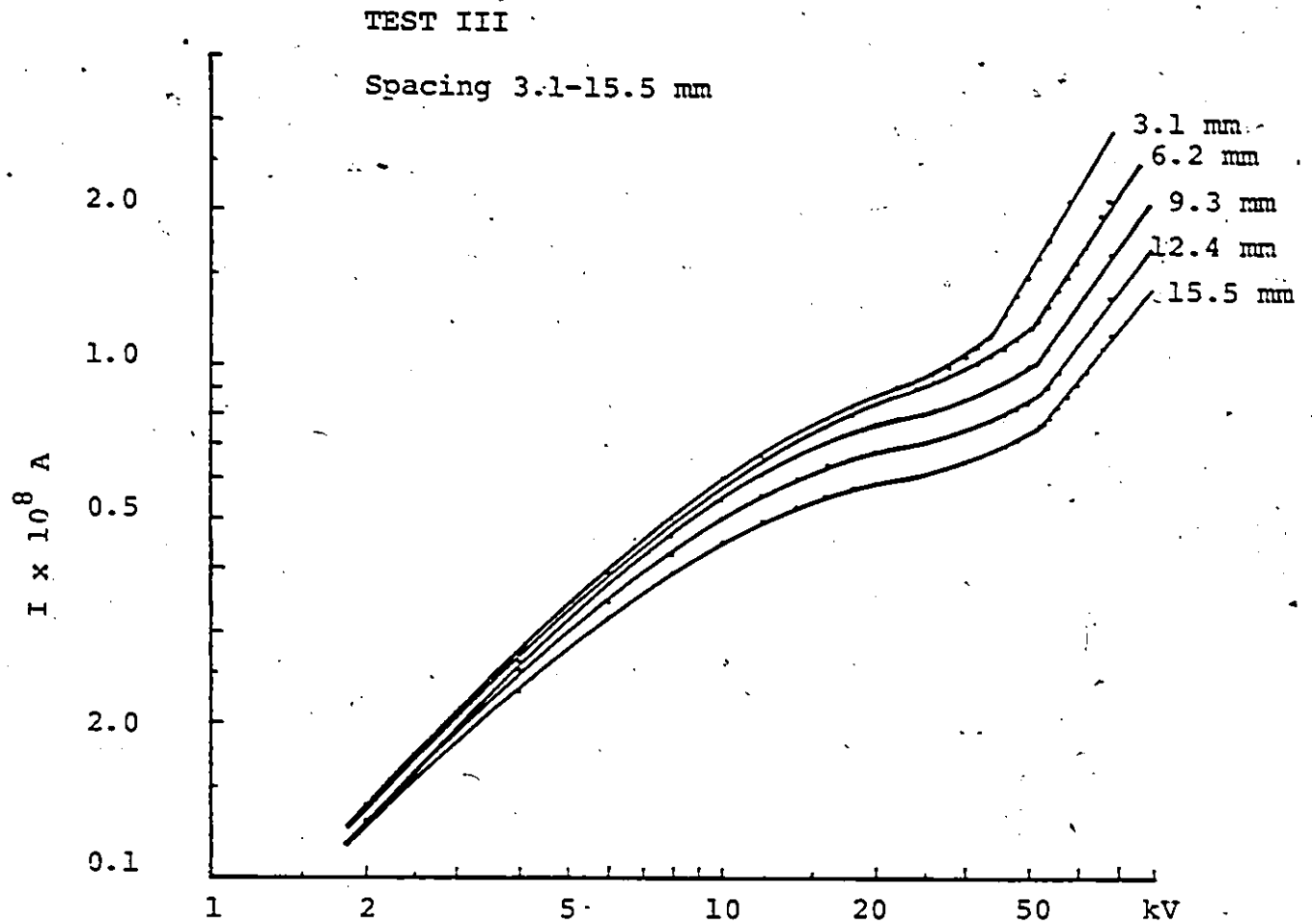


Figure 4.10.8: The Current-Voltage Characteristics (log-log) for Magnesium Electrodes and 350C-S. Silicone Oil at Room Temperature and 55% Relative Humidity

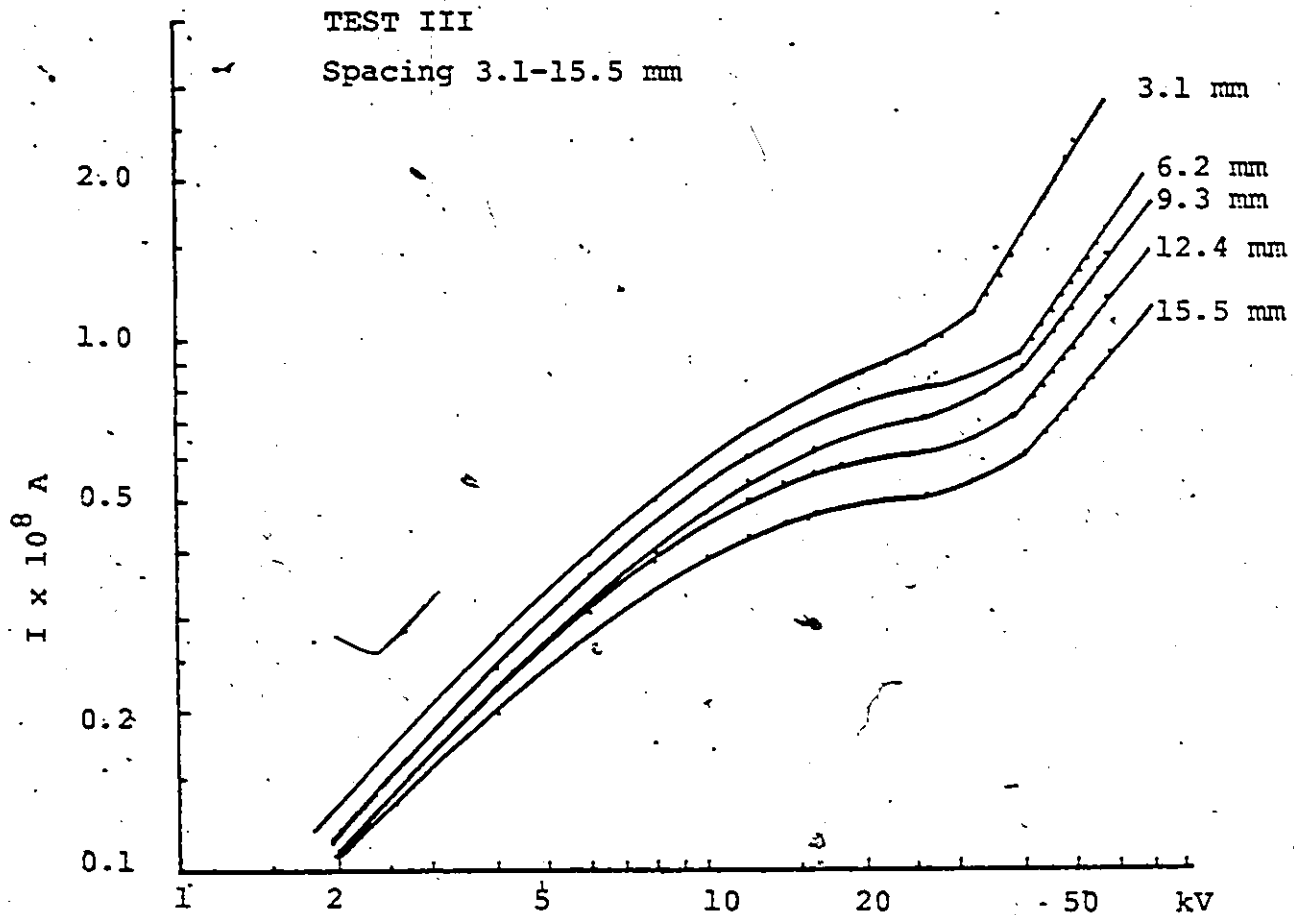


Figure 4.10.9: The Current-Voltage Characteristics (log-log) for Magnesium Electrodes and 1000C-S. Silicone Oil at Room Temperature and 55% Relative Humidity

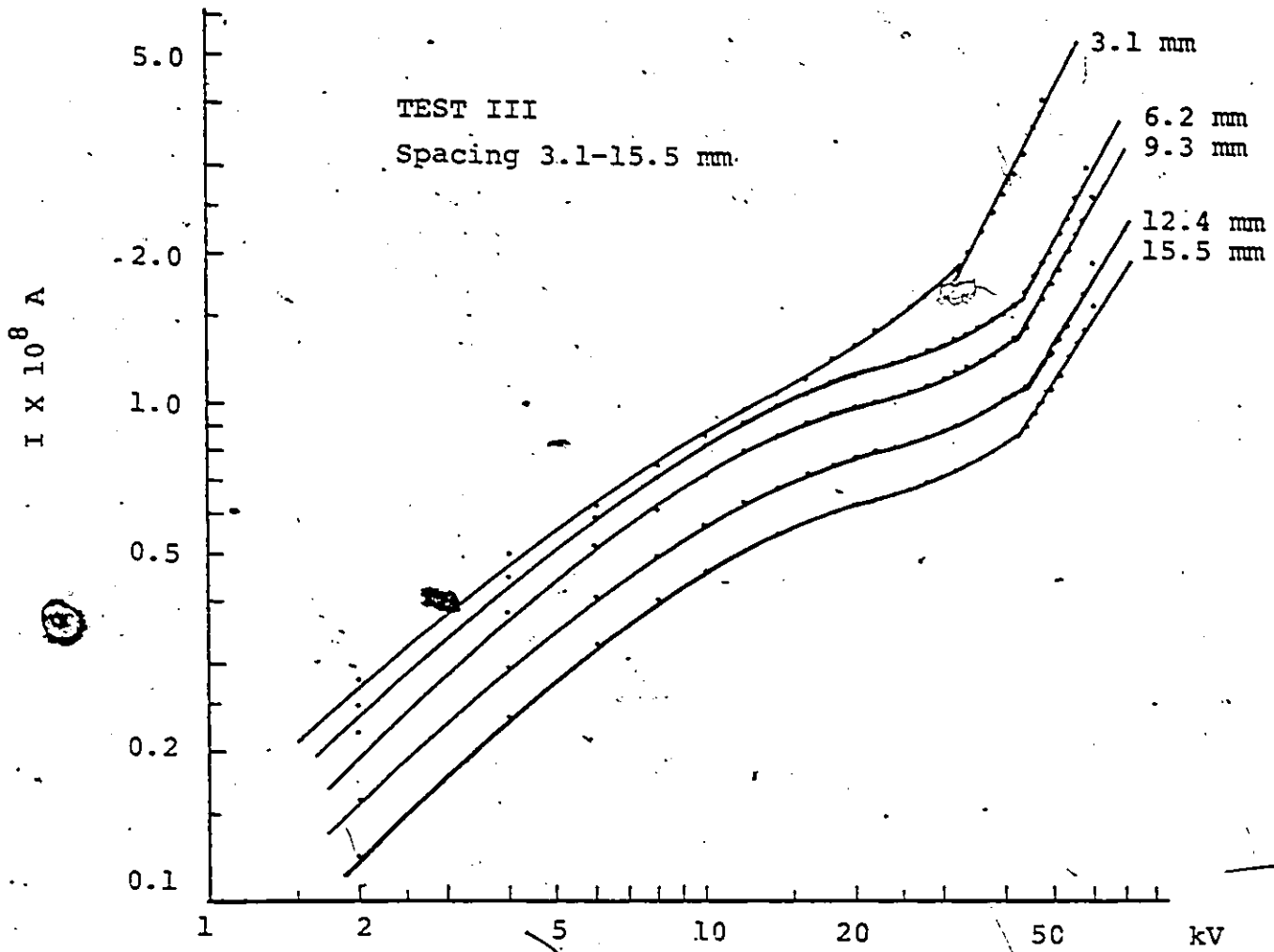


Figure 4.10.10: The Current-Voltage Characteristics (log-log) for Zinc Electrodes and 5c.s. Silicone Oil at Room Temperature and 55% Relative Humidity

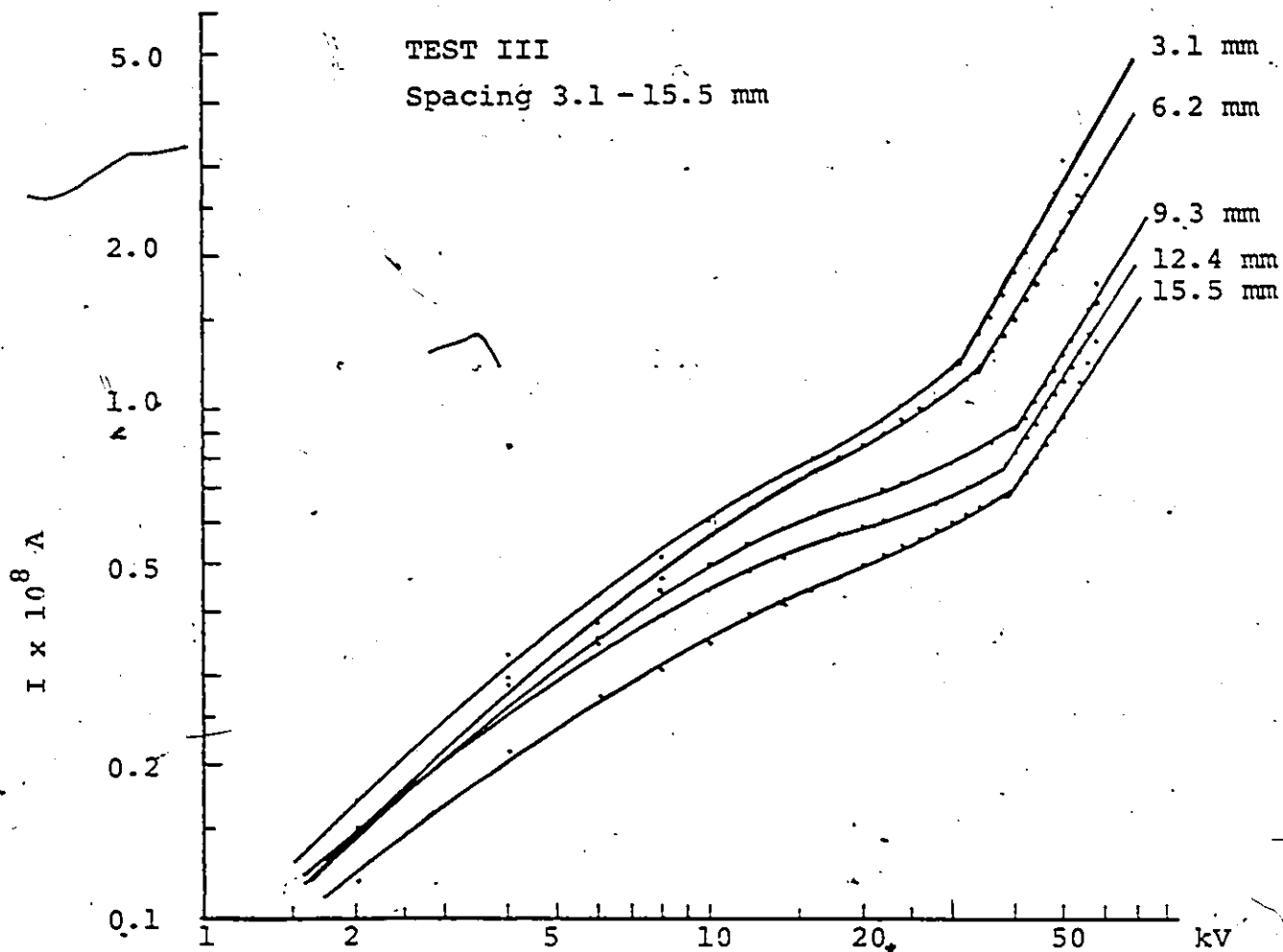


Figure 4.10.11: The Current-Voltage Characteristics (log-log) for Zinc Electrodes and 350^{c.s.} Silicone Oil at Room Temperature and 55% Relative Humidity

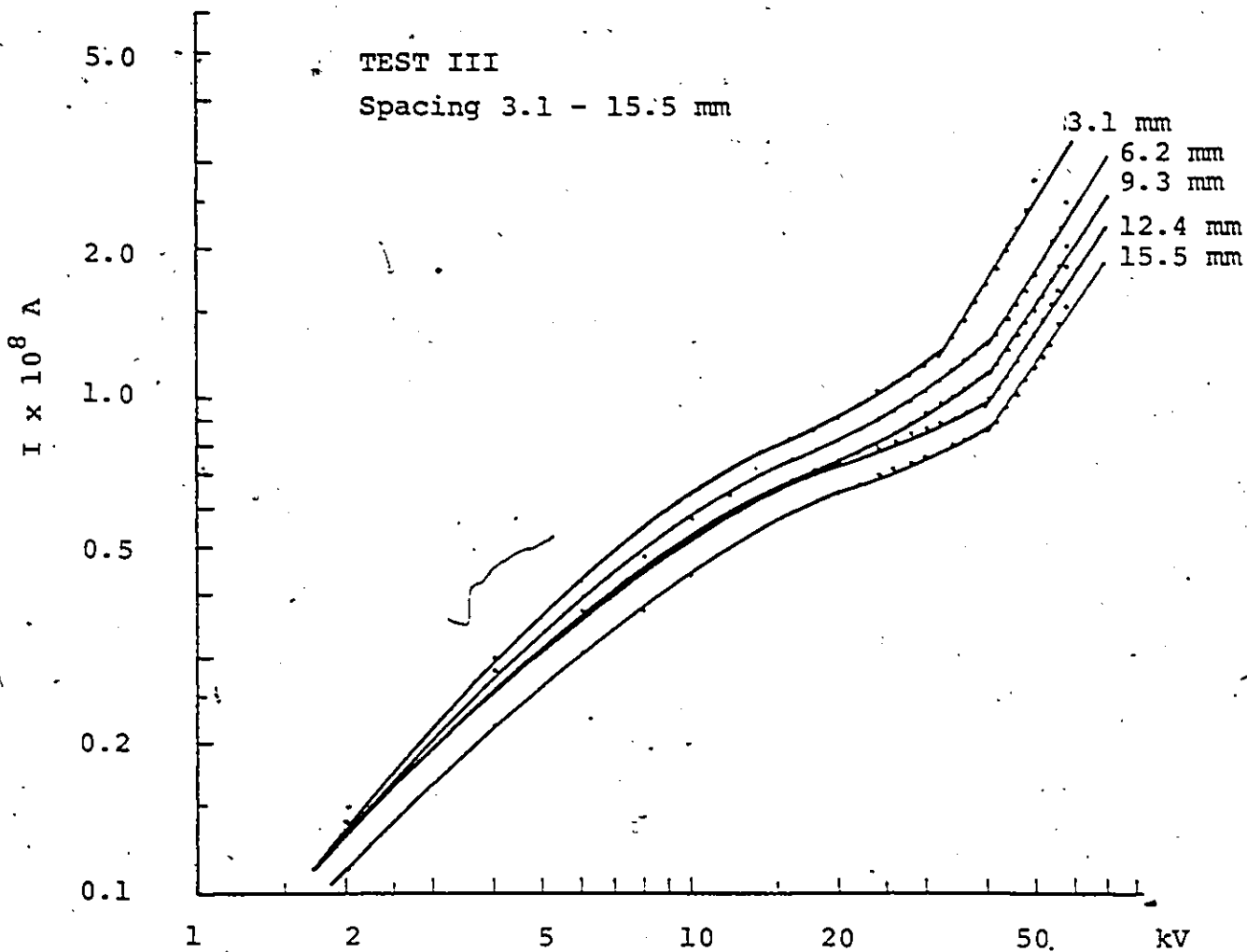


Figure 4.10.12: The Current-Voltage Characteristics (log-log) for Zinc Electrodes and $1000^{\text{C.S.}}$ Silicone Oil at Room Temperature and 55% Relative Humidity

reduces to a straight line in logarithmic co-ordinates, the equation is a power relationship and can be expressed as $I = KV^n$, indicating that for relatively large electrode spacing the prebreakdown "conduction" current varies as a power of the applied voltage, which is of the same form of equation as was previously found by Ostroumov [48] for small electrode spacings. As an example Fig. (4.10.2) shows a I-V plot that in the high field regime reduces to a straight line in logarithmic co-ordinates.

Two selected points of 1.0 R electrode spacing give,

$$V_1 = 39 \text{ KV} \quad I_1 = 1.0 \times 10^{-8} \text{ A}$$

$$V_2 = 81 \text{ KV} \quad I_2 = 3.0 \times 10^{-8} \text{ A}$$

because the plot is logarithmic,

$$\frac{\log I - \log I_1}{\log V - \log V_1} = \frac{\log I_2 - \log I_1}{\log V_2 - \log V_1}$$

hence,

$$\log I = -10.39 + 1.51 \log V$$

and

$$I = 10^{-10.39} V^{1.51}$$

Fig. (4.10) shows also that the experimental points fall very well onto straight lines of different slopes with electrode spacing.

The "conduction" current of silicone oil is found to be dependent on the ambient humidity. It was seen that, at the

same field, the "conduction" current of an immediately vacuum filtered sample decreases as compared with a sample already exposed to the ambient conditions. A comparison of the I-V characteristics of these two is shown in Fig. (4.11).

For low viscosity oil ($5^{\text{C.S.}}$) series 1 to 4 were interesting in that at small electrode spacings, 3.1-6.2 mm and 50 KV stress the reproducibility begins to fail and becomes progressively worse as stress conditioning proceeds. This was at $5^{\text{C.S.}}$ for which it is known (from the breakdown data) that breakdown voltage was also poorly reproducible. At $350^{\text{C.S.}}$ and $1,000^{\text{C.S.}}$ with different electrode material the reproducibility was very good. It was seen, in most cases, that the V-I characteristics for series 1-4 were not equally reproducible. Some of these graphs for different electrode spacings and different viscosities are given in Appendix II.

If now the slope of the resultant lines of the Fig. (4.10) is related with electrode spacing, the plot shown in Fig. (4.12) is obtained, from which it is seen that the inverse value of the slope (n^{-1}) representing the derivative $d(\ln V)/d(\ln I)$ varies linearly with electrode spacing (d). Each point of the Fig. (4.12) is the average value of four sets of 15 superimposed V-I plots which were recorded over 210 cycles. Similar results were found by other investigators [5], for $350^{\text{C.S.}}$ silicone liquid and copper electrodes, but with different slope and the ordinate intercept. Fig. (4.12) shows, however, that for a specified current the voltage

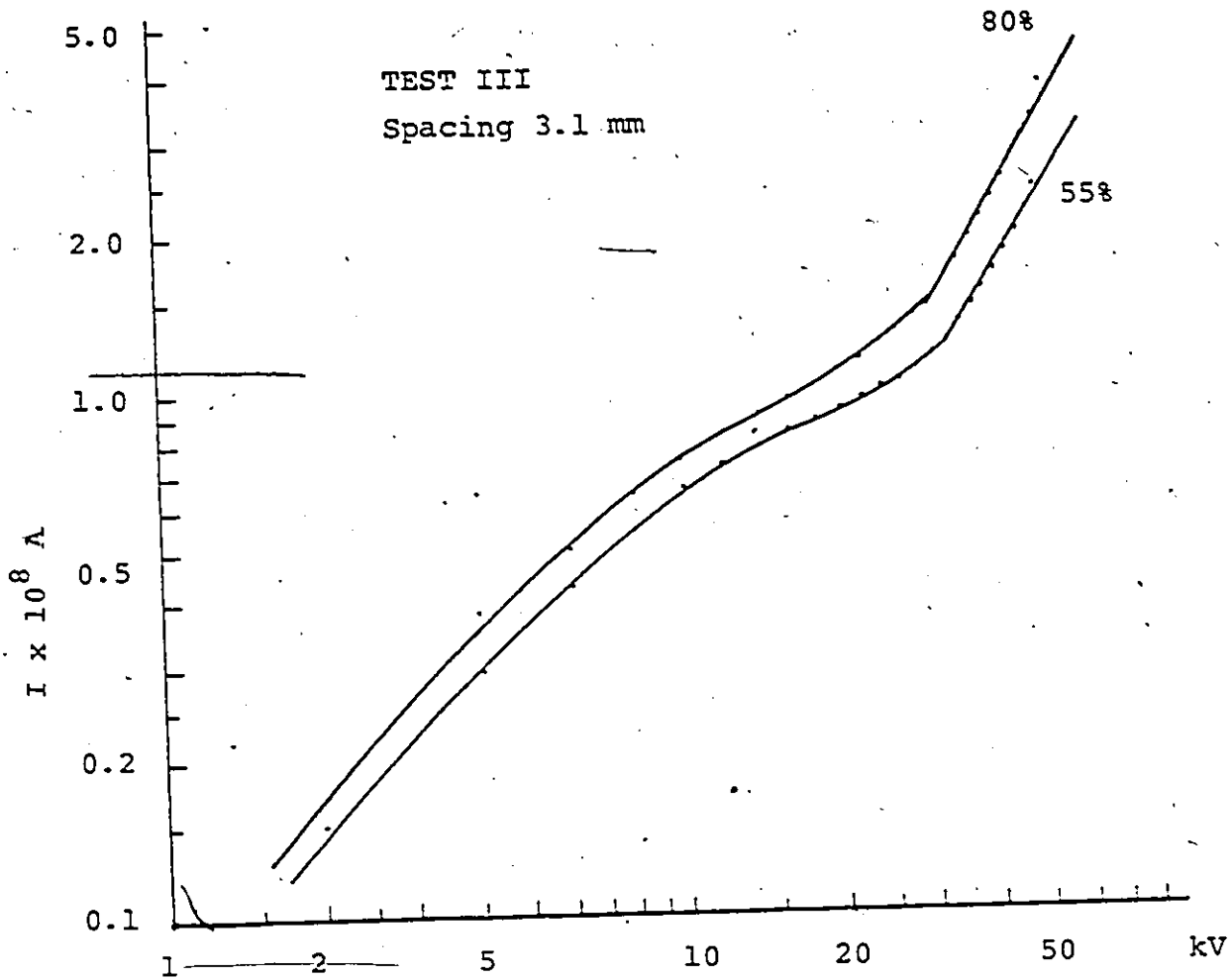


Figure 4.11: The Current-Voltage Characteristics (log-log) at Room Temperature for Different Relative Humidities Using Copper Electrodes and 350^{c.s.} Silicone Oil

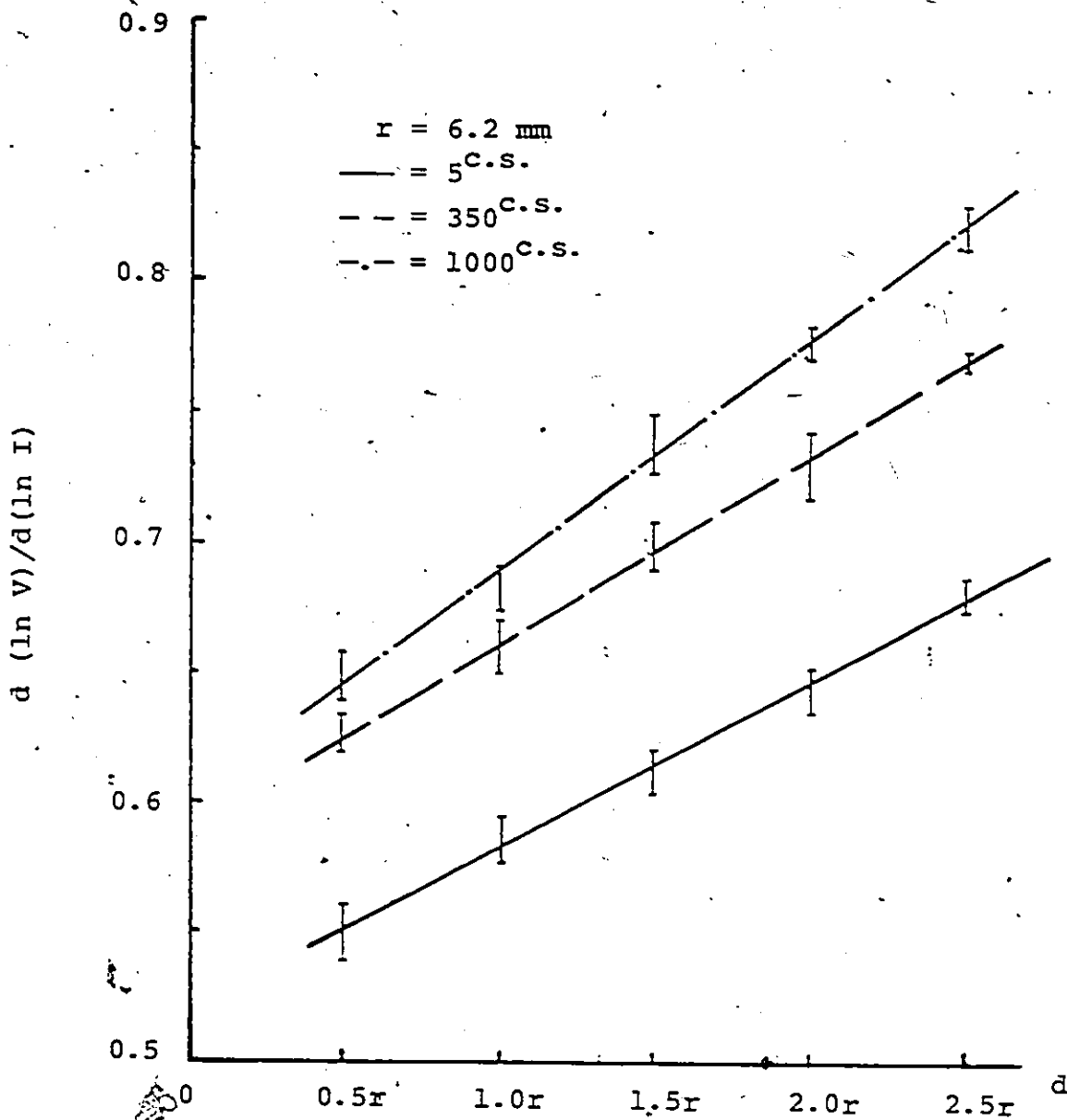


Figure 4.12.1: $-d(\ln V)/d(\ln I)$ as a Function of Electrode Spacing for Hemispherical Copper Electrodes

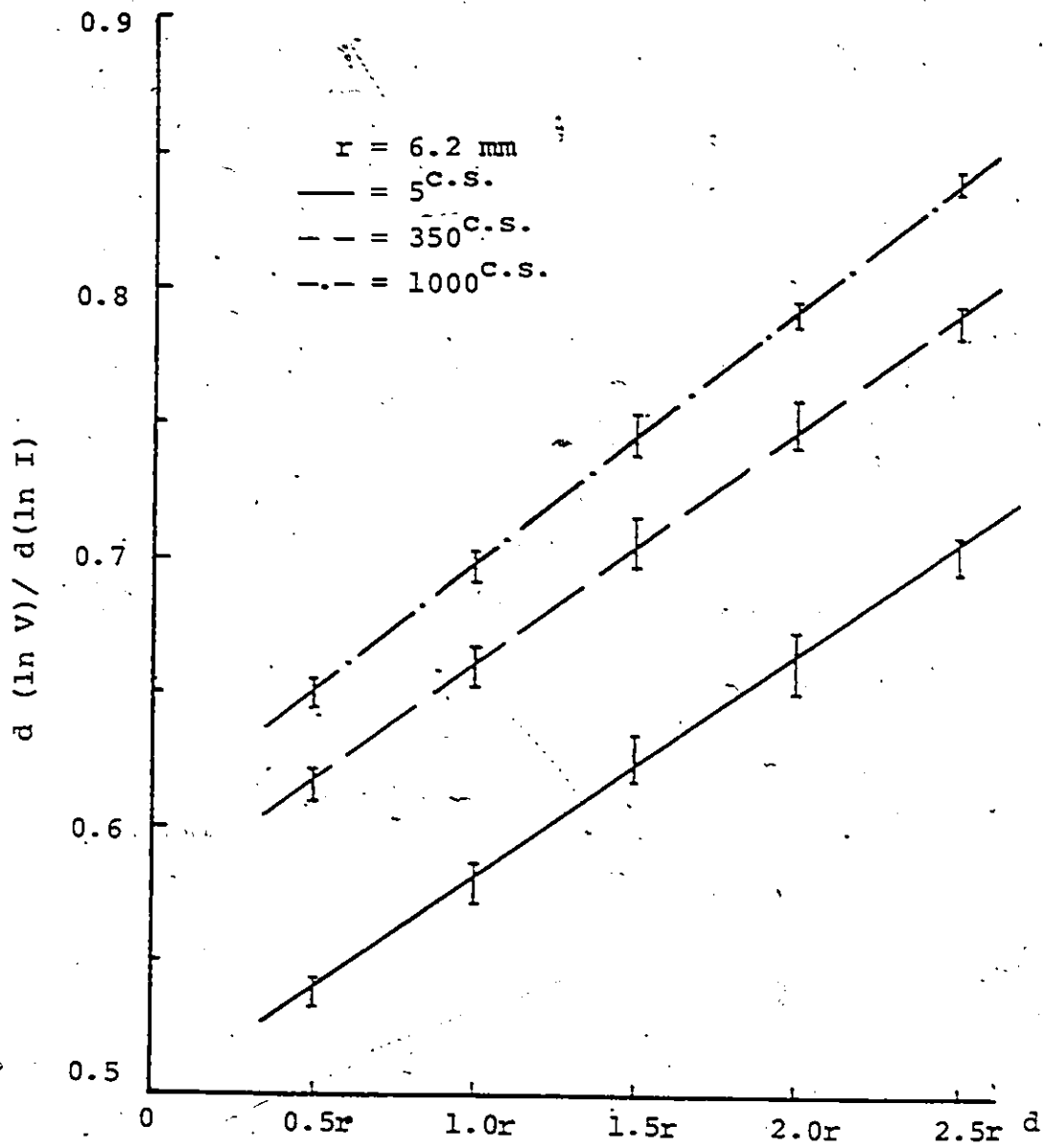


Figure 4.12.2: $d(\ln V)/d(\ln I)$ as a Function of Electrode Spacing for Hemispherical Aluminum Electrodes

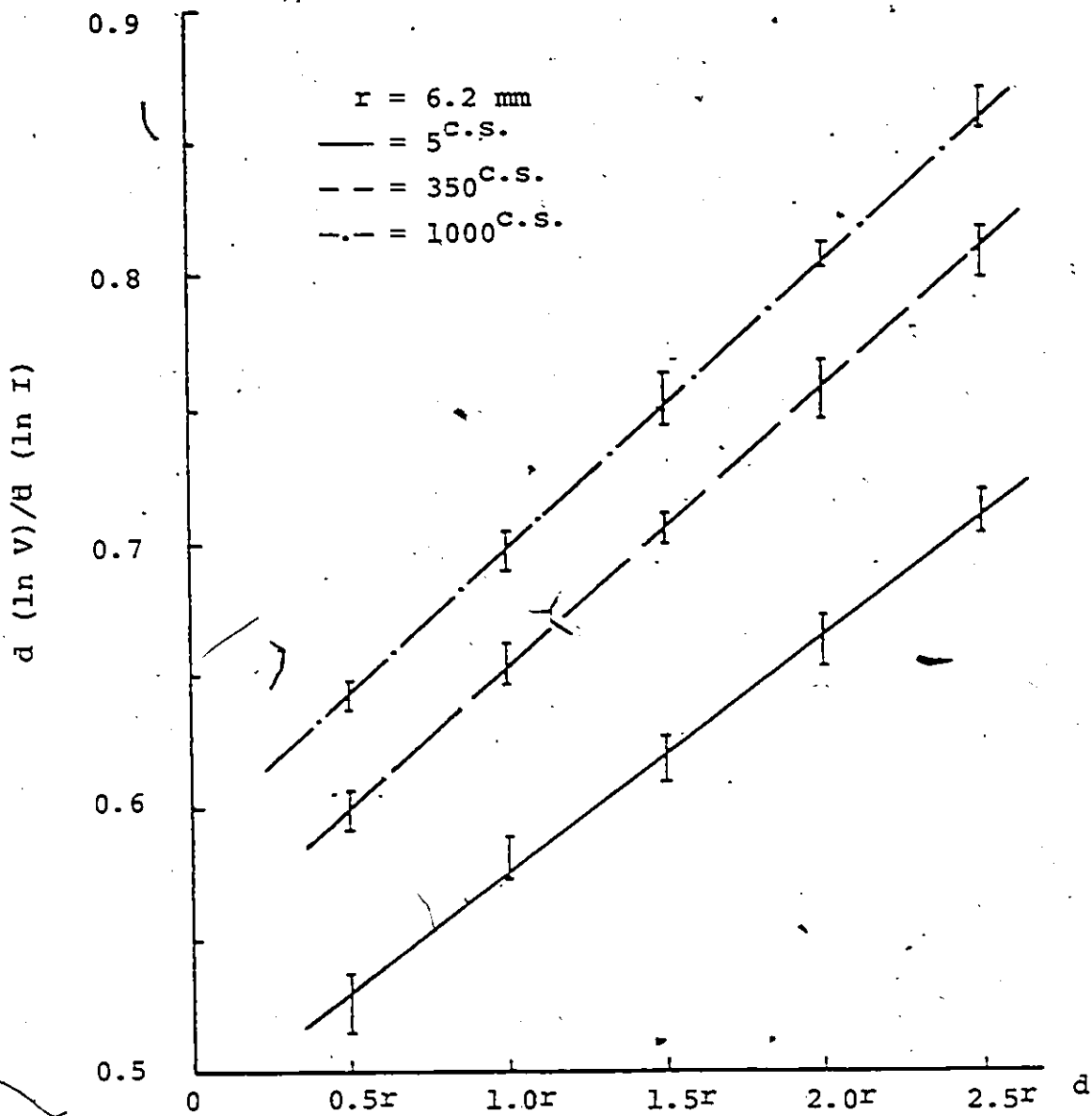


Figure 4.12.3: $d(\ln V)/d(\ln I)$ as a Function of Electrode Spacing for Hemispherical Magnesium Electrodes

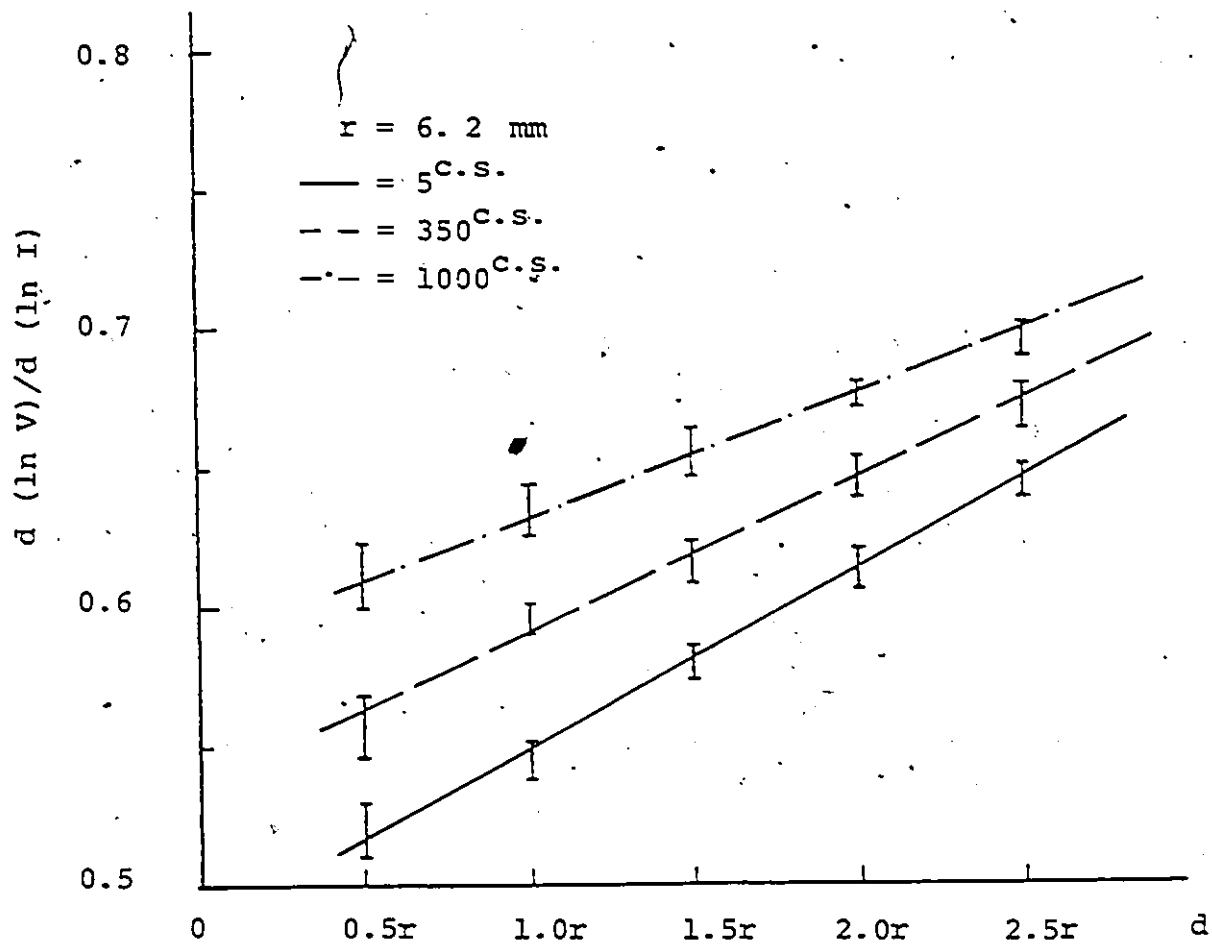


Figure 4.12.4: $d(\ln V)/d(\ln I)$ as a Function of Electrode Spacing for Hemispherical Zinc Electrodes

applied to the liquid is linearly dependent to the distance between electrodes. Three such curves are presented in Fig. (4.12) to show the influence of varying the viscosity of the silicone dielectric oil in different experiments. It can easily be seen that, in general, oils of higher viscosity indicate an increase in the inverse of the slope, i.e., a decrease of the V-I slope at high field. This results in extension of the field range to higher values with the viscosity of the liquid sample. It can also be observed that the slope of the straight lines is not influenced significantly by varying the viscosity but the ordinate intercept is moved upwards for more viscous oil.

The four sets of curves shown in Fig. (4.13) for different electrode materials are superimposed to show that for each viscosity value the influence of changing the electrode material was to vary both the slope and the intercept. Although this influence seems to be significant, it is not so dramatic a change as can be seen from Figs. (4.12.1-4.12.4) when the nature of the liquid alone is varied.

In order to search for a magnetic field effect upon the prebreakdown "conduction" current the early treatment by Watson [5] is extended to higher magnetic field (200 gauss). The complete experimental procedure described earlier was repeated with all the electrode materials, one type of oil (350^{C.S.}), and a number of electrode spacings ranging from 3.1 mm to 15.5 mm.

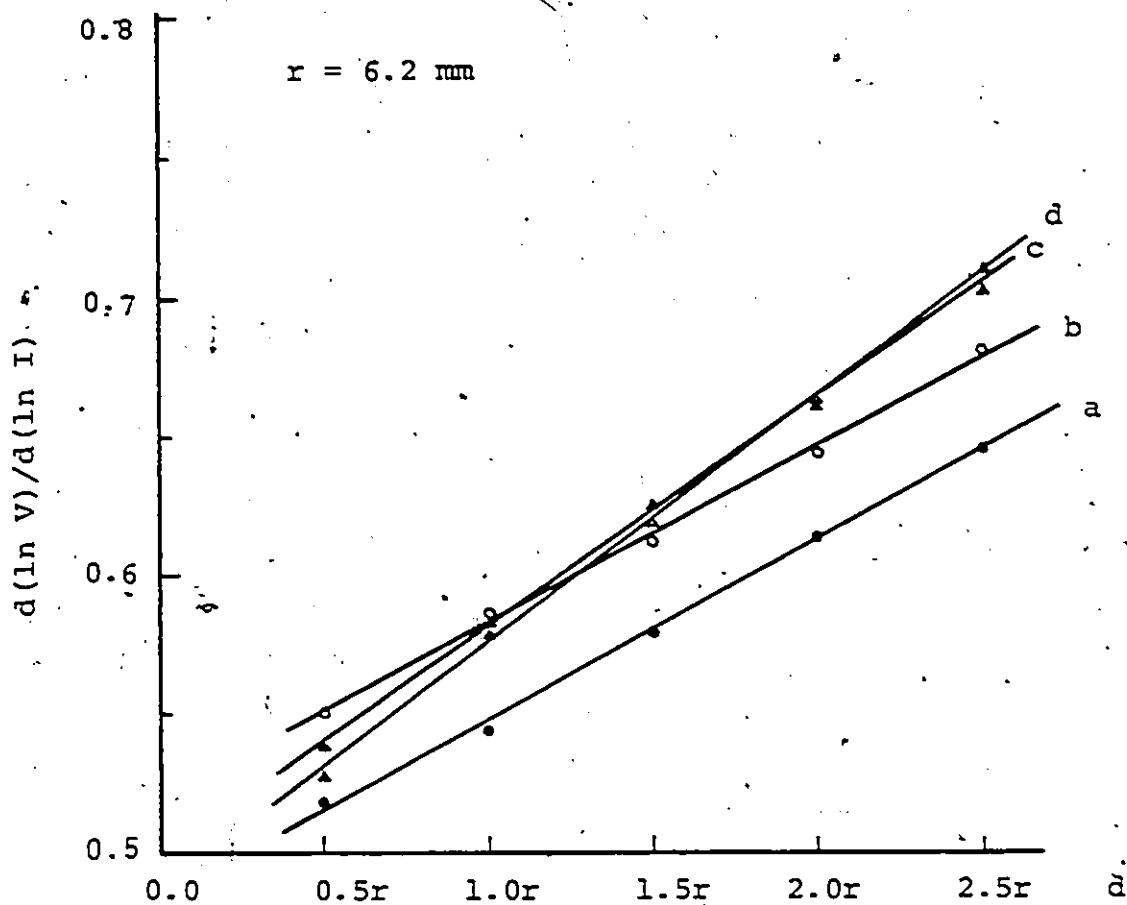


Figure 4.13.1: Dependence of $d(\ln V)/d(\ln I)$ on Electrode Spacing for a Number of Electrode Materials a) Zn, b) Cu, c) Al, d) Mg (hemispherical electrodes), using 5^{C-5} Silicone Oil

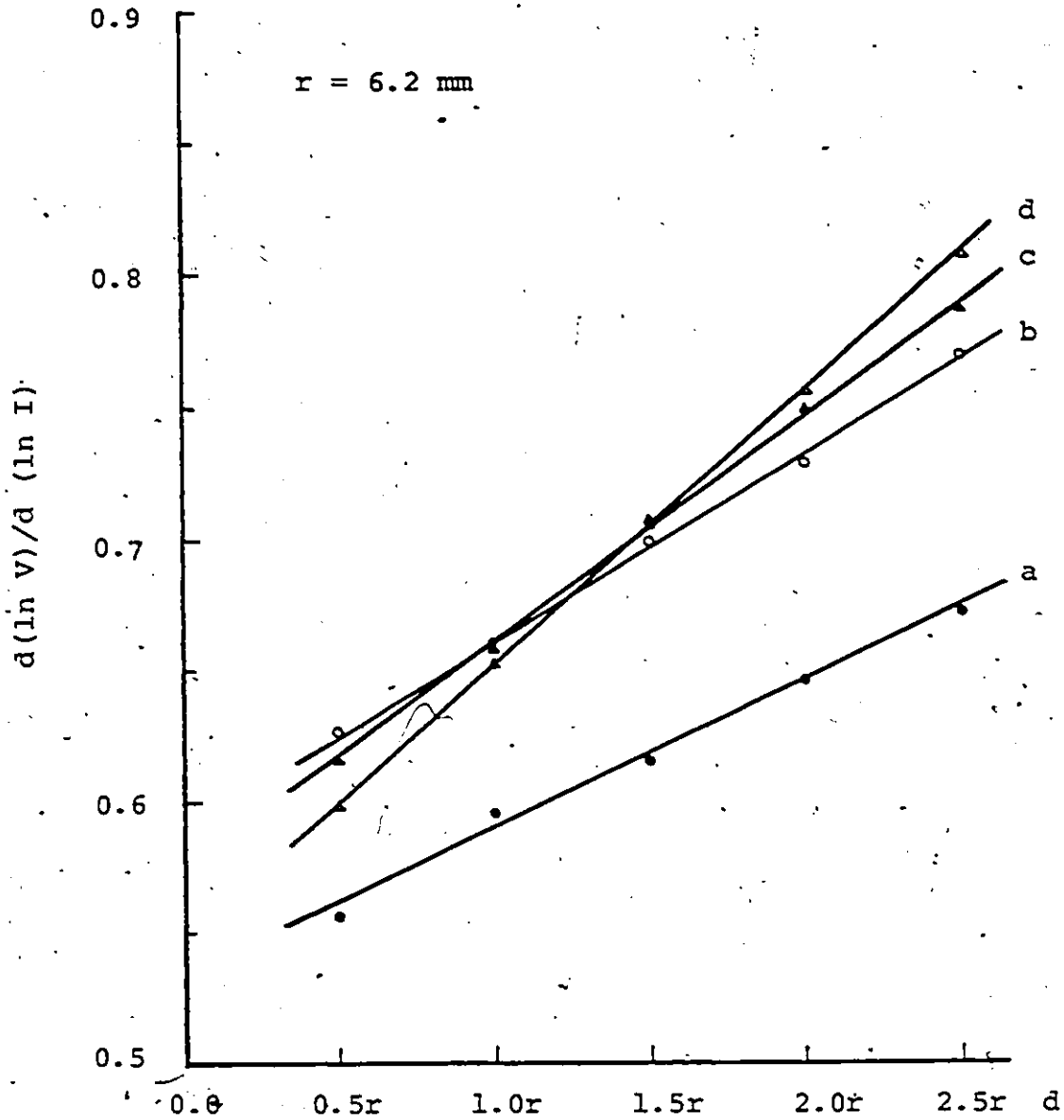


Figure 4.13.2: Dependence of $d(\ln V)/d(\ln I)$ on Electrode Spacing for a Number of Electrode Materials
 a) Zn, b) Cu, c) Al, d) Mg (Hemispherical Electrodes), using 350^{c.s.} Silicone Oil

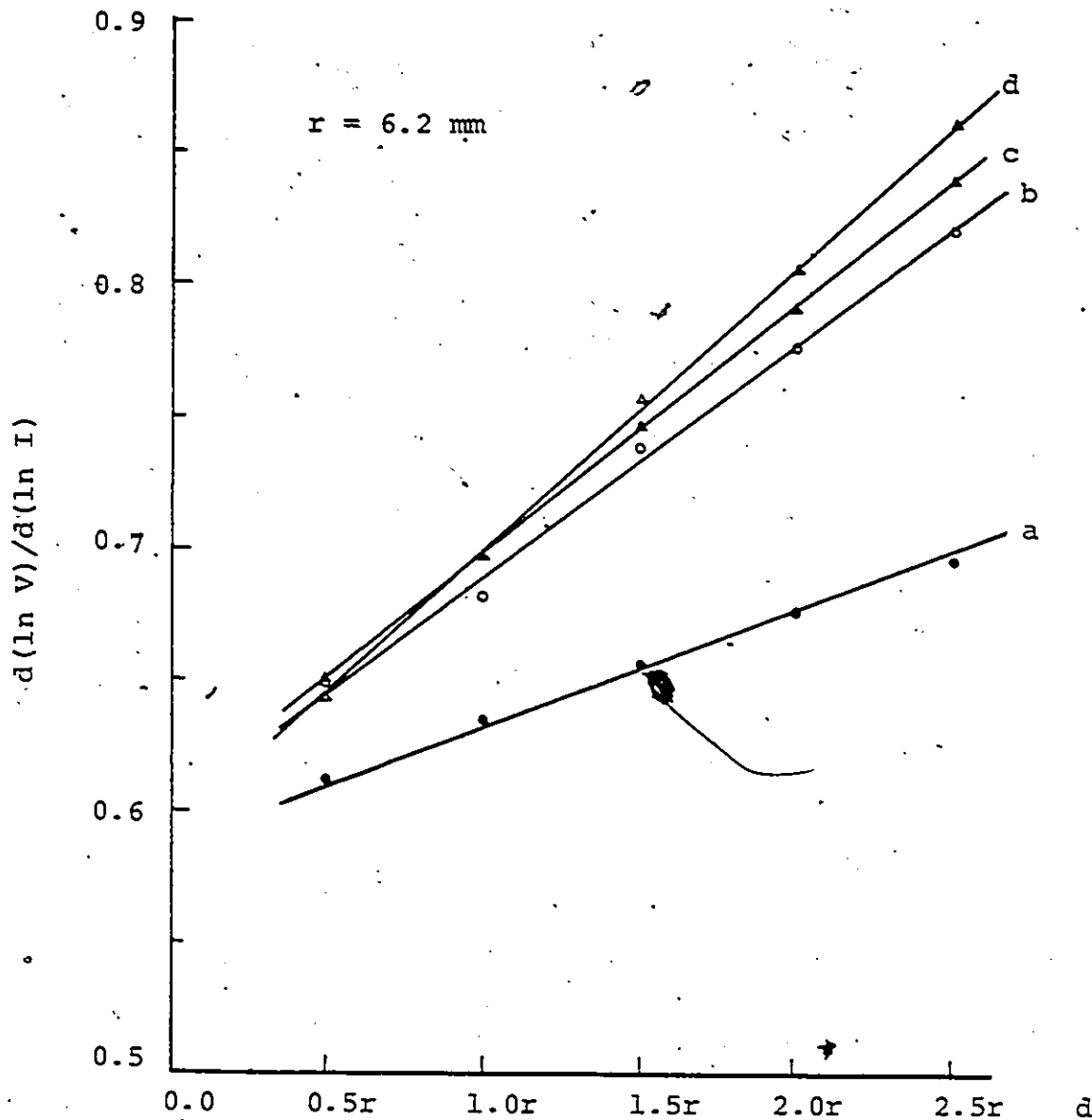


Figure 4.13.3: Dependence of $d(\ln V)/d(\ln I)$ on Electrode Spacing for a Number of Electrode Materials
 a) Zn , b) Cu , c) Al , d) Mg , (Hemispherical Electrodes), using $1000^{\text{C-S}}$ Silicone Oil

The application of a crossed magnetic field of 200 gauss upon prebreakdown "conduction" current of copper electrodes under the action of an electric field enabled the results depicted in Fig. (4.14) to be obtained. Fig. (4.14) shows the relationship between the slopes representing the exponent $d (\ln V) / d (\ln I)$ and electrode spacings for four sets of experiments recorded over 210 cycles at the presence of a 200 gauss crossed magnetic field. It will be seen that in this case the linear relationship between the inverse slope and the electrode spacing disappears, giving a randomly displaced set of concave down curves. There is, however, a little doubt in the position of each curve which is due to the statistical error associated with the electrode conditioning phenomenon just as in the case of the straight line parametric variations.

It should be noted, however, that if the magnetic field were applied after the electric field had conditioned the electrodes the slope would remain the same as if only the electric field were applied. Similar experiments were carried out for a number of electrode materials and the average values of the results obtained over 210 cycles are shown in Fig. (4.15). This is a common procedure to repeat the test in order to obtain a reliable average value of the data. In Fig. (4.15) the average values of the results are superimposed to show that for a fixed magnetic flux density the influence of changing the electrode material was to move the curves slightly. In every case both anode and cathode

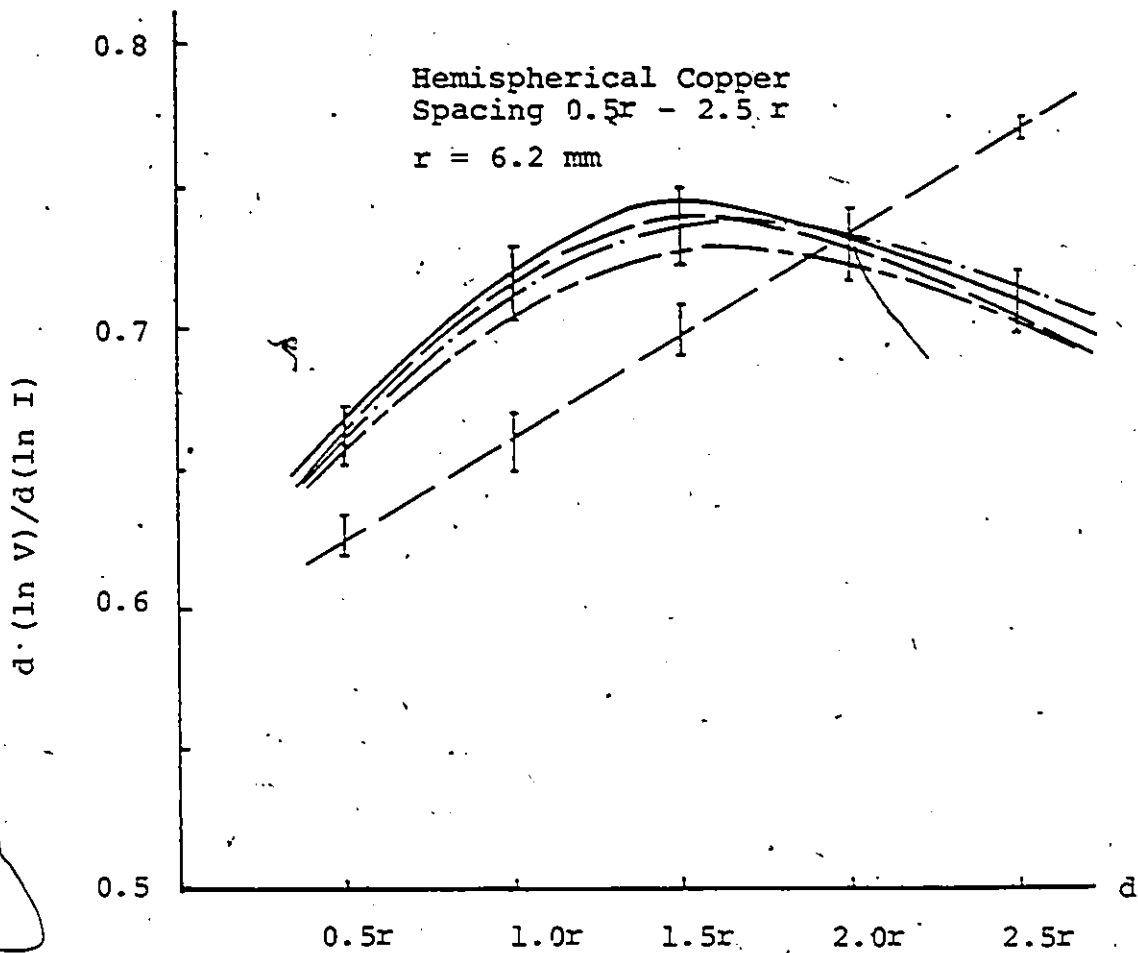


Figure 4.14: $d (\ln V) / d (\ln I)$ for Hemispherical Copper Electrodes as a Function of Electrode Spacing for Four Successive Sets of 15 Recordings in the Presence of a Magnetic Field Using 350C-s. Silicone Oil

(The broken straight line indicates comparative curve in the absence of a magnetic field (reproduced from Fig. 4.12.1 for comparison).

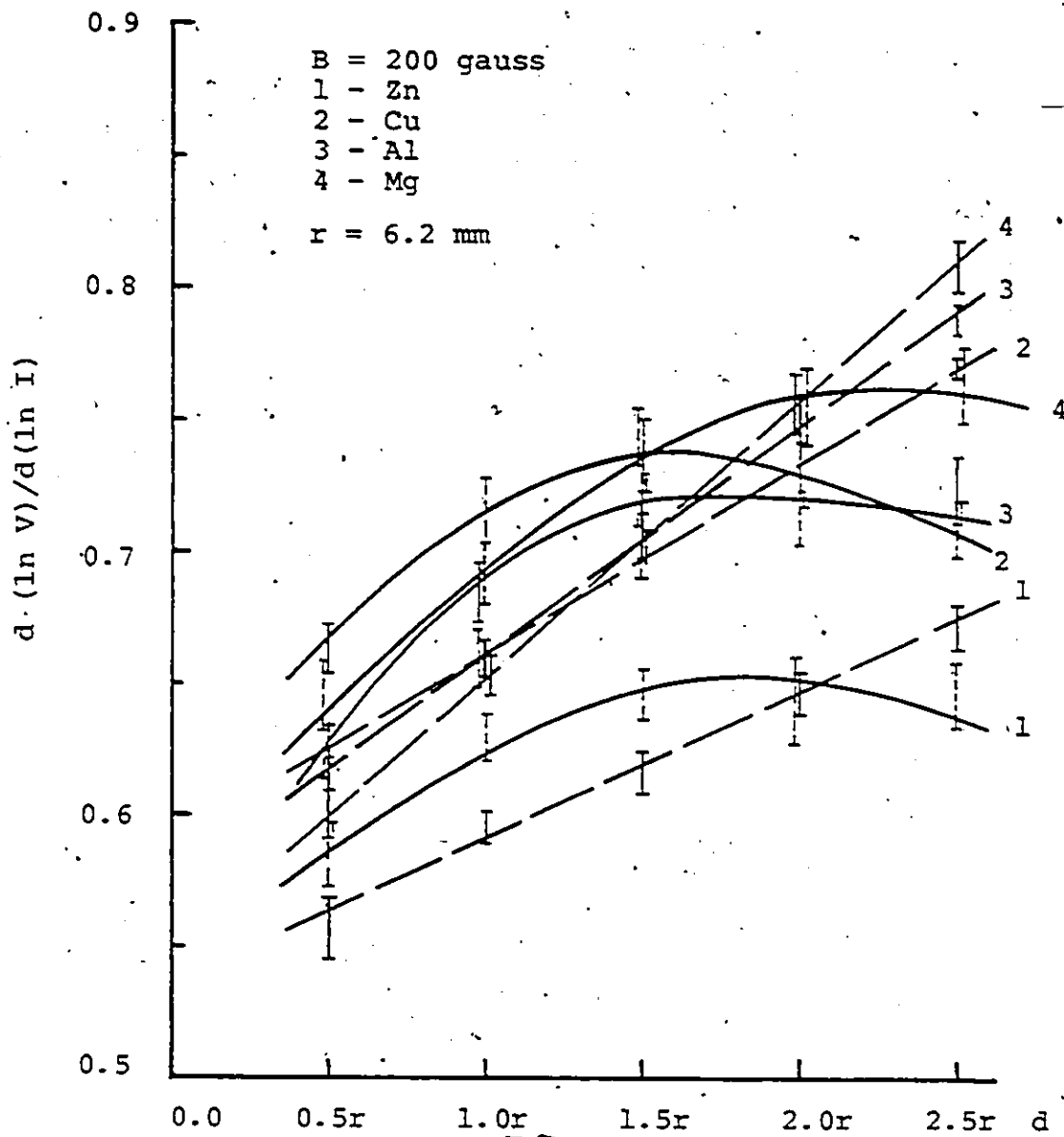


Figure 4.15: The Average $d(\ln V)/d(\ln I)$ for Different Electrode Materials as a Function of Electrode Spacing With and Without Applying a Magnetic Field and Using 350°C . Silicone Oil

were treated indentially.

An experiment was made with a fixed electrode spacing, a pair of copper electrodes, and one type of oil (350^{C.S.}) for different rates of ramping. The results are shown in Fig. (4:16) in which the general characteristics are slightly moved upwards as the rate of ramping increased but the slope of the $d(\ln I) / d(\ln V)$ in the ultimate high field remained unchanged.



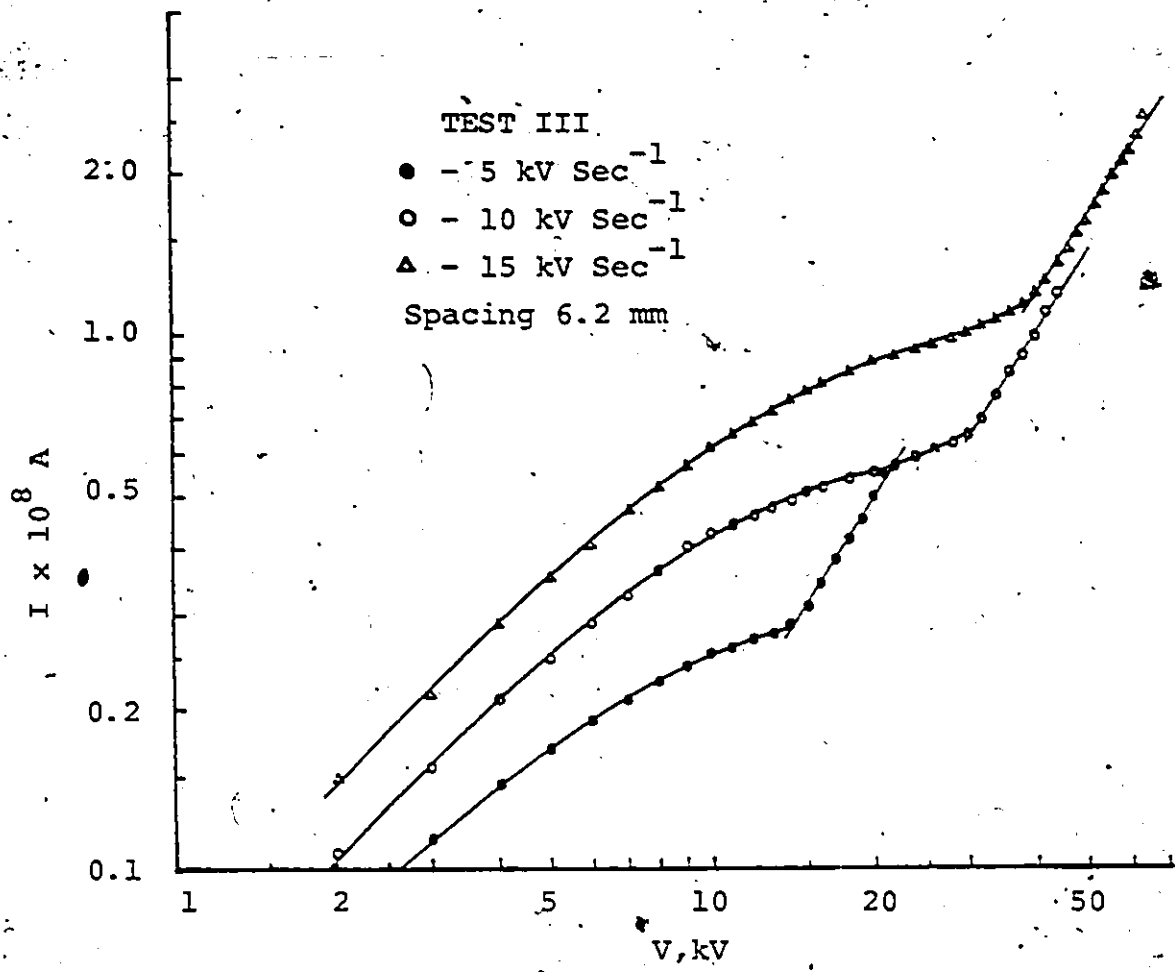


Figure 4.16: The Current-Voltage Characteristics with Copper Electrodes and 350°C. Silicone Oil, for Different Ramp Slew Rates

V. CONCLUSIONS AND DISCUSSION

5.1 Summary

The principal purpose of this research was to investigate:

- a) The influence of viscosity of the liquid upon the prebreakdown current.
- b) The influence of electrode material upon the prebreakdown current.
- c) The magnetic field effects on each of the materials of part (b) with one type of oil, 350 C.S.

Silicone oil (Dow Corning DC 200) 5, 350, and 1,000 C.S. were used as a working dielectric, the electrodes remaining uncontaminated throughout the experiments so long as tests were not carried out up to breakdown.

The application of a ramp voltage in the manner reported by Secker and Hilton [11] and Watson and Girgis [5] was found to permit the acquisition of reproducible current versus voltage characteristics. The current versus voltage relations, Fig. (4.3), gave characteristics of a consistent shape, i.e., after an initial rise of the current as a function of the applied voltage, the current shows a tendency toward saturation and rises strongly again in the high field regime.

The plot of $\log I$ versus $\log V$ has been obtained for large spacings with copper, aluminum, zinc, and magnesium electrodes and with three types of oil all of which displayed a linear portion in the high field regime.

The slope of the final portion of $\log I$ versus $\log V$ was seen to vary with the electrode spacings and its inverse value, n^{-1} , was found to increase linearly with electrode spacing when no magnetic field was applied. When the results were extrapolated to zero electrode spacing they failed to pass through the origin. Similar findings have been reported in previous measurements [5] for large spacings, 350^{C.S.} silicone oil, and copper electrodes. These are, however, in contradiction with the data reported by Ostroumov [48] for small spacings. In a previous publication [5] it was shown that the linearity between $d(\ln V)/d(\ln I)$ and the electrode spacing d was consistent with the notion of charge injection from the cathode by the Fowler-Nordheim mechanism. These results have now been further confirmed.

The test results showed that with a constant electrode area, increase in the electrode spacing, and hence in the volume of the oil tests, would significantly decrease the current flowing. The change in the volume of the test vessel (at least in the range of volumes, 35 cc and 70 cc, used), however, has no measureable effect on the prebreakdown current results.

Experimental data with non-zero magnetic field acting at right angles to the rotational symmetry axis of the electrodes showed a non-linear relationship between the inverse slope $d(\ln V)/d(\ln I)$ and electrode spacings.

5.2 Major Conclusions

The experimental results led the author to the following

major conclusions.

a) The influence of varying the viscosity of the silicone dielectric oil was one in which the slope of the straight lines for all the electrode materials was not influenced, but the ordinate intercept was shifted upwards for more viscous oil [49] showing that the slopes of the lines are independent of viscosity which are in contradiction with the simple theory of charge transport mechanism given by Watson [5]. It can be, therefore, suggested that mobility of the liquid plays no part and the given theory should be modified [Appendix (II)].

b) When the curves of part (a) for all the electrode materials were superimposed they showed that for each viscosity value the influence of changing the solid emitting material was to vary the slope and thus is in accord with what would be expected of the Fowler-Nordheim mechanism. Although this influence is seen to be significant, it is not so dramatic a change as when the nature of the liquid alone is varied.

c) When a magnetic field of 200 gauss was applied at right angles to the axis of rotational symmetry of the electrodes the prebreakdown current changed significantly at a number of electrode spacings ranging from 3.1 to 15.5 mm. It was found that the derivative $d(\ln V)/d(\ln I)$ is non-linear with electrode spacings; the value of the prebreakdown current is to be either increased slightly or reduced according to the electrode spacings. The magnetic field did, however, perturb the conduction current if it was on throughout the

conditioning. If, however, it were applied after the electric field had conditioned the electrodes the slope would remain the same as if only the electric field were applied. The results showed that the curves were slightly shifted as the nature of the electrode was changed under similar conditions. The results are consistent with the idea that the strength of the liquid is greatly influenced by the nature of the cathode surface oxide layer.

d) Using a similar gap setting and the same treatments for liquid and electrodes, different rates of ramping, dv/dt , changes the level of the general characteristics but does not alter the slope of $d(\ln I)/d(\ln V)$ in the ultimate high field regime.

5.3 Discussion

It is evident from Fig. (4.3) that the general shape of the curve showing the relationship between the steady-state current and the applied voltage for silicone oil is similar to the results obtained by other investigators using different liquid insulators [8-10]. The "conduction" current at low field, however, was attributed mainly to the presence of impurities which are inevitably present in the wall of the test cell, the electrodes, and the liquid sample itself. This may be supported from Fig. (4.5) which indicates that the "conduction" current is dependent upon impurities. At high fields (above 100 KV cm^{-1}) the nonlinear portion becomes dominant and is attributed mainly to electron emission from the cathode [50]. In the intermediate stress regime, the

characteristics do not show a true saturation value but a small rise in current with increasing stress. This slight increase is known [8] to be due to the spherical geometry of the electrode configuration used: For such electrodes the current from the highly stressed inner volume will reach a saturation value whilst that from the surrounding space will still be in the low field region and so will contribute to the increase in the total current. During the saturation, under the action of the applied voltage, an accumulation of ions at the surface of the cathode takes place; evidence of positive space charge formation near the cathode has been reported by other investigators [8, 51]. Since even with the most careful preparation of the electrodes a semi-insulating film will be formed on their surfaces, this film will hinder their immediate neutralization. The present experimental results are consistent with all this previously reported work.

The plotted experimental results of Fig. (4.10) (the log of the flowing current I versus the log of the applied voltage V) show an abscissa intercept whose average is approximately 1.4^{kv} for copper and 1.6^{kv} for magnesium. This part of the voltage is known [48] to be needed to overcome the surface resistance on the boundary of the electrodes and to produce a current of sufficient strength. These intercepts are, however, much higher than the one reported previously [48]. The pre-breakdown current of silicone oil was observed to have a tendency to decrease when it was purified through filters of pore size down to 2.0-2.5 micron. This decrease may be

accounted through the presence of impurities in the unfiltered liquid sample. A small particle, when charged, would oscillate between the electrodes as the voltage is ramped up and down and could be compared to a large heavy ion which, when approaching an electrode, causes a local increase in the field. In very high fields this may develop into a complete breakdown.

It was observed that, in general, the prebreakdown current values decrease progressively during conditioning with the ramp application. The time required for the current to reach its steady value, however, varied between samples of low viscosity, 5^{C.S.}, liquid, taken from the same batch but it was lowered for the liquids of higher viscosities, 350, and 1,000^{C.S.} This decrease may be associated with the process at the cathode where positive ions are neutralized. Since nearly all clean metals rapidly acquire an invisible protective film when exposed to a laboratory atmosphere, a dielectric or semi-conducting layer is almost inevitably present as an oxide film on the electrode surfaces [8, 52, 53]. This layer tends to prevent the ionic charge carriers from being immediately neutralized. The great difference between current of different electrode materials is evidence that it is dependent upon the electrode surfaces themselves and probably upon the nature of the oxide layer. This continued accumulation of ions on the layer enhances the field at the electrodes, increasing neutralization until the rate of neutralization and rate of arrival of ions are in dynamic equilibrium [54]. These processes may reduce the concentration and drift velocity of

the charge carriers which could explain the decrease of current with the time of ramp application.

It was found that upon application of a magnetic field the slope $d(\ln V) / d(\ln I)$ is non-linear with electrode spacing. The exponent $d(\ln V) / d(\ln I)$ is observed either increased or reduced slightly depending upon the electrode spacings.

Secker [11] reported a similar magnetic field effect on the breakdown voltage of n-hexane at a fixed electrode spacing. He assumed that the magnetic field interacts with charge-carriers in the interelectrode spacing. For such interaction, he suggested that the majority of the charged particles must be free electrons to explain such effects.

Watson [12] however, reported a similar pattern of variation in the case of static breakdown voltage of copper electrodes in vacuum. He has suggested that the phenomenon is an electrode surface effect and magneto-transport of electrons through the surface layer of oxide is capable of modifying the field emission and so influences the Fowler-Nordheim equation. This effect is significantly influenced by the relative magnitude of the oxide work function and that of the inner potential barrier at the underlying metallic junction.

In liquids before breakdown, however, a field strength above 100 Kv cm^{-1} exists at the liquid-cathode interface [50], a stress at which field aided electron emission can take place from cathode protrusions, causing local field enhancement and

therefore large local electron emission. The similarity between this phenomenon and vacuum field emission suggests, therefore, the existence of a common mechanism.

The results of Fig. (4.15) show that the curves are slightly shifted as the nature of the electrode is changed under similar conditions. There is no theory to determine the unusual behaviour of pre-breakdown current with electrode spacing as well as the alteration due to change of electrode material at fixed applied magnetic field. There is close agreement, however, between the results obtained here and those reported by Watson and Girgis [5].

Perturbation of the prebreakdown mechanism by a magnetic field in the lowering portion of the prebreakdown current might be explained in terms of the deflection of the electron beam from emitting cathode protrusion by the Lorentz field. The magnetic field would give the electrons a transverse component of drift velocity and an associated decrease in their drift velocity in the electric field direction [55]. This will suggest that magnetic field can be applied to control the resistance of a liquid, i.e. to sweep the electrons from the region between the electrodes until it can no longer impinge upon the anode. It is however possible that such a perturbation mechanism could exist in the cathode oxide layer and modify the current through it in a similar manner [12].

There is evidence that the curve (a) of Fig. (4.13) which gave greater current and scatter measurements than those of b, c, and d might be due to the natural surface roughness of

the commercially available zinc metal which could not be removed even by intense polishing; due to patches having low work function, and geometrical irregularities, a freshly prepared cathode surface will always be non-uniform in structure and certain sites will be able to emit more freely than others [56]. The probability of breakdown being initiated at one of these sites is therefore high, i.e. there might be a correlation between the nature of the cathode and the breakdown instability.

As far as the author is aware this is the first time that the influence of different electrode material upon the pre-breakdown "conduction" current has been examined in the presence of an applied magnetic field under similar conditions. It is likely that different electrode materials will influence prebreakdown "conduction" current but the solid deposits and adsorbed layers will completely mask any variations in the properties of the underlying surface. The technique used here, however, allowed slight changes of the electrode materials to be effective by virtue of their possessing different types of surface oxide layers.

5.4 Suggestions for Further Studies

The variation of the prebreakdown current with different electrode material shows that the nature and structure of the electrode surface is important as far as the electron emission is concerned. The results obtained here, however, can not demonstrate this conclusively, because the liquid-metal interface at the cathode and the thickness of the surface

layer itself makes the surface phenomena very complex and would need further studies both experimentally and theoretically. Moreover, other factors such as temperature, hydrostatic pressure, additives, electrode area, anode material, and circulation of large volume of the liquid (and thus more representative of practical conditions in transformers) that may affect the prebreakdown current of liquid dielectrics should also be studied.

LIST OF REFERENCES

1. Rouse, T.O., Evaluation of Alternate Mineral Oils for Use in Transformers and Other Electrical Apparatus, International Symposium on Electrical Insulation, IEEE Conference Record, pp. 250-260, 1978.
2. Burrow, R.F., et al, Methods for Evaluating New Dielectric Liquids for Use in High Voltage Electrical Equipment, International Conference on Liquid Dielectrics, pp. 172-175, 1972.
3. Lockie, A.M., Time to Re-Examine Your Transformer Protection?, Electric Light and Power, T & D Edition, pp. 52-53, 1970.
4. Hosticka, C., Insulating Characteristic of Dimethyl Silicone in Bare and Insulated Uniform Field Gaps, IEEE Trans. EI - 12, pp 389-394, 1977.
5. Watson, A., and Girgis, S.S., The Influence of Electrode Separation, Geometry and an Applied Magnetic Field Upon Current Conduction in Silicone Oil, J. Electrostatic, 2, pg. 175-186, 1976.
6. Hakim, R.M., Oliver, R.G., and St.-Onge, H., The Dielectric Properties of Silicone Fluids, IEEE Trans. EI-12, pp. 360-369, 1977.
7. Nikuradse, A., Das Flussige Dielectrikum, Springer-Verleg, Heidelberg, 1934, (Text not available).
8. Zaky, A.A., Tropper, H., and House, H., Electrical Conduction in Organic Liquids, B.J. Applied Physics, 14, pp. 651-656, 1963.

9. Zaky, A.A., and Hawley, R., Conduction and Breakdown in Mineral Oil, Peter Peregrinus Limited, On behalf of the Institute of Electrical Engineering, London, 1973.
10. Kao, K.C., and Calderwood, J.H., Effects of Hydrostatic Pressure, Temperature and Impurity on Electric Conduction in Liquid Dielectrics, Proceedings, IEEE, 112, pp. 597-601, 1965.
11. Secker, P.E., and Hilton, K.J., Measurement of Breakdown Stress in Hexane Subjected to a Transverse Magnetic Field, Proceedings 4th International Conference on Conduction and Breakdown in Dielectric Liquids, Dublin, pp. 206-209, 1972.
12. Watson, A., Magneto-Surface Effects in Vacuum Breakdown, Proceedings 4th International Symposium on Discharges and Electrical Insulation in Vacuum, pp. 18-22, 1970.
13. Watson, A., Perturbation of the Static Voltage Breakdown Mechanism in Vacuum by a Weak Magnetic Field, Canadian Journal of Physics, 54, pp. 2403-2417, 1976.
14. Saveanu, L., and Mondescu, D., Phenomenes de Conduction dans les Liquides Isolants, Grenoble, pp. 385, 1968, (Text of paper unavailable).
15. Gallagher, T.J., The Influence of a Magnetic Field on the Breakdown of a Liquid, Proceedings 4th International Conference on Conduction and Breakdown in Dielectric Liquids, Dublin, pp. 210-213, 1972
16. Lewis, T.J., The Electric Strength and High-Field Conductivity of Dielectric Liquids, Prog. in Dielectrics,

1, pp. 97-140, 1959.

17. Adamczenski, I., Ionization, Conductivity and Breakdown in Dielectric Liquids, London: Taylor-Francis Ltd. pp. 335-352, 1969.
18. Sletten, A.M., Electric Strength and High-Field Conduction in n-Hexane, Nature, 183, pp. 311-312, 1959.
19. Sletten, A.M., and Lewis, T.J., The Influence of Dissolved Gasses on the Electric Strength of n-Hexane, B.J. Applied Physics, 14, pp. 883-888, 1964.
20. Gosling, C.H., and Tropper, H., The Direct Voltage Breakdown Strength of Purified Mineral Oils, Proceedings IEEE Conference of Dielectric and Insulating Materials, 1964.
21. Nelson, J.K., Salvage, B., and Sharpley, W.A., Electric Strength of Transformer Oil for Large Electrode Areas, Proceedings IEEE, 118, 2, pp. 388-393, 1971.
22. Nossier, A., and Hawley, R., Effect of Dissolved Sulphur Hexafluoride on Electrical Breakdown in Mineral Oil, Proceedings IEE, 113, 2, pp. 359-363, 1966.
23. Zein Eldine, M.E., and Tropper H., The Electric Strength of Transformer Oil, Proceedings IEE, 103c, pp. 35-45, 1956.
24. Ganger, B.E., The Breakdown Voltage of Oil Gaps with High D.C. Voltage, IEEE Transcript, PAS-98, pp. 1840-1843, 1968.
25. Kao, K.C. and Higham, J.B., The Effects of Hydrostatic Pressure, Temperature, and Voltage Duration on the Electric Strengths of Hydrocarbon Liquids, J. Electrochem. Soc., 108, pp. 522-528, 1961.

26. Lewis, T.J., Electrical Breakdown in Organic Liquids, Proceedings IEE, Part IIA, 100, pp. 141-148, 1953.
27. Farazmand, B., Study of Electric Breakdown of Liquid Dielectrics Using Schlieren Optical Techniques, B.J. Applied Physics, 12, pp. 251-254, 1961.
28. Chadband, W.G., and Wright, G.T., A Prebreakdown Phenomenon in the Liquid Dielectric Hexane, B.J. Applied Physics, 16, pp. 305-313, 1965.
29. Watson, A., Some Factors and Associated Mechanisms Influencing High Voltage Insulation Failure in Vacuum, A Ph.D. Thesis, Gesamthochschule, Kassel, W. Germany, 1978.
30. Swan, D.W., and Lewis, T.J., The Influence of Cathode and Anode Surfaces on the Electric Strength of Liquid Argon, Proceedings, Phys. Soc., 78, pp. 448-459, 1961.
31. Gallagher, T.J., and Lewis, T.J., The Influence of Electrode Surfaces on the Electric Strength of Liquid Argon at Small Spacings, B.J. Applied Physics, 15, pp. 491-498, 1964.
32. Cullingford, M.C., Zaky, A.A., ZeinEldine, M., and Hawley, R., Influence of Electrode Coatings on Conduction Currents in Transformer Oil, Nature, 199, pp. 1082-1083, 1963.
33. ZeinEldine, M.E., Zaky, A.A., Hawley, R., and Cullingford, M.C., Influence of Insulating Films on Conduction, Proceedings IEE, 112, 3, pp. 580-585, 1965.
34. Zaky, A.A., ZeinEldine, M.E., and Hawley, R., Influence of Electrode Coatings in the Breakdown Strength of Transformer Oil, Nature, 202, pp. 687-688, 1964.

35. Zaky, A.A., ZeinEldine, M.E., and Hawley, R., Electric Strength of Mineral Oil Using Bare and Coated Electrodes, B.J. Applied Physics, 16, pp. 437-440, 1965
36. Zaky, A.A., Nossiers, A., and Megahed, I.Y., The Effect of Surface Oxide Films on the Apparent Zero-Gap Breakdown Voltage in Mineral Oil, J. Physics, 10, pp. L43-L45, 1977.
37. Weber, K.H., and Endicott, H.S., Area Effect and its External Basis for the Electric Breakdown of Transformer Oil, Trans. Am. Inst. Elec. Eng., 75, pp. 371-381, 1956.
38. Weber, K.H., and Endicott, H.S., Extremal Effect for Large Area Electrodes for the Electric Breakdown of Transformer Oil, Ibid, 76, pp. 1091-1098, 1957
39. Sharbaugh, A.H., Cox, E.B., Crowe, R.W., and Aver, P.L., The Effect of Electrode Configuration on the Electric Strength of Hexane, National Academy of Science, NRC, Washington, D.C., Annual Report of the Conference on Electrical Insulation, 396, pp. 16-20, 1955, (Text of report unavailable).
40. Dickson, M.R., The Causes and Effects of Water in Oil-Immersed Transformers, J. Inst. Petroleum, 37, pp. 373-379, 1951.
41. Kaufman, R.B., Shimanski, E.J. and McFadyen, K.W., Gas and Moisture Equilibrium in Transformer Oil, Trans. Am. Inst. Elec. Eng., 74, pp. 312-318, 1955.
42. Fallou, B., and Thibault, M., Quelques Motions Relatives a l'Humidification des Huiles Isolants Usagees, Revue Gen. Elec. 72, pp. 242-247, 1963, (Text of paper unavailable)

43. Abed, J., The Effect of Water on the Dielectric Strength of Mineral Oil for Very Small Electrode Gaps, (In Polish) Prace Naukowe Inst. Podstaw Elektrotech & Elektrochnol. Politech. Wroctawskiej, 1, pp. 5-21, 1968 (Text of paper unavailable).
44. Kaplan, D.A., and Kutchinski, G.C., Influence of Humidity on the Electric Strength of Transformer Oil, (In Russian) Elektrotehnika, 35, pp. 30-33, 1964, (Text of paper unavailable).
45. Ferrant, W., Effect of Pressure on Breakdown in Liquid Dielectrics, Z. Phys. 89, pp. 317-356, 1934, (Text of paper unavailable).
46. Maksiejewski, J.L., and Tropper, H., Some Factors Affecting the Measurement of the Electric Strength of Organic Liquids, Proceedings IEE, 101, pp. 183-190, 1954.
47. Hug, A.M.Z., and Tropper, H., Conduction Current Pulses in Organic Insulating Liquids Under Electrical Stress, B.J. Applied Physics, 15, pp. 481-490, 1964.
48. Ostroumov, G.A., Results of Measurements of the Electrical Conductivity of Insulating Liquids, Soviet Phys. JETP, 14, pp. 317-319, 1962.
49. Abiri, M.A., Watson, A., and Raghuveer, M.R., The Influence of Electrode Material Upon Prebreakdown Current in Viscous Dielectric Oil, Conference on Electrical Insulation and Dielectric Phenomena, paper No. F-7, Assembly of Engineering, NRC, Washington, D.C., 1980.
50. Alston, L.L., High Voltage Technology, Oxford University

- Press, pp. 95-128, 1968.
51. Hart, J., and Mungall, A.G., The Electrical Conductivity of Chlorinated Hydrocarbons, Trans. Am. Inst. Elec. Eng., 76, pp. 1295-1301, 1958.
 52. Swan, D.W., A Review of Recent Investigations into Electrical Conduction and Breakdown of Dielectric Liquids, B.J. Applied Physics, 13, pp. 208, 1962.
 53. Harper, H.R., Contact and Frictional Electrification, Oxford University Press, pp. 184-186, 1967.
 54. Mirza, J.S., Smith, C.W., and Calderwood, J.H., Liquid Motion and Internal Pressure in Electrically Stressed Insulating Liquids, J. Phys. D., 3, pp. 580-585, 1970.
 55. Heylen, A.E.D., and Bunting, K.A., Electron Drift Velocities in a Moderate and in a Strong Crossed Magnetic Field, Vol. 27, 1, pp. 1-12, 1969.
 56. Lewis, T.J., High Field Electron Emission from Irregular Cathode Surfaces, T. Applied Physics, 26, pp. 1405-1410, 1955.
 57. Sillars, R.W., Electrical Insulating Materials and their Application, Peter Peregrinus Ltd., on behalf of the IEE, London, pp 50-60, 1973.
 58. Fowler, R.H., and Nordheim, L.W., Electron Emission in Intense Electric Fields, Proc. Roy. Soc. A119, pp 173-181, 1928.
 59. Girgis, S.S., The Influence of a Magnetic Field upon the Prebreakdown Current in Silicone Oil, M.Sc. Thesis, University of Western Ontario, London, Ontario, 1974.

APPENDICES

APPENDIX I

SPECIFICATIONS OF THE VARIABLE AUTO TRANSFORMER AND
MODEL 616 DIGITAL ELECTROMETER

1. The variable autotransformer was with the following specifications:

Primary voltage 240 V, 1 Ph, 50/60 HZ

Output voltage 0 - 280 V

Maximum A 28, maximum KVA 7.8

The driving motor was specified as:

Volts 120, A 0.4, Frequency 50/60 cps

Travel time - 5 sec and 72 rpm

2. The condensed specifications of the Model 616 electrometer as an ammeter were as follows:

Range: $\pm 10^{-16}$ A per digit (10^{-13} A full range)
to ± 0.1 A full range in 13 decade ranges. 100% over
ranging to 1999 on all ranges.

Accuracy (20°C to 30°C)

Range Switch Setting

Accuracy

10^{-1} to 10^{-7} A

\pm (0.5% of reading + 0.1% of range)

10^{-8} A

\pm (2% of reading + 0.1% of full range)

10^{-9} to 10^{-11} A

\pm (5% of reading + 0.1% of range)

Noise: 2×10^{-15} A peak to peak on the most sensitive range, exclusive of alpha particle disturbance.

Offset Current: Less than 5×10^{-15} A

Analog Output: 1 volt output for monitoring an analog signal.

For DC inputs, output is equal to ± 1 volt at up to 1 mA corresponding to a full scale input. In both modes the output polarity is opposite input polarity.

To use the Model 616 as a pico ammeter, the front panel controls were set as follows:

Range - 10^{-5} A

Sensitivity - Auto

FAST/NORMAL - FAST

Connections to the Model 616 were made using a shield triaxial cable. The zero control needed occasional adjustment to reduce voltage offset due to temperature variations. To zero the Model 616, the ZERO CHECK switch was set to CHECK position and the front panel ZERO control was adjusted for a 0.00-0.00 display.

APPENDIX II

Figures (II.1-II.15) are examples of some of the results obtained for different ramp application time. In the experimental work the main source of error was due to non-reproducibility of short term conditions. The voltage versus current characteristics were obtained by taking the average value of the curves (1) and (2) of Figure (II). These curves represent the average value of fifteen experiments. As can be seen from the Figure (II.4) the curves approximately coincided with each other for the long term conditioning. To have an idea of the uncertainty of the linearity of the ultimate section of the Fig. (4.10) four sets of experiments were carried out. From series II-IV it was seen that there is no doubt about the shape of the curve which was always linear. There is, however, uncertainty in the position of each curve and this is due to the statistical error associated with the electrode conditioning phenomenon.

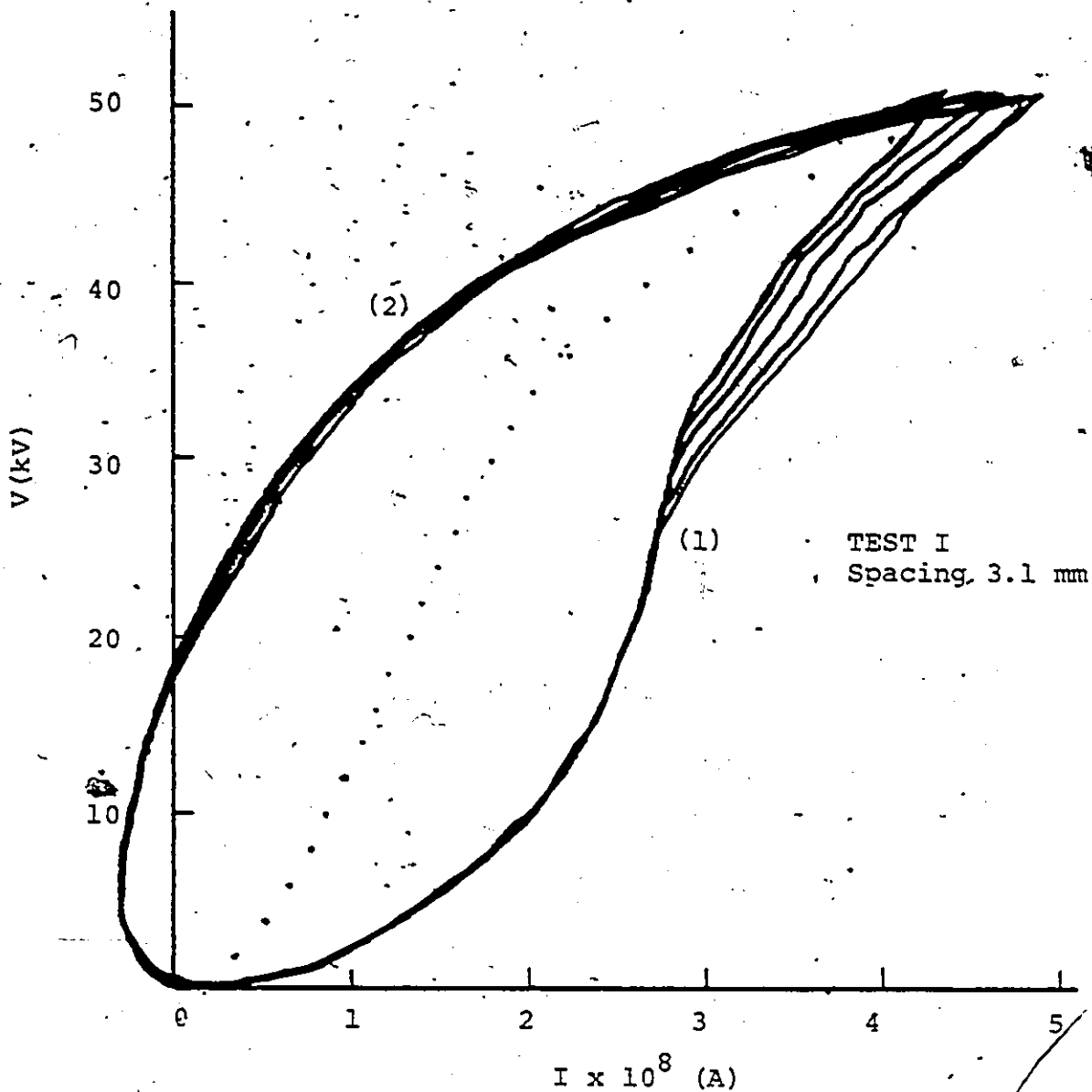


Figure II.1: Voltage Versus Current Characteristics for Hemispherical Zinc Electrodes using 5^C.S. Silicone Oil at Room Temperature and 55% Humidity. (Dotted Points Represent Average of the Curves 1 and 2).

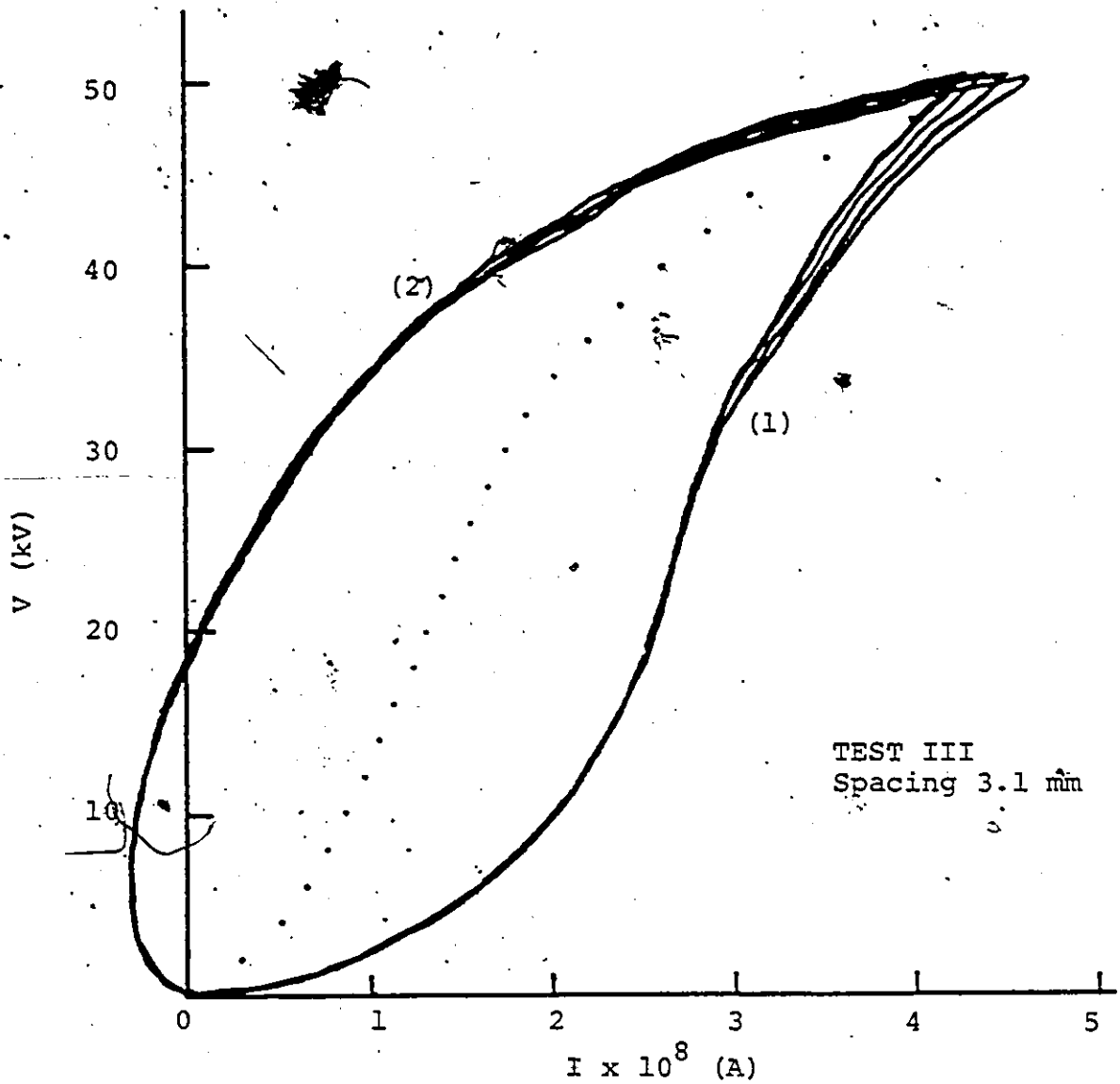


Figure II.2: Voltage Versus Current Characteristics for Hemispherical Zinc Electrodes using 5°C.S. Silicone Oil at Room Temperature and 55% Humidity
(Dotted Points Represent Average of the Curves 1 and 2)

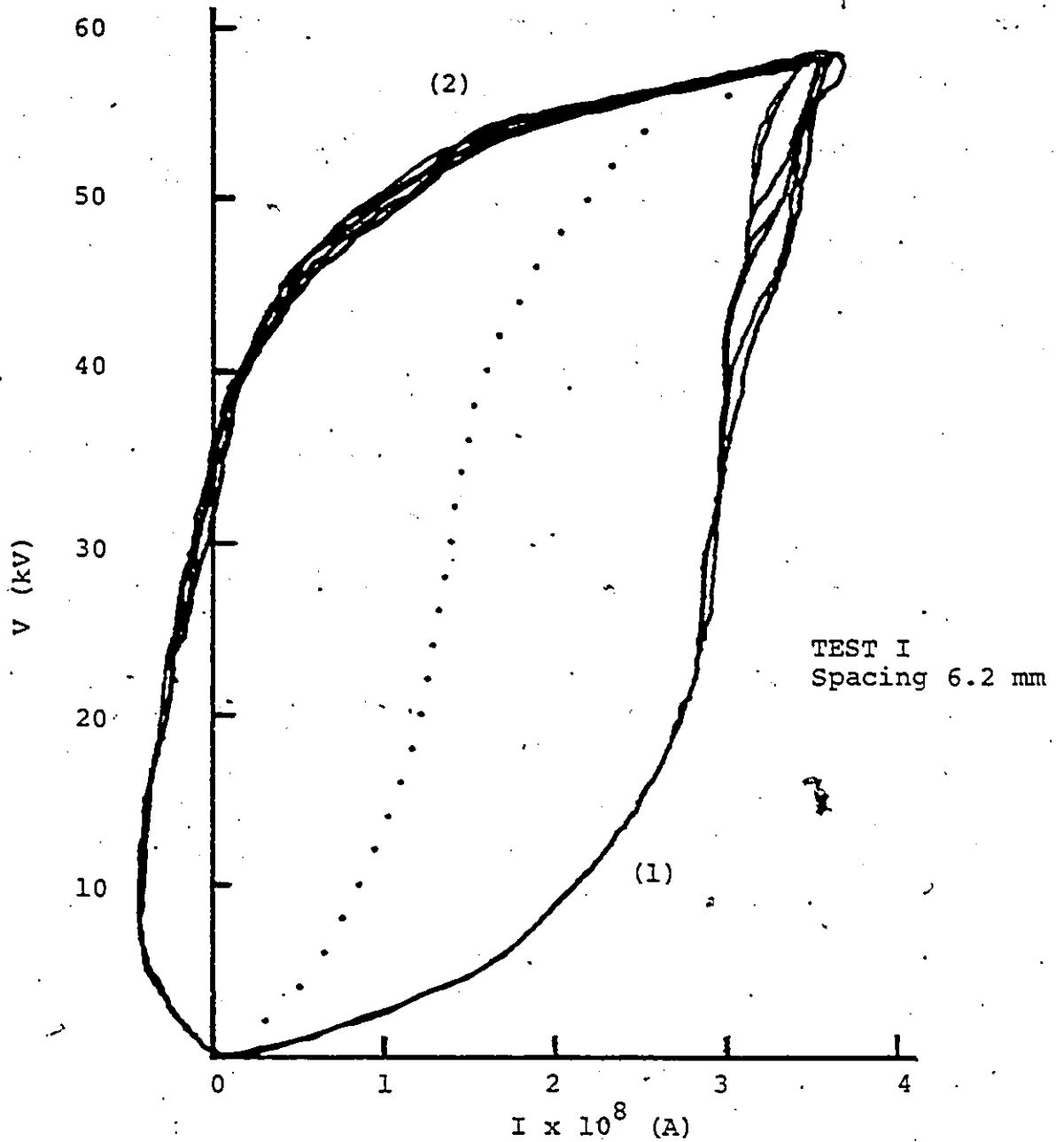


Figure II.3: Voltage Versus Current Characteristics for Hemispherical Zinc Electrodes using 5^{c.s.} Silicone Oil at Room Temperature and 55% Humidity
(Dotted Points Represent Average of the Curves 1 and 2)

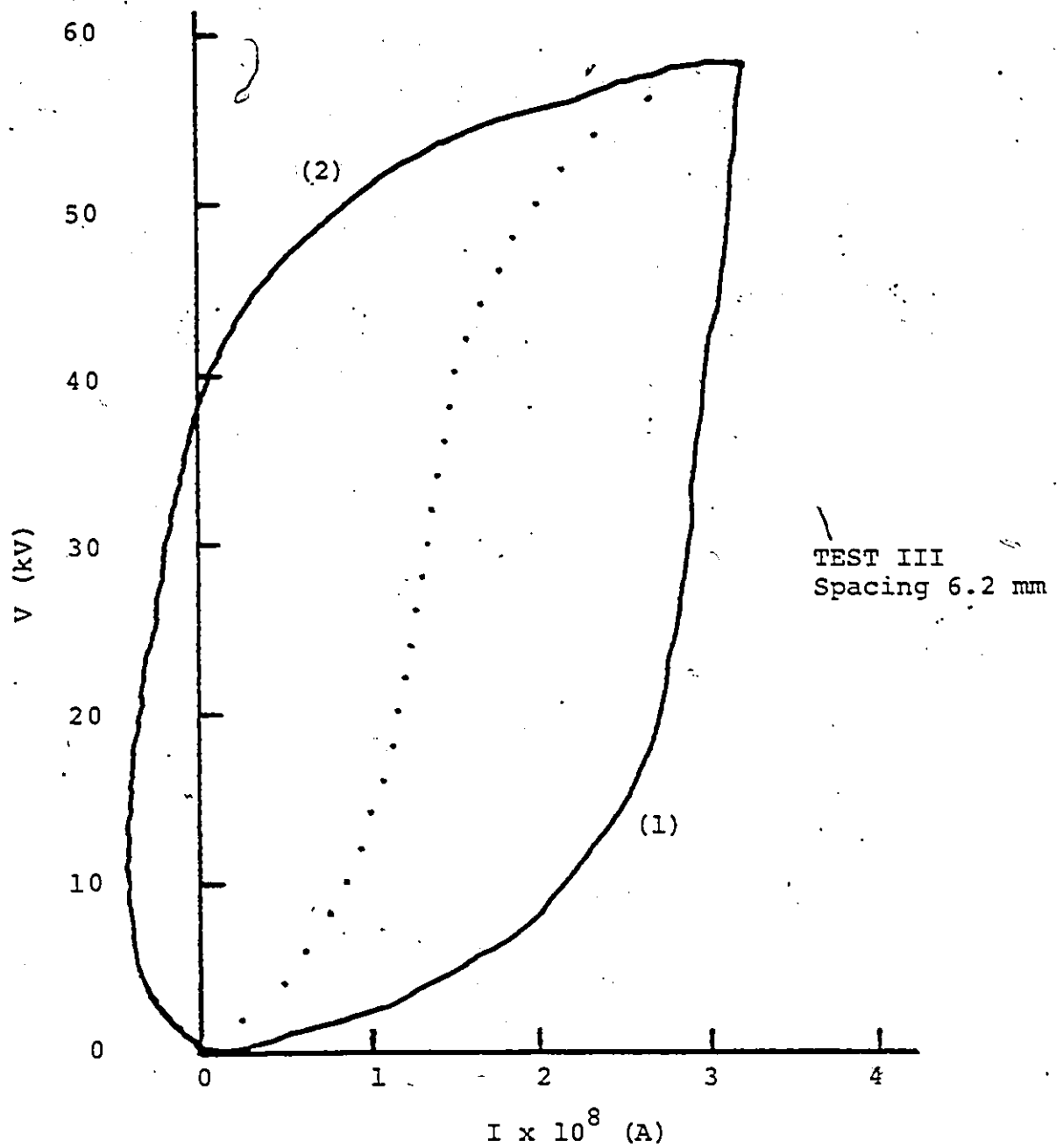


Figure II.4: Voltage Versus Current Characteristics for Hemispherical Zinc Electrodes using 5^{C.S.} Silicone Oil at Room Temperature and 55% Humidity
(Dotted Points Represent Average of the Curve 1 and 2)

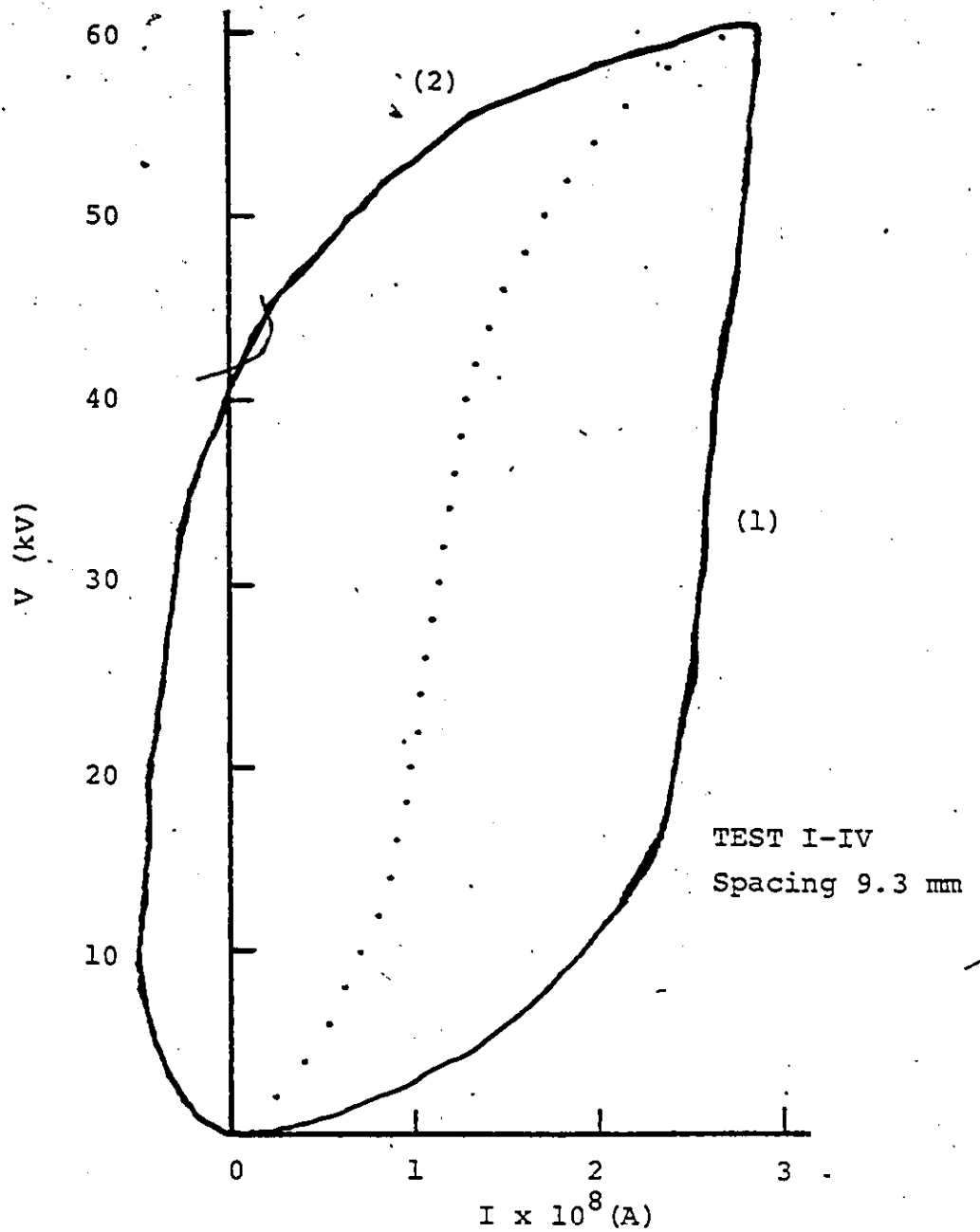


Figure II.5: Voltage Versus Current Characteristics for Hemispherical Zinc Electrodes using 5C-S-Silicone Oil at Room Temperature and 55% Humidity
(Dotted Points Represent Average of the Curve 1 and 2)

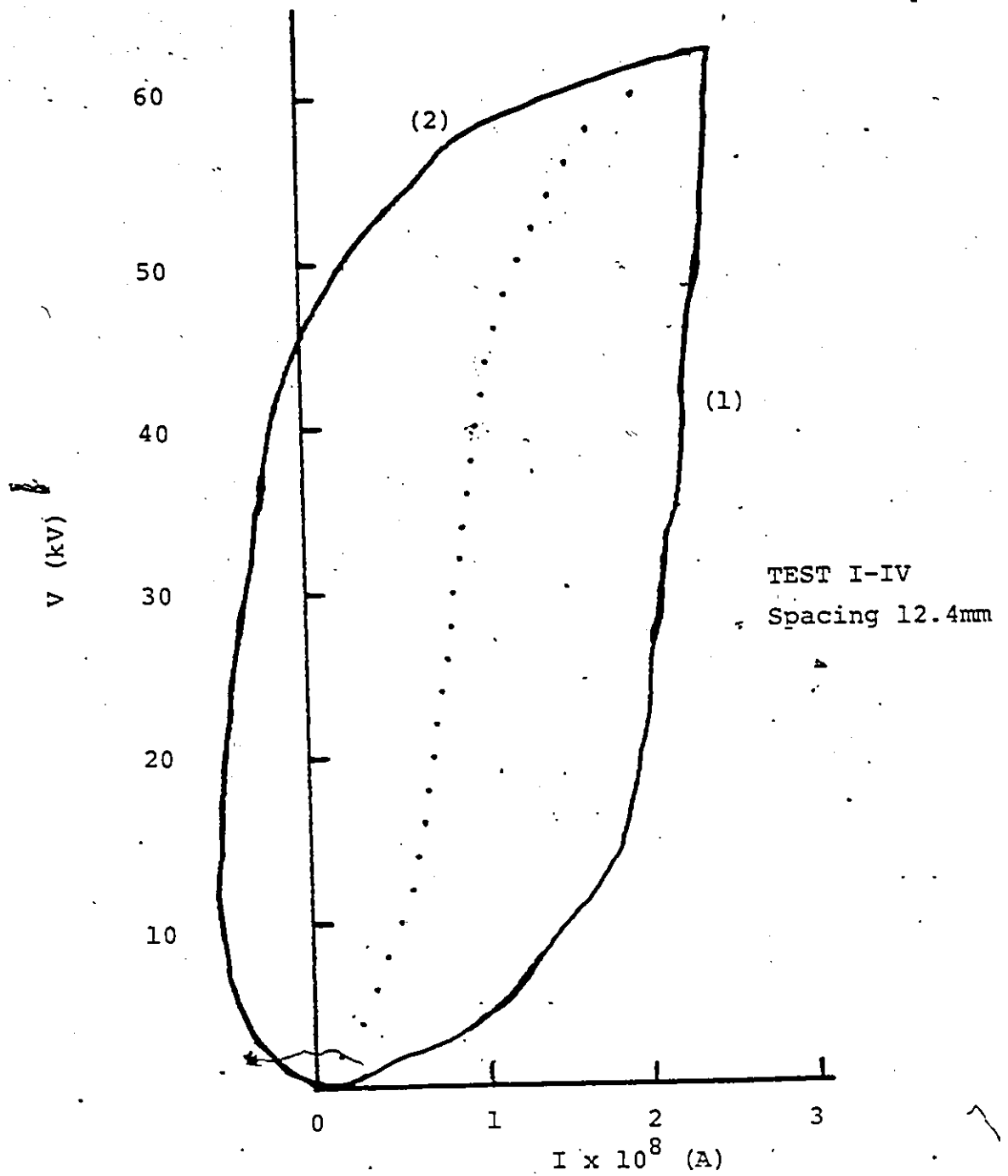


Figure II.6: Voltage Versus Current Characteristics for Hemispherical Zinc Electrodes using 5^{C.S.} Silicone Oil at Room Temperature and 55% Humidity (Dotted Points Represent Average of the Curve 1 and 2)

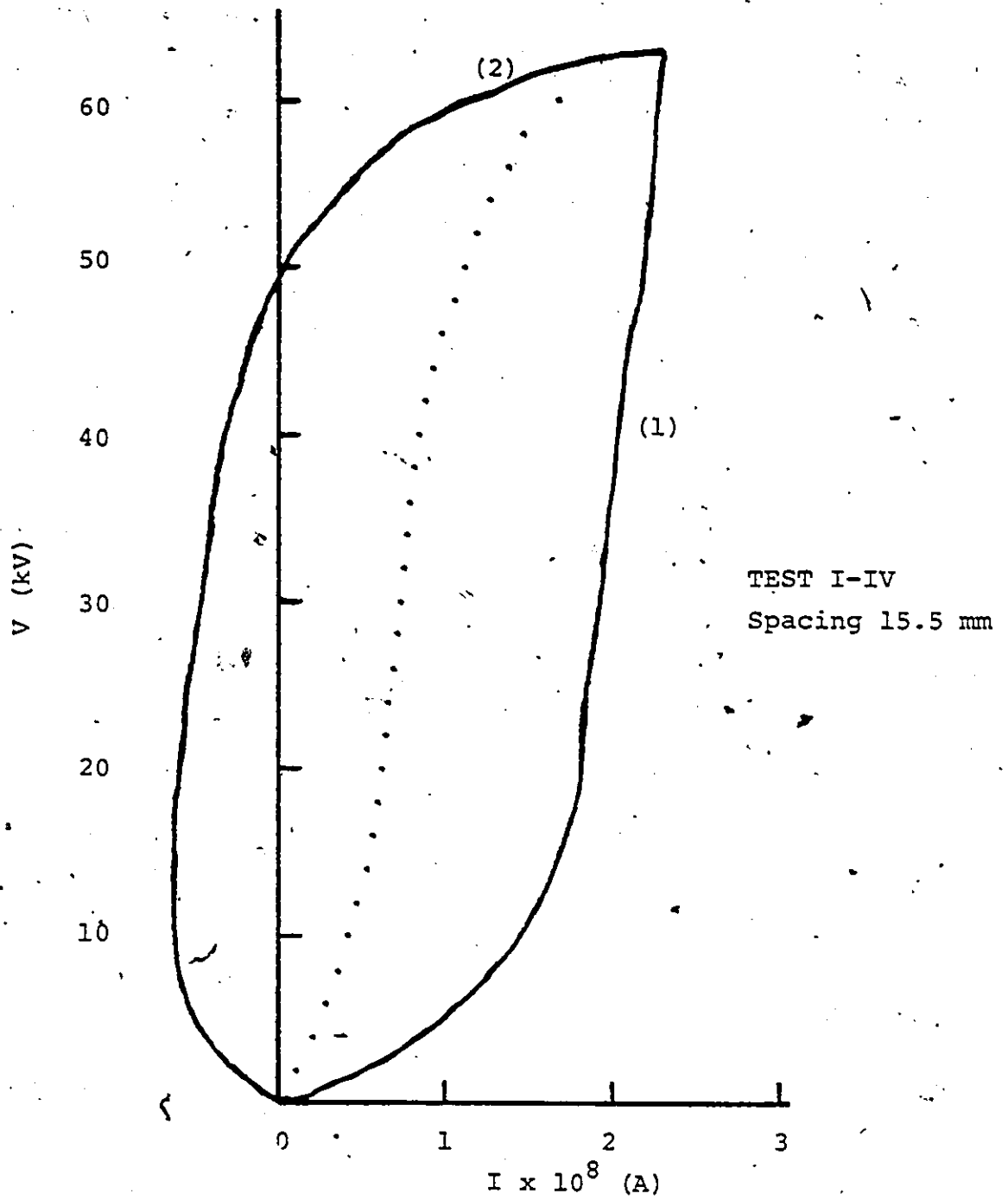


Figure II.7: Voltage Versus Current Characteristics for Hemispherical Zinc Electrodes using 5^{C.S.} Silicone Oil at Room Temperature and 55% Humidity (Dotted Points Represent Average of the Curve 1 and 2)

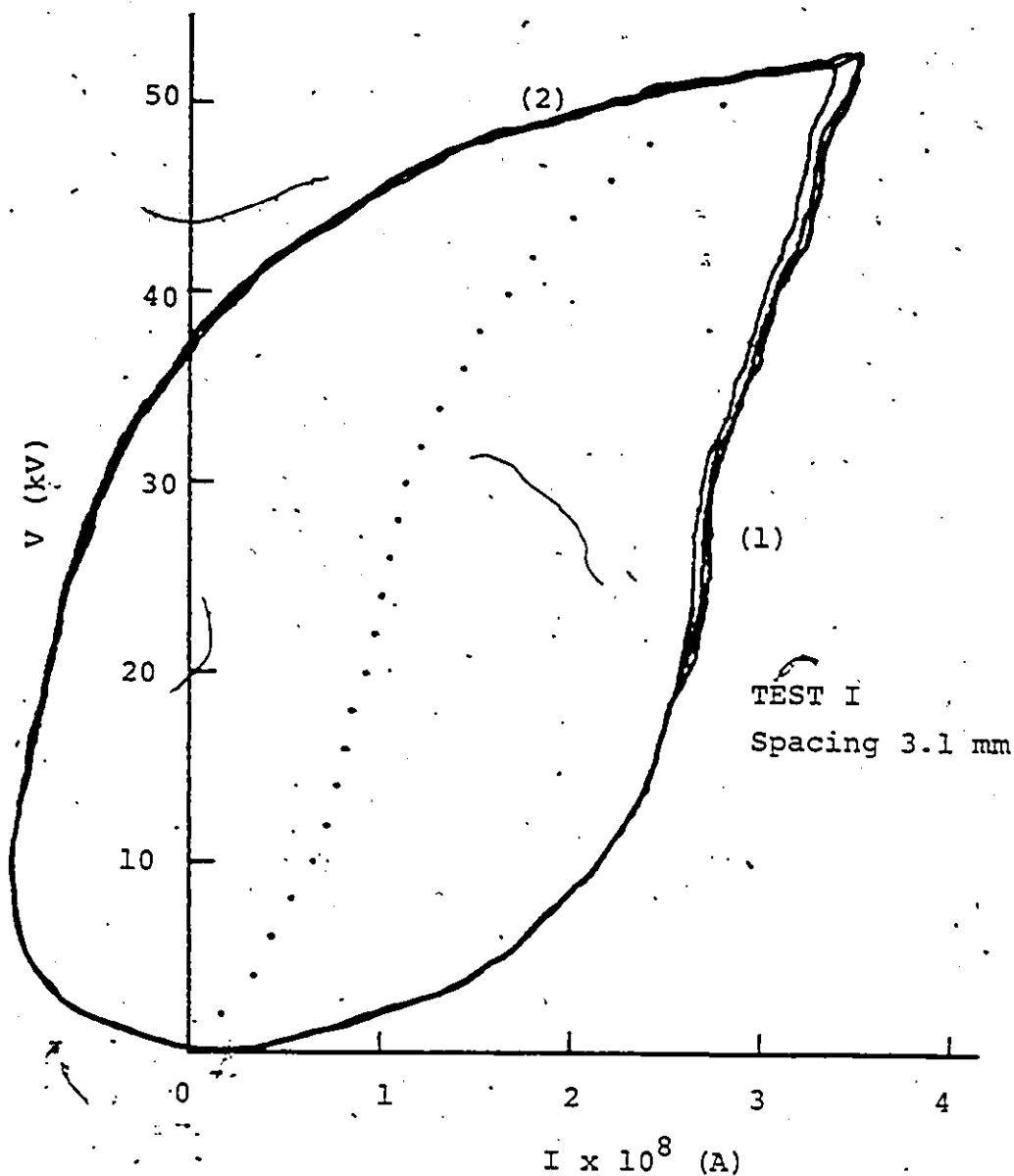


Figure II.8: Voltage Versus Current Characteristics for Hemispherical Zinc Electrodes using 350^{C.S.} Silicone Oil at Room Temperature and 55% Humidity (Dotted Points Represent Average of the Curve 1 and 2)

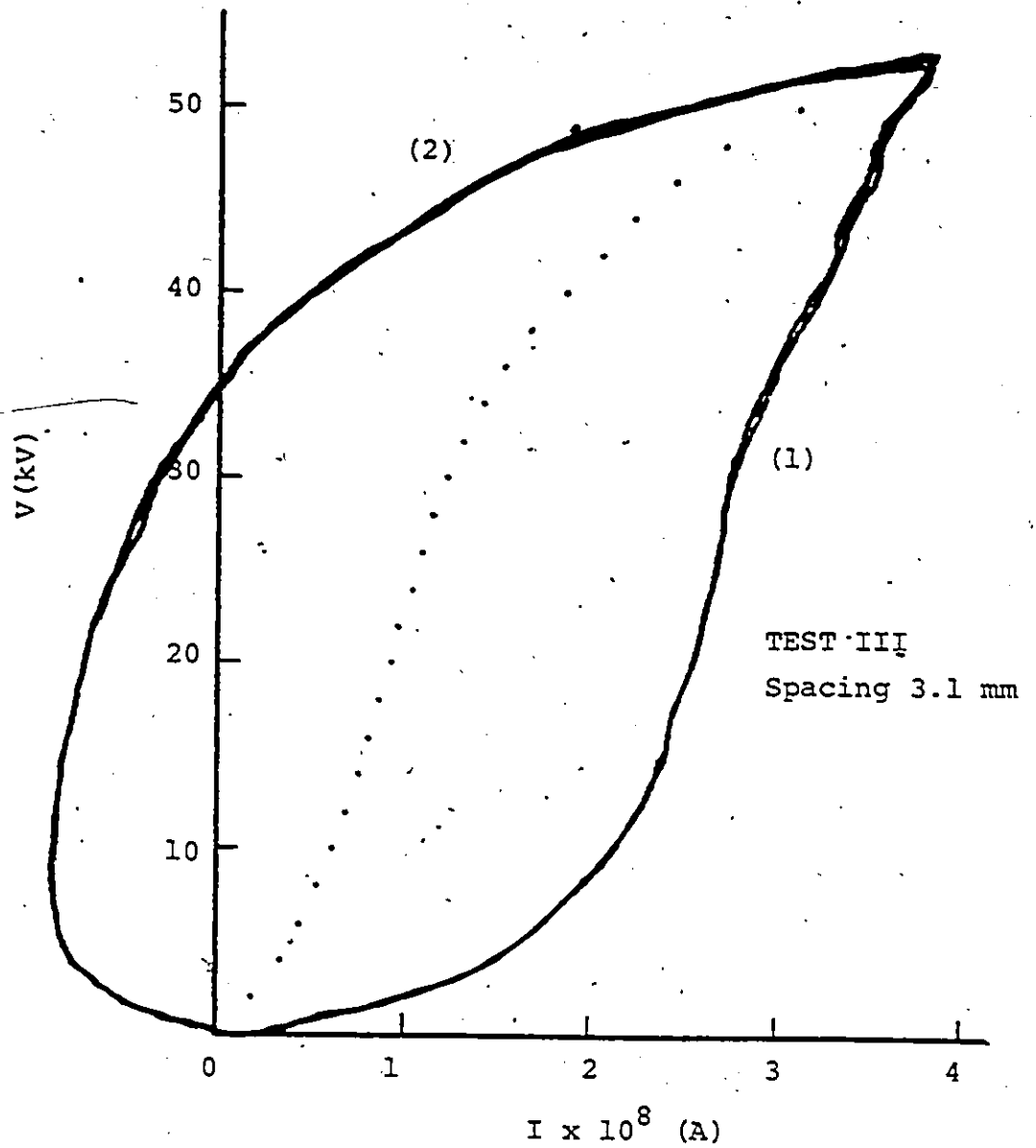


Figure II.9: Voltage Versus Current Characteristics for Hemispherical Zinc Electrodes using 350°C.S. Silicone Oil at Room Temperature and 55% Humidity
(Dotted Points Represent Average of the Curve 1 and 2)

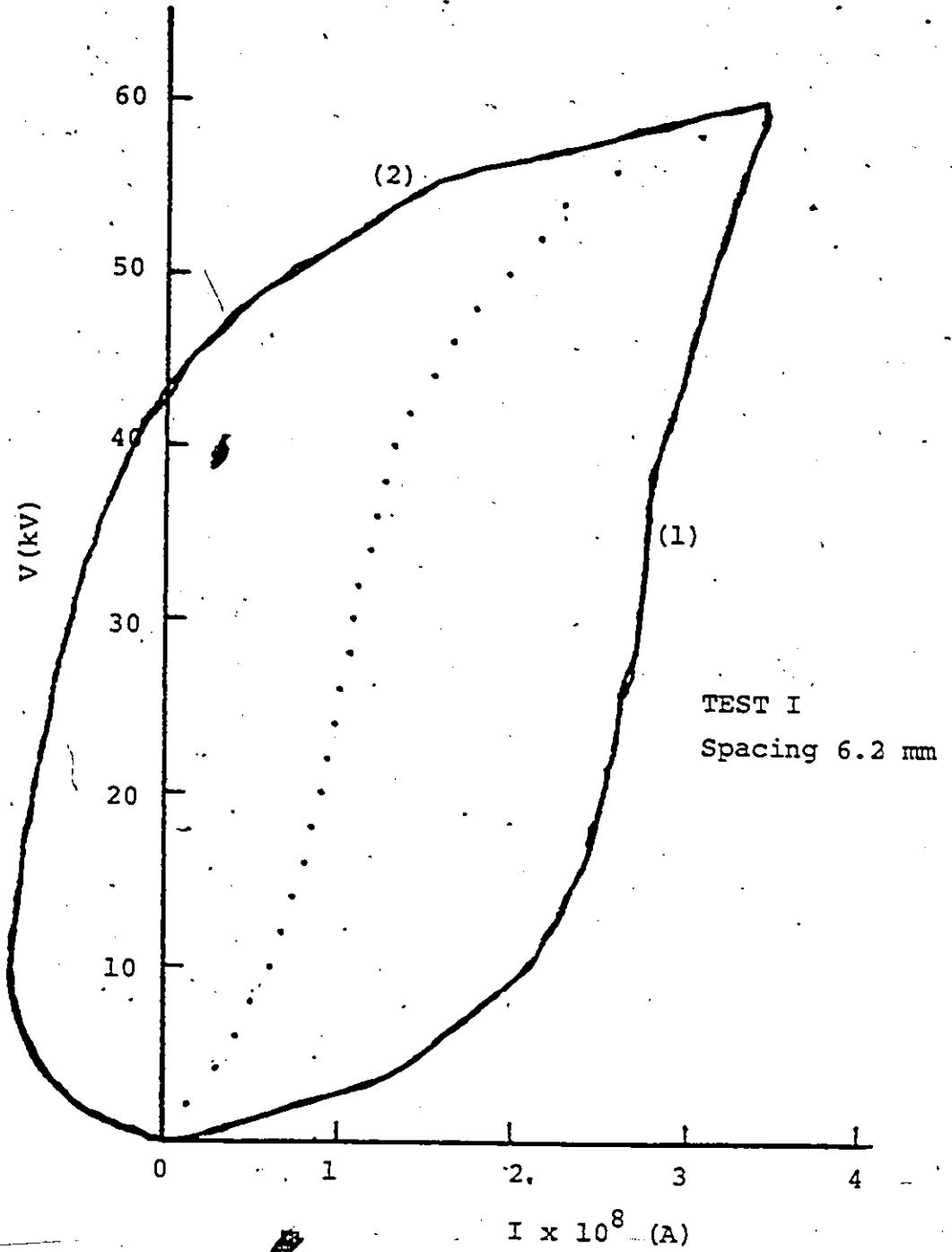


Figure II.10: Voltage Versus Current Characteristics for Hemispherical Zinc Electrodes using 350C.S. Silicone Oil at Room Temperature and 55% Humidity (Dotted Points Represent Average of the Curve 1 and 2)

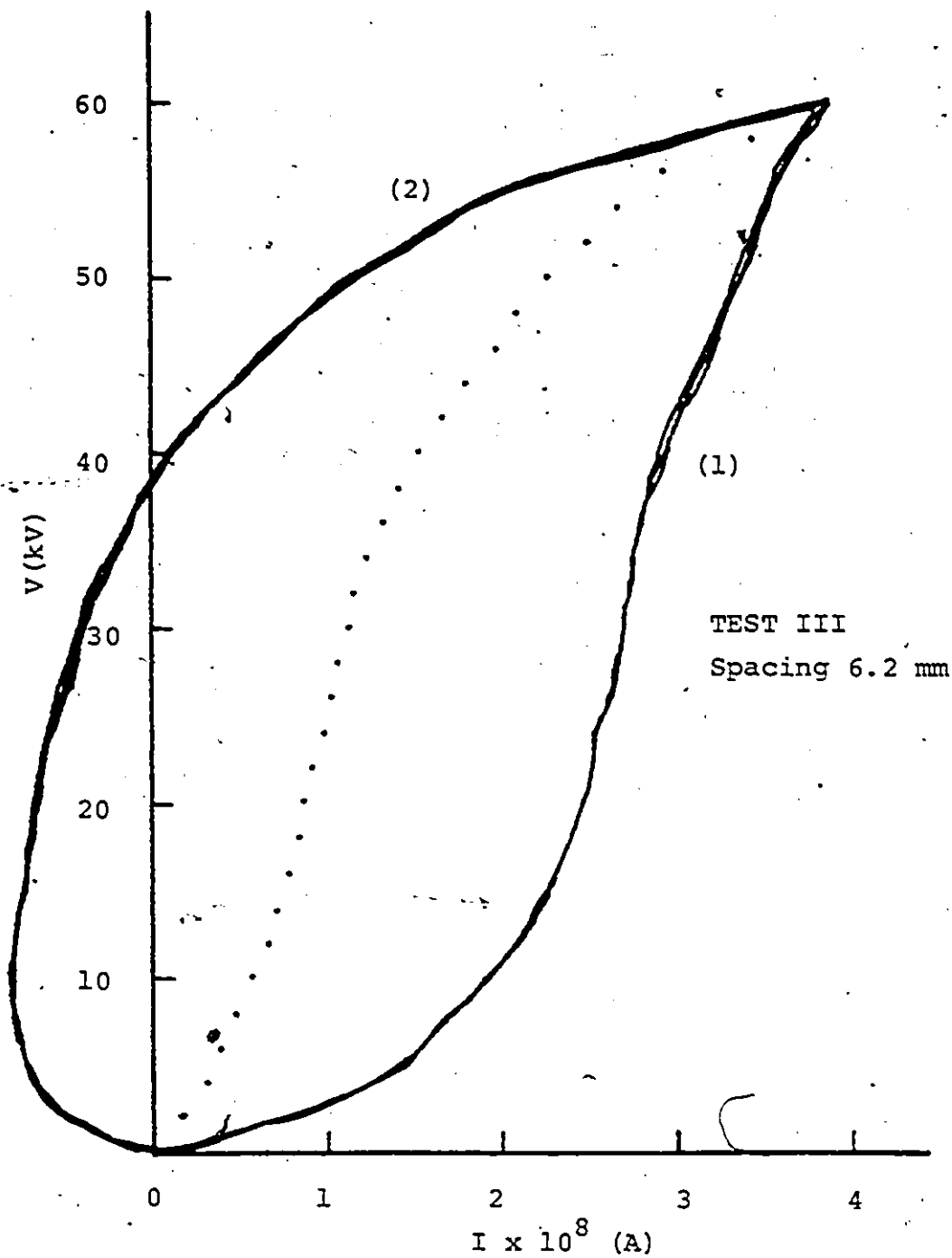


Figure II.11: Voltage Versus Current Characteristics for Hemispherical Zinc Electrodes using 350C.S. Silicone Oil at Room Temperature and 55% Humidity
(Dotted Points Represent Average of the Curve 1 and 2)

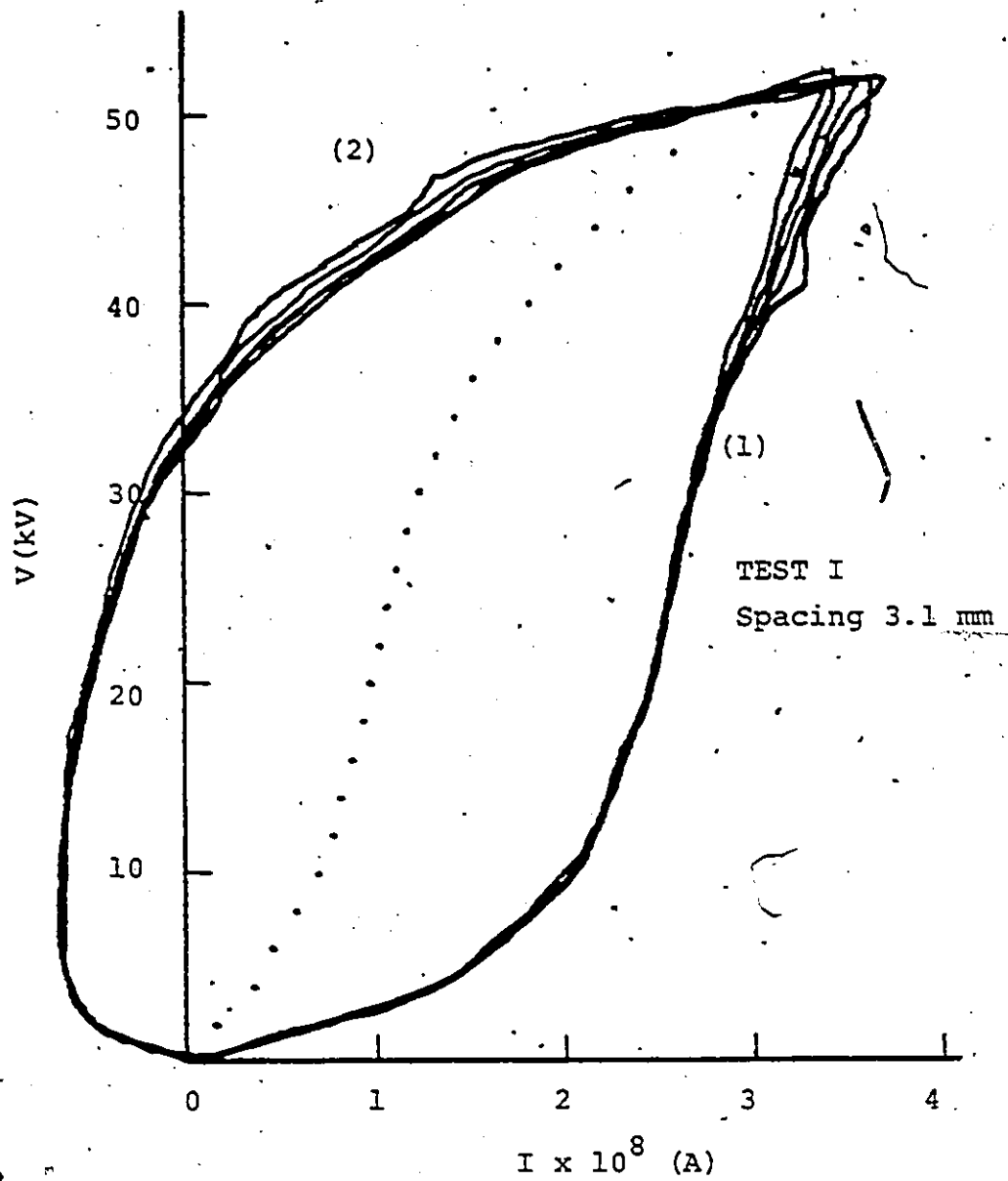


Figure II.12: Voltage Versus Current Characteristics for Hemispherical Zinc Electrodes using 1000^{C.S.} Silicone Oil at Room Temperature and 55% Humidity
(Dotted Points Represent Average of the Curve 1 and 2)

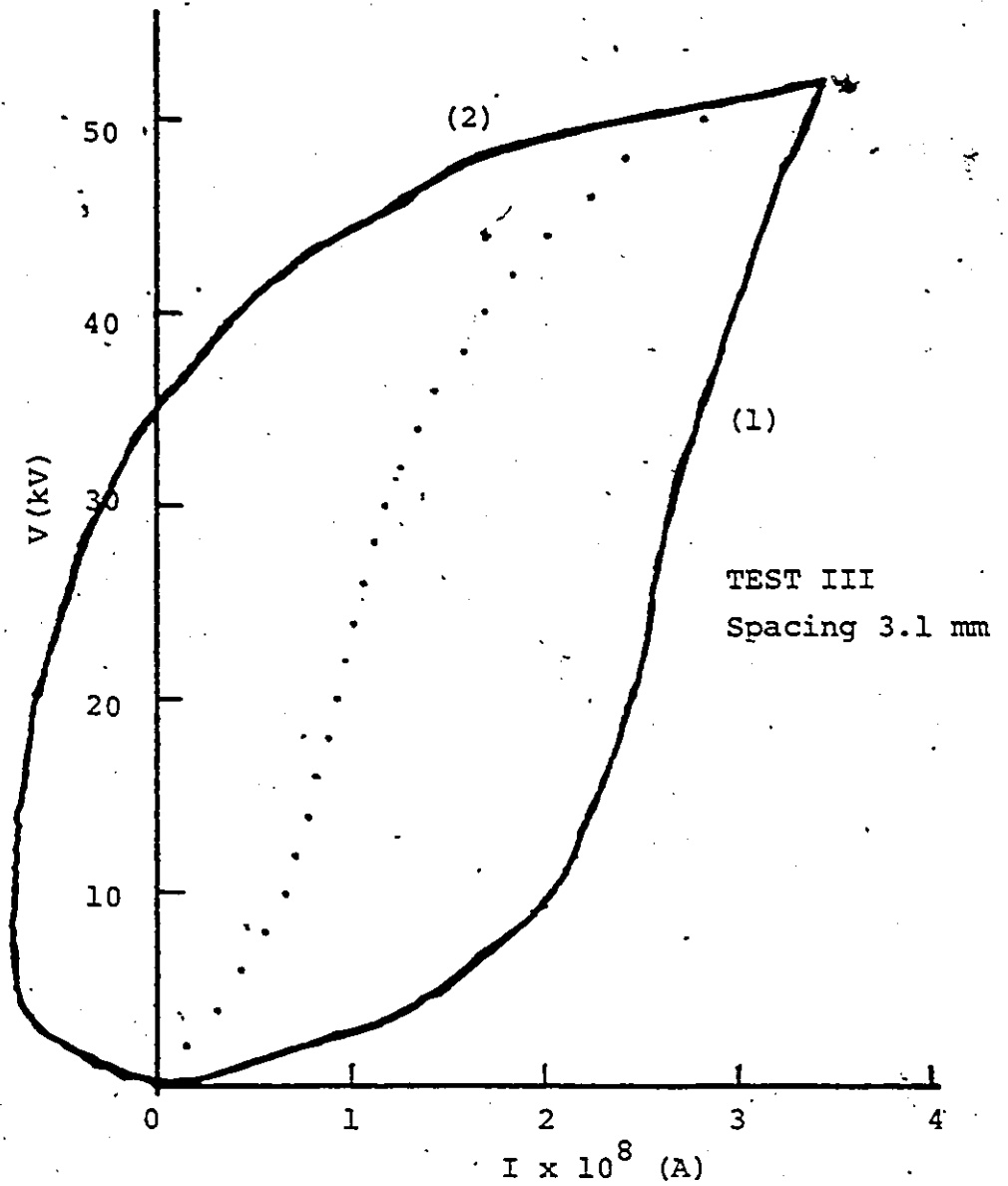


Figure II.13: Voltage Versus Current Characteristics for Hemispherical Zinc Electrodes using 1000C.S. Silicone Oil at Room Temperature and 55% Humidity (Dotted Points Represent Average of the Curve 1 and 2)

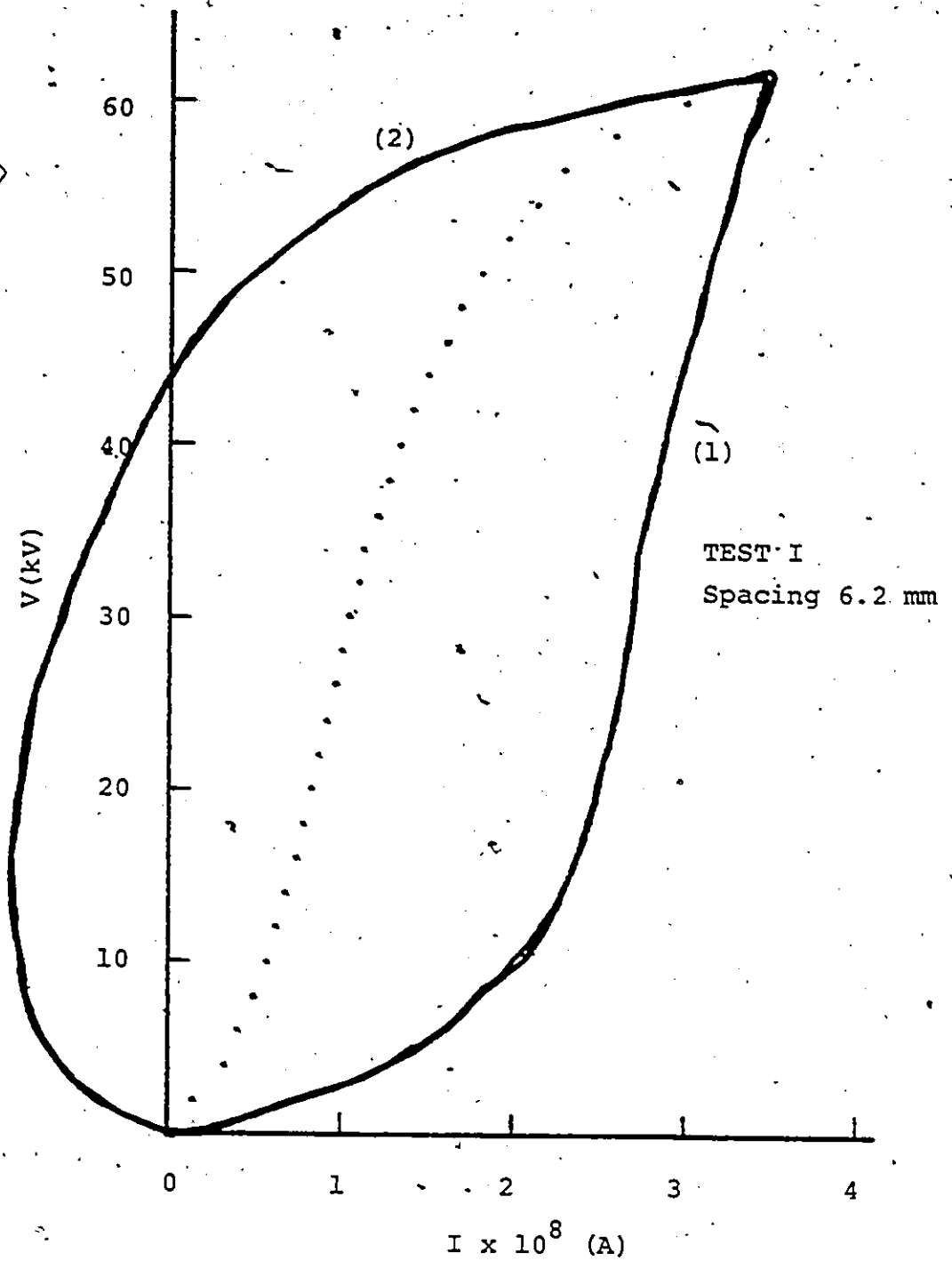


Figure II.14: Voltage Versus Current Characteristics for Hemispherical Zinc Electrodes using 1000C.S. Silicone Oil at Room Temperature and 55% Humidity (Dotted Points Represent Average of the Curve 1 and 2)

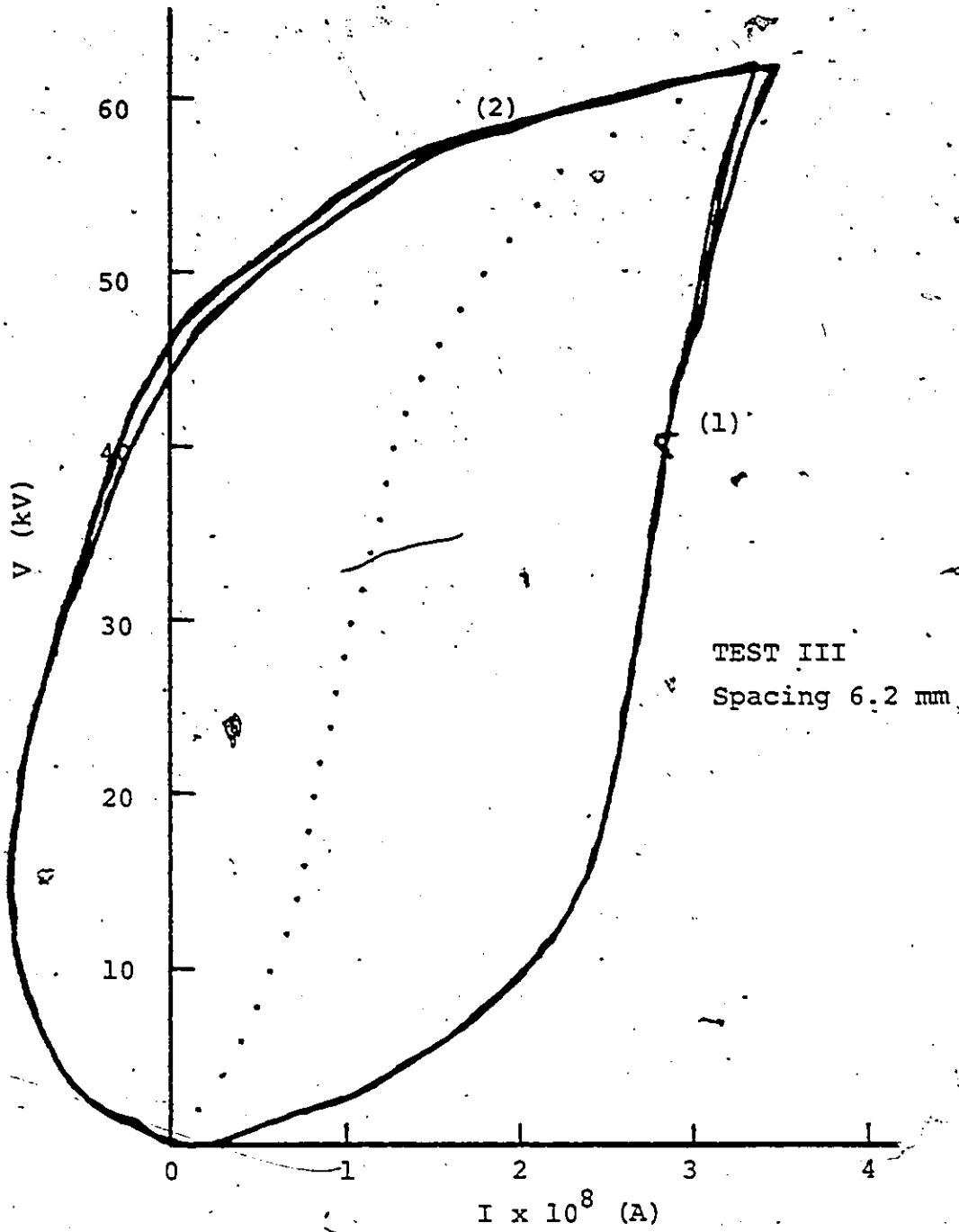


Figure II.15: Voltage Versus Current Characteristics for Hemispherical Zinc Electrodes using 1000^{C.S.} Silicone Oil at Room Temperature and 55% Humidity (Dotted Points Represent Average of the Curve 1 and 2)

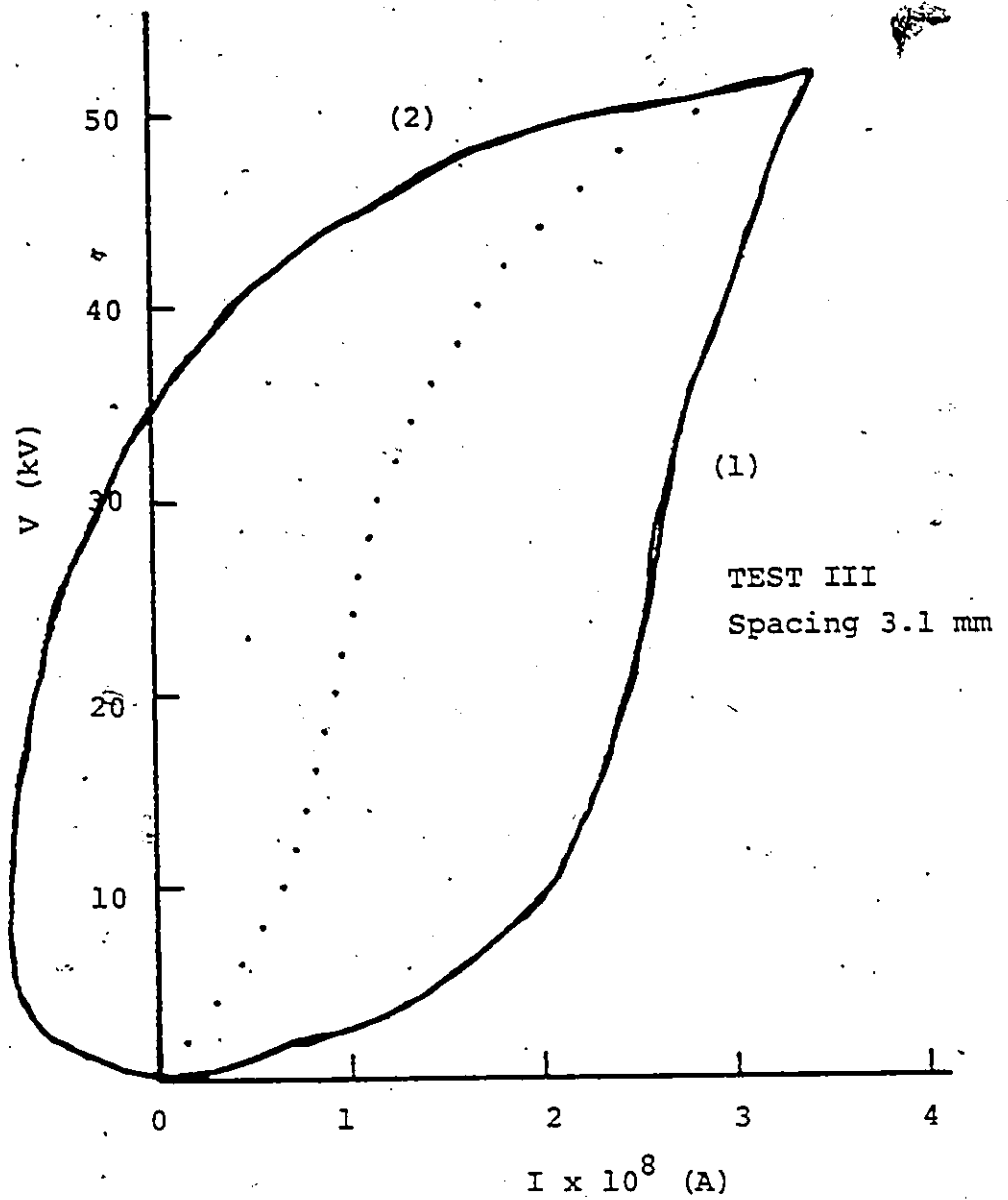


Figure II.16: Voltage Versus Current Characteristics for Hemispherical Copper Electrodes using 350c.s. Silicone Oil at Room Temperature and 55% Relative Humidity (Dotted Points Represent Average of the Curve 1 and 2)

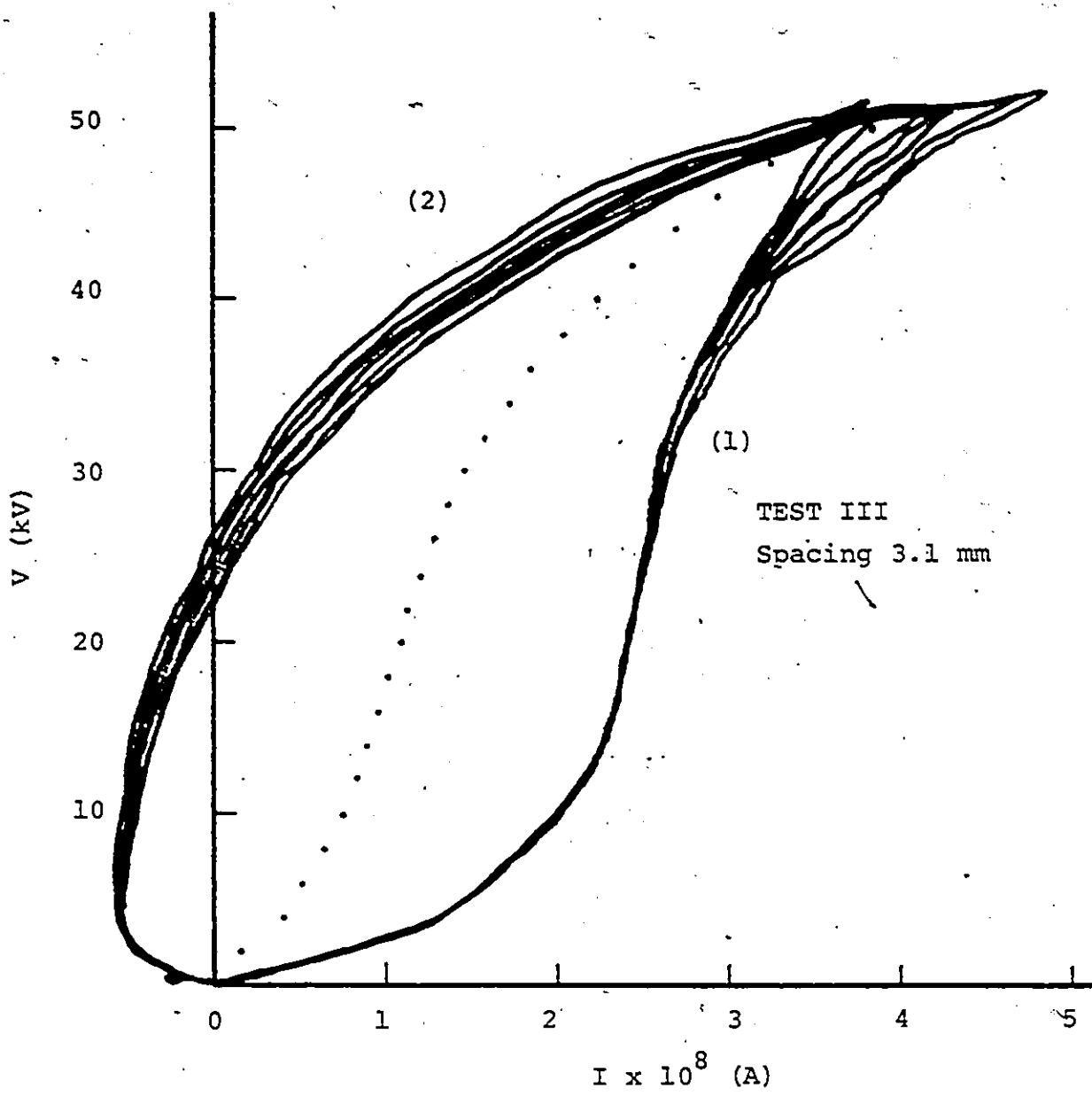


Figure II.17: Voltage Versus Current Characteristics for Hemispherical Copper Electrodes using 350C.S. Silicone Oil at Room Temperature and 80% Relative Humidity
(Dotted Points Represent Average of the Curve 1 and 2)

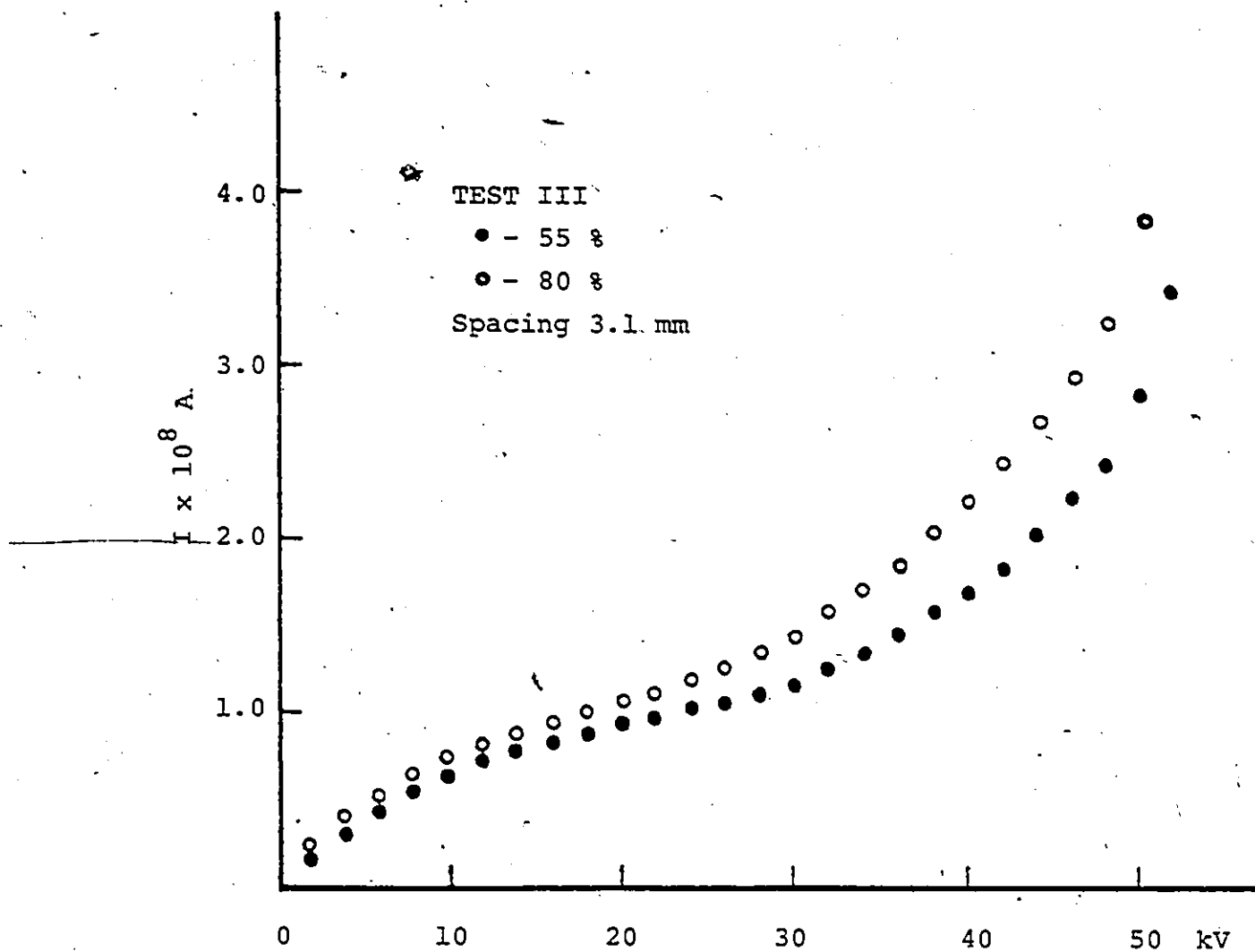


Figure II.18: The Current-Voltage Characteristics for Hemispherical Copper Electrodes using 350^{C.S.} Silicone Oil at Room Temperature and Different Relative Humidities

APPENDIX III

The well known tendency of oil to display movement when under stress suggests that charges injected into the liquid from an electrode attaching themselves to oil molecules in the neighbourhood cause this oil to be attracted to the opposite electrode where some of its charge may be given up, thus producing a convection of charge independent of conductivity. These movements have been observed by many authors (e.g. Hewish and Brignell, 1972). Watson [5] considered the motion of the liquid in the form of a vortex cell enclosing a steady (ρ_m and $u = \text{const.}$) irrotational (this is the case when vorticity, ω , vanishes) funnel flow through its core. Negative charge is trapped in the moving core of liquid dielectric and the space charge is contained laterally by the tendency of the vortex ring to resist stretching by the outward component of the electrostatic Maxwell stress. Upon raising the applied voltage the Maxwell stress from this space charge will increase and extend the vortex with strength ω which results in a stationary current channel of diameter λ after emission from a cathode protrusion at an expansion rate $(dx^2)/(dt)$ which is equal to the dynamic viscosity of the fluid, η .

The experimental results of current "conduction" in silicone oil lead us to the following expression:

$$\frac{d(\ln V)}{d(\ln I)} = md + c \quad \dots \text{A3.1}$$

where d is the electrode spacing and m and c are constants.

The behaviour expressed by Eqn. (A3.1) has been accounted for [5] in terms of the Fowler-Nordheim equation for field emission of electrons into the liquid dielectric, under any assumption that conduction current consists wholly of electrons injected in this way. Changes in this current occur when the voltage is raised and hence,

$$\frac{d(\ln V)}{d(\ln I)} = \left[\frac{d(\ln E_s)^2}{d(\ln V)} \right]^{-1} \left[1 + \frac{B}{2\beta V} d \right] \quad [5] \quad \dots \text{A3.2}$$

where E_s is the local field strength and given by $(-\beta V)/d$, β being the field intensification factor and B is the Fowler-Nordheim constant and is material dependent. This equation can be written as,

$$\frac{d(\ln V)}{d(\ln I)} = M \left[1 + \frac{B}{2\beta V} d \right] \quad \dots \text{A3.3}$$

which is of the form of Eqn. (A3.1).

Fluid flows away from the tip of the electrode upon charge injection so that dx/dt is equal to the drift velocity $U_d = bE_s$ where b is the electronic mobility [5]. Thus,

$$\frac{dx^2}{dt} = 2X \frac{dx}{dt} = 2XU_d = 2XbE_s = \eta$$

hence,

$$XE_s = \frac{\eta}{2b} \quad \dots \text{A3.4}$$

On the other hand, mobility is roughly proportional to the inverse of viscosity (Sillars, 1973), then,

$$XE_s = \frac{\eta}{2b} \propto \frac{\eta^2}{2}$$

but,

$$XE_s = -\beta V$$

thus,

$$\frac{d(\ln V)}{d(\ln I)} = M \left[1 + \frac{B'}{\eta} d \right] \quad \dots A3.5$$

therefore, slope $\propto \eta^2$

and this is what Watson's analysis says. But the author's experimental results indicate that viscosity moves the lines (changes the ordinate intercept) while the slope remains constant [49] and this is in contradiction with what Watson's simple theory says, therefore, suggests that mobility of the liquid plays no part and it should be convection that takes place, meaning that a charge Q is fixed relative to fluid but fluid moves to create a current column.

To make any headway in our study we take a vortex ring which expands just as smoke rings do when they rise, Fig. (A.3.1). Since the flow is axially symmetric, with a suitable choice of cylindrical polar co-ordinates r, θ, z every physical variable is independent of the angle θ .

The expansion acceleration equal to the vector cross product $\underline{\omega} \times \underline{u}$ is oppositely directed at two locations. The electrostatic force can be written as $F_e = \rho_o E$ which is equal to the inertial force with acceleration $\underline{\omega} \times \underline{u}$. Therefore,

$$\begin{aligned} F_e &= \rho_o E = \rho_m (\underline{\omega} \times \underline{U}) = \rho_m (\nabla \times \underline{U}) \times \underline{U} = -\rho_m \underline{U} \times (\nabla \times \underline{U}) \\ &= -\rho_m \underline{U} \times (\text{curl } \underline{U}) \end{aligned} \quad \dots A3.6$$

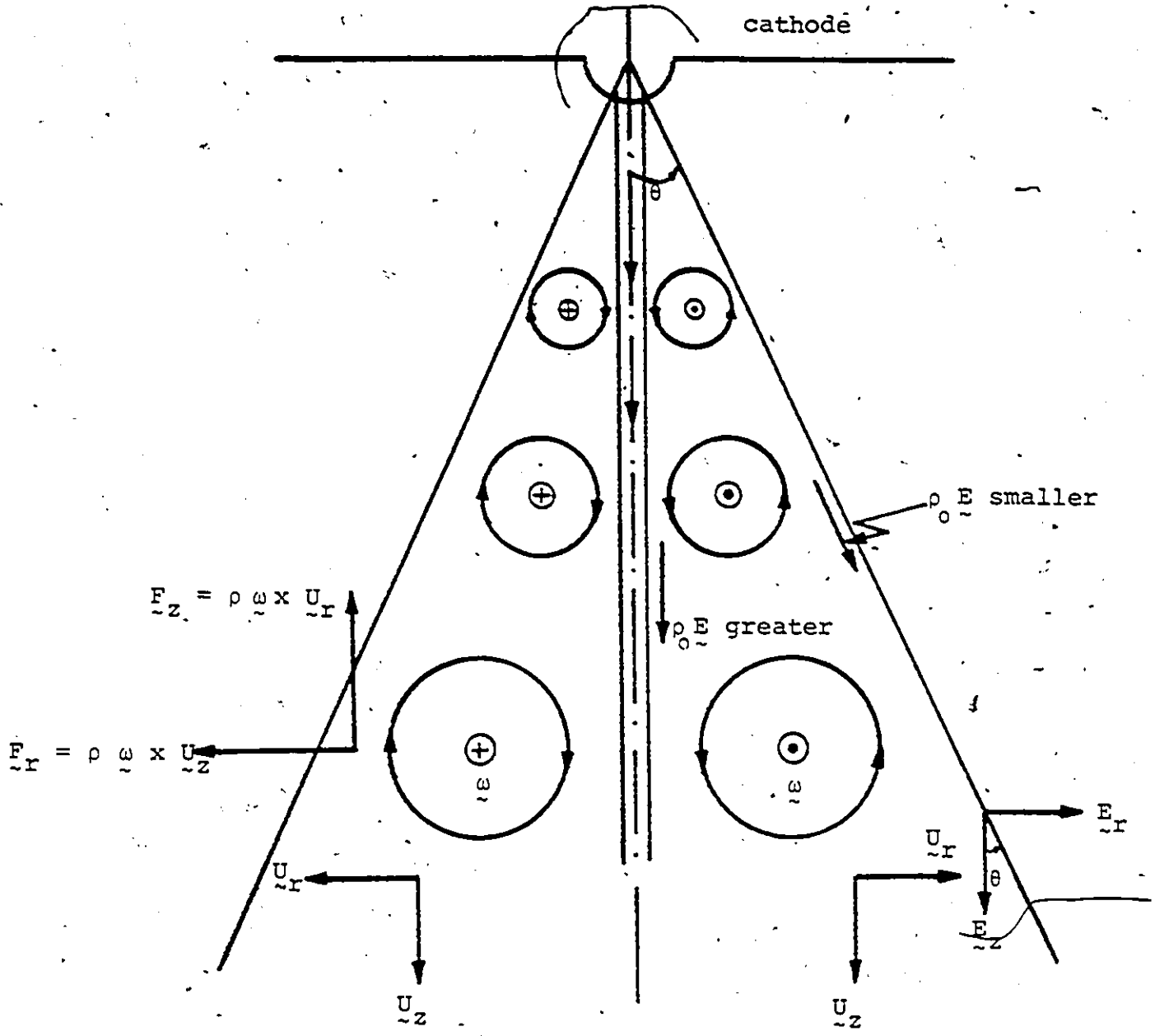


Figure A.3.1: Schematic Illustration of Current and Fluid Flow Configuration.

(The cylindrical column illustrates current channel before the vortex is developed.)

where,

$\nabla \times \underline{U}$ is the vorticity vector

and,

$$\nabla \cdot \underline{E} = \frac{1}{r} \frac{d}{dr} (rE) + \frac{\partial E}{\partial z} = \frac{\rho_0}{\epsilon_0} \quad \dots A3.7$$

therefore,

$$\epsilon_0 \nabla \cdot \underline{E} = -\rho_m \underline{U} \times (\nabla \times \underline{U}) \quad \dots A3.8$$

If E_r , E_z be the components of \underline{E} in vertical and axial directions, then the electrostatic force at each location can be written as,

$$\rho_0 E_r = \rho_m \omega \times U_z \quad \dots A3.9$$

similarly,

$$\rho_0 E_z = \rho_m \omega \times U_r \quad \dots A3.10$$

hence,

$$\frac{E_r}{E_z} = \frac{U_z}{U_r} \quad \dots A3.11$$

If we consider that electrons to be emitted radially from the centre of curvature of the tip of the cathode within a conical section of half angle θ , (Fig. A.3.1), then,

$$\frac{E_r}{E_z} = \tan \theta \quad \dots A3.12$$

If we suppose that the motion is along the surface of the cone then $\tan \theta = \text{constant}$.

The rate of change of a value V attached to some particular particle of the fluid can be expressed as DV/Dt where,

$$V = V(r, \theta, z, t)$$

but if the displacement is the same as that made by the particle of fluid in time we must have,

$$\begin{aligned} \frac{DV}{Dt} &= \frac{dv}{dt} + U \cdot \nabla V = \frac{dv}{dt} - U \cdot E = \frac{dv}{dt} - (U_r E_r + U_z E_z) \\ &= \frac{dv}{dt} - 2U_r E_r = \frac{dv}{dt} - 2U_z E_z \end{aligned} \quad \dots \text{A3.13}$$

This is Euler's equation of motion.

Now suppose we move on an equipotential line as it "drifts" into the electrode spacing when dv/dt rises, i.e. $DV/Dt = 0$, which seems to imply that we move with a fixed vorticity. Then the Euler mobile time derivative reduces to,

$$\frac{DV}{Dt} = \frac{dv}{dt} - 2U_r E_r = \frac{dv}{dt} - 2U_z E_z = 0 \quad \dots \text{A3.14}$$

therefore,

$$\dot{V} = 2U_r E_r = 2U_z E_z \quad \dots \text{A3.15}$$

Now we assume that the fluid flows away from the tip upon charge injection so that dx/dt is equal to the drift velocity in the axial direction $U_z = KE_z$ where K is the mobility. Thus,

$$\rho_m \tilde{\omega} \times \tilde{U}_z = K \rho_m \tilde{\omega} \times \tilde{E}_z \quad \dots \text{A3.16}$$

Substituting E_z from the Eqn. (A3.10) into the Eqn. (A3.16) we obtain,

$$\tilde{\omega} \times \tilde{U}_z = K \frac{\rho_m}{\rho_0} \tilde{\omega} \times (\tilde{\omega} \times \tilde{U}_r) \quad \dots \text{A3.17}$$

or in scalar form,

$$\omega U_z = K \frac{\rho_m}{\rho_o} \omega^2 U_r$$

hence,

$$|U_z| = K \frac{\rho_m}{\rho_o} \omega |U_r| \quad \dots \text{A3.18}$$

Therefore,

$$K = - (U_z/U_r) / (\rho_m/\rho_o) \omega = -(E_r/E_z) / (\rho_m/\rho_o) \omega$$

So,

$$K = - \frac{\rho_o}{\rho_m} \frac{\tan \theta}{\omega} \quad \dots \text{A3.19}$$

and

$$U_z = - \frac{\rho_o}{\rho_m} \frac{E_r}{\omega} \quad \dots \text{A3.20}$$

Similarly by substituting $E_r = E_z \frac{U_z}{U_r}$ in the above we get,

$$U_r = - \frac{\rho_o}{\rho_m} \frac{E_z}{\omega} \quad \dots \text{A3.21}$$

Now if,

$$\frac{\eta}{2K} = \frac{\eta \rho_m \omega}{2 \rho_o \tan \theta} = \frac{\mu \omega}{2 \rho_o \tan \theta}$$

where

$$\mu = \rho_m \eta$$

and μ , η are viscosity and dynamic viscosity of the fluid respectively, is constant then Watson's model is validated.

Since $\rho = \text{constant}$, this is the case of incompressible flow of a homogeneous fluid and is particular applicable in the motion of a liquid [Rutherford, 1959] then $\eta/2K$ is

constant iff $\eta\omega$ is constant, meaning that vortex strength is inversely proportional to the viscosity of the fluid. But on the other hand,

$$\underline{\mu\omega} = \underline{\mu \text{ curl } \underline{U}} = \underline{T} \quad \dots \text{A3.22}$$

where T is shear stress in fluid, which must be present in the Maxwell stress to be balanced at all time.

and,

$$\frac{\eta}{2K} = \beta V \quad [5]$$

therefore,

$$\text{slope} \propto \beta V = \frac{\eta}{2K} = \frac{\mu\omega}{2\rho_0 \tan \theta} = \frac{T}{2\rho_0 \tan \theta} = \text{constant}$$

... A3.23

The invariance of slope with η implies that shear stress T is invariant (depends only on electrode material). By having $\eta = \omega^{-1}$, T is constant and the invariance of the slope with η can be explained.

Since we supposed movement along a path where $V = \text{constant}$ then,

$$\text{Maxwell stress component} = \rho_0 V = -\epsilon E^2/2 = \text{constant}$$

but $T = \text{constant}$ implies that the shear component of Maxwell stress is constant which is consistent with our model.

Now,

$$\frac{dv}{dt} = 2U_z E_z = 2KE_z^2 = \frac{2(\tan \theta)}{\omega} \cdot \frac{\rho_0}{\rho_m} E_z^2 \quad \dots \text{A3.24}$$

So it seems that the fixed K ("vortex mobility") implies the

motion of the vortex with a fixed Maxwell stress tensor.

In short from the experiment slope is invariant with viscosity η and so if the modified analysis above is true, then the flow must be assumed to proceed with an invariant shear component of the Maxwell stress.

VITA AUCTORIS

Mohammad A. Abiri

- 1946 Born on September 16, Iran
- 1960 Completed primary school education at Khayyam Elementary School, Tehran, Iran
- 1963 Completed lower secondary education at Parvaresh High School, Tehran, Iran
- 1966 Completed higher secondary education at Dar-ol-Phonoun High School, Tehran, Iran, in Mathematics.
- 1968 Terminated from Literary corps (Military service), Tehran, Iran
- 1972 Graduated from Iran University of Science and Technology, Tehran, Iran with the degree of Bachelor of Science in Electrical Engineering
- 1972-76 Karun & Marun Project, KWPA, in corporation with Harza Engineering Company, International, MIS, Khuzestan, Iran
- 1977-80 Laboratory Instructor, University of Windsor, Windsor, Ontario, Canada
- 1980 Candidate for the Degree of Master of Applied Science in Electrical Engineering at the University of Windsor, Windsor, Ontario, Canada.